P. A. LEPCZYK
M.S.
2005

LIBRARY
Michigan State
University

67799181

This is to certify that the
thesis entitled

LABORATORY AND NUMERICAL SIMULATIONS OF THREE-DIMENSIONAL MICROBIAL TRANSPORT AND BIODEGRADATION

presented by

Peter A. Lepczyk

has been accepted towards fulfillment
of the requirements for the

M.S. degree in Geological Sciences

David Hyndman
Major Professor's Signature

5/6/2005
Date

MSU is an Affirmative Action/Equal Opportunity Institution

PLACE IN RETURN BOX to remove this checkout from your record.
TO AVOID FINES return on or before date due.
MAY BE RECALLED with earlier due date if requested.

DATE DUE	DATE DUE	DATE DUE

2/05 c:/CIRC/DateDue.indd-p.15

LABORATORY AND NUMERICAL SIMULATIONS OF THREE-DIMENSIONAL MICROBIAL TRANSPORT AND BIODEGRADATION

By

Peter Alexander Lepczyk

A THESIS

Submitted to
Michigan State University
in partial fulfillment of the requirements
for the degree of

MASTER OF SCIENCE IN ENVIRONMENTAL GEOSCIENCES

Department of Geology

2005

ABSTRACT

LABORATORY AND NUMERICAL SIMULATIONS OF THREE-DIMENSIONAL MICROBIAL TRANSPORT AND BIODEGRADATION

By

Peter Alexander Lepczyk

A three-dimensional column experiment was created to provide insight into the bioaugmentation of carbon tetrachloride by *Pseudomonas stutzeri* KC. The goals of this experiment were to increase our understanding of the transport of *Pseudomonas stutzeri* KC and to collect high-resolution datasets to conduct a case study using a numerical model developed by the Departments of Geological Sciences and Civil and Environmental Engineering at Michigan State University that accounts for the three-dimensional microbial transport and biodegradation specific to the Schoolcraft Plume A project. The laboratory model results exhibit effective transport of the mobile phase microbe and degradation of CT; however, the results indicate a lag between the transport of mobile *Pseudomonas stutzeri* KC and a conservative tracer, which was not produced in the numerical simulation. The simulated CT degradation exhibited a higher degree of mass removal than what was observed, though detailed qualitative comparisons could not be made.

ACKNOWLEDGMENTS

I would first like to thank my wife, Xiomara, whose encouragement, love, and patience was instrumental in the completion of this thesis. I would also like to acknowledge all of my family, friends, and co-workers who provided me with additional strength and support.

Next, I would like to thank my committee members, starting with my advisor, David Hyndman, without whom this thesis would not have had direction. His comments and suggestions were always appreciated and more importantly, his belief in me through this arduous process will never be forgotten. I would also like to thank Phanikumar Mantha, who was constantly willing to help and provide insight into the numerical modeling aspects of this work. Lastly, Dave Long's constructive criticism and flexibility in meeting my time constraints was greatly appreciated. In addition to my committee members, I would like to express my gratitude towards the rest of the Department of Geological Sciences for allowing me this opportunity to learn and grow as a scientist.

Finally, I would like to acknowledge the entire Schoolcraft laboratory column research team, including Mike Dybas, Xianda Zhao, Roger Wallace, Georgina Vidal-Gavilan, Emily King, and Chris Ritchie, all of who played major roles in this project and I am very appreciative of their hard work and dedication. Specifically, I would like to thank Mike Dybas, Xianda Zhao, and Roger Wallace for their contributions to the design of this laboratory experiment, and Xianda Zhao, Georgina Vidal-Gavilan, Emily King, and Chris

Ritchie for the data collection and sample analyses. Working as a member of this interdisciplinary research group taught me a great deal about teamwork, of which I am very thankful.

TABLE OF CONTENTS

LIST OF TABLES

LIST OF FIGURES

1 INTRODUCTION

Carbon tetrachloride (CT) is a carcinogenic compound that has been widely used as a degreaser, solvent, fumigant, and fire extinguisher. Unfortunately due to disposal practices prevalent in the past it has also become a common groundwater contaminant (Lewis and Crawford, 1999; Hyndman et al., 2000; Dybas et al., 2002). Traditional clean up methods for removing CT, include pump and treat coupled with activated carbon sorption or air stripping. However, these techniques are costly and time consuming. Moreover, these methods only treat aqueous phase constituents and do not address the contaminants sorbed onto the aquifer media, which may pose a future threat to the site if the contaminants were released after the treatment operations have been completed (Davis, 1995; Fetter, 1999).

Novel strategies, such as bioremediation, are necessary to clean up CT contaminated groundwater. Three distinct types of bioremediation strategies have been developed: natural attenuation, biostimulation, and bioaugmentation. Natural attenuation is the process by which the native flora are left alone to degrade contaminants and mitigate the size and extent of the plume. This may be a reasonable option when the natural rate of biodegradation is fast enough to prevent significant contaminant migration. Biostimulation involves stimulating indigenous microbes to transform target contaminants through the addition of either an electron acceptor, (i.e., oxygen or nitrate), an electron donor (i.e., acetate or lactate), or both. Bioaugmentation is the process of adding a non-indigenous microbe into the aquifer to transform target contaminants that

indigenous microbes either could not transform at an acceptable rate or the results of the transformation are undesirable. Bioaugmentation may also require addition of electron donors and/or acceptors (Hyndman et al., 2000; Chapelle, 2001; Dybas et al., 2002).

Bioaugmentation offers an advantage over biostimulation and monitored natural attenuation because it creates a controlled pathway for degradation to occur. This is an important distinction from the other bioremediation strategies, which may lead to end products that are more hazardous than the original contaminant. In the case of CT, Criddle et al. (1990) demonstrated that chloroform (CF) is a common end product of CT transformation by many indigenous microbes. Therefore, it was critical to discover a microbe capable of transforming CT into non-hazardous end products. In 1987, Criddle et al. (1990) found such a microbe, later named *Pseudomonas stutzeri* KC (KC), in an aquifer in Seal Beach, California. This discovery provided the basis for a significant amount of research on the mechanisms and kinetics of this bioremediation process (Criddle et al., 1990; Lewis and Crawford, 1993; Tatara et al., 1993 and 1995; Dybas et al., 1995; Davis, 1995; Mayotte et al., 1996; Witt et al., 1995 and 1998), and led to tests of strain-KC bioaugmentation of a CT contaminated aquifer in Schoolcraft, Michigan (Dybas et al., 1998; Hyndman et al., 2000; Dybas et al., 2002; Phanikumar et al., 2005).

This thesis presents a subset of the results of a three-dimensional column experiment created to provide insight into the full-scale biocurtain used to remediate dissolved phase carbon tetrachloride at a contaminated aquifer located near Schoolcraft, Michigan (Hyndman et al., 2000; Dybas et al., 2002). The objectives of this laboratory model

aquifer experiment were to (a) improve our understanding of how well *Pseudomonas stutzeri* KC was transported in the subsurface, (b) to visualize the spatial distribution of biomass after an inoculation event, and (c) to conduct a case study using a numerical reactive transport model developed by the Departments of Geological Sciences and Civil and Environmental Engineering at Michigan State University that accounts for the three-dimensional microbial transport and biodegradation associated with the Schoolcraft project.

2 SCHOOLCRAFT BACKGROUND

In 1987, the Michigan Department of Natural Resources (MDNR) began investigation of an aquifer near Schoolcraft, Michigan (Figure 1), which was impacted with dissolved phase CT and nitrate. This plume has later been referred to as Schoolcraft Plume A. In accordance with common technologies at the time, the MDNR proposed a pump and treat system coupled with air stripping. According to Halliburton NUS Environmental Co. (1991), the remedial action for this site would take approximately 25 years. As was previously mentioned, 1987 also marked the discovery of strain KC. Utilizing this microbe, researchers at Michigan State University conducted batch and one-dimensional column studies (Mayotte et al., 1996; Witt et al., 1995 and 1999). These experiments demonstrated the rapid transformation of CT into CO_2, formate and an unidentified non-volatile product; this transformation required denitrifying conditions, the presence of an electron donor (like acetate), alkaline pH (7.8 to 8.3), and typical aquifer temperatures (5-25 °C); (Criddle et al., 1990, Tatara et al., 1993; Lewis and Crawford, 1993; Davis, 1995; Mayotte et al., 1996; Witt et al., 1995 and 1998; and Dybas et al., 1995 and 1998). It was later demonstrated that the transformation was mediated by a secreted factor determined to be pyridine-2,6-bis(thiocarbonxylate) or PDTC, which is produced under the fore mentioned conditions (Lee et al., 1999). Encouraged by the results, the state of Michigan funded an interdisciplinary research team to test the field applicability of a bioaugmentation system using strain KC at the Schoolcraft Plume A site. This team conducted a field pilot test (Dybas et al., 1998), engineered a full-scale bioaugmentation system (Hyndman et al., 2000 and Dybas et al., 2002), and later designed this three-dimensional laboratory model aquifer experiment (Vidal-Gavilan, 2000).

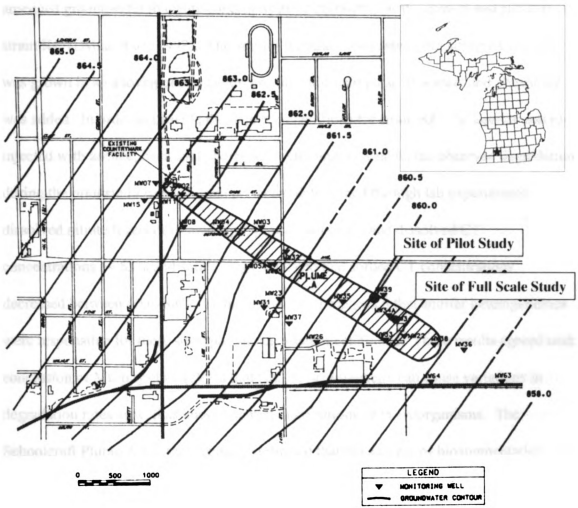

Figure 1. Map illustrating the location of Schoolcraft, Michigan, the position of plume A, and hydraulic head contours in feet. Also identified are the locations of the pilot study and the full-scale biocurtain, reprinted from Hyndman et al (2000).

2.1 PILOT STUDY

A pilot test was conducted at Schoolcraft Plume A in 1994 to test the effectiveness of bioaugmentation with strain KC under field conditions (Dybas et al., 1998). In general, the groundwater in Schoolcraft Plume A contains CT, up to roughly 100 ppb, nitrate at roughly 65 ppm, dissolved oxygen between 2 to 5 ppm, pH between 7.2 and 7.4, and is phosphorous and carbon limited. The pilot test entailed pulsing base and phosphate

amended groundwater to create conditions more favorable for the growth and survival of strain KC (Dybas et al., 1998). The aquifer was then inoculated with strain KC, which was grown in an aboveground reactor, and an additional pulse of acetate and phosphate was added. In order to provide the required conditions for strain KC, the aquifer was re-injected with acetate, base, and phosphate. Although favorable, the observed degradation during the pilot study was less than predicted determined through lab experiments; dissolved nitrate levels decreased by approximately 85% and dissolved CT concentrations by 65% and soil borings indicated that sorbed CT concentrations decreased between 60 to 88%. Dybas et al (1998) suggested that aquifer heterogeneities were responsible for these sub-optimal degradation conditions. These results agreed with conclusion of Murphy et al. (1997) that aquifer heterogeneity can cause variations in degradation rates as well as uneven spatial distributions of microorganisms. The Schoolcraft Plume A pilot test results confirmed that the success of bioaugmentation requires an understanding of the aquifer heterogeneities and a remedial design that accounts for them (Hyndman et al., 2000).

2.2 FULL-SCALE BIOCURTAIN

Following the analyses of the pilot test, a full-scale biocurtain was designed and installed at the Schoolcraft site (Hyndman et al., 2000; Dybas et al., 2002). Conceptually, this entailed creating a biologically active zone perpendicular to natural gradient flow. The contaminated groundwater flows by natural gradient into the biocurtain and is degraded when the microbes are stimulated with the appropriate pH, acetate, and phosphorous

concentrations through a series of delivery wells. The objectives of the biocurtain design were to (a) decrease the concentrations of CT and nitrate to below Michigan Department of Environmental Quality residential drinking water criteria (5 ppb and 10 ppm, respectively) from the original concentrations of 100 ppb and 65 ppm, respectively, (b) develop an effective treatment zone across a vertical transect through the contaminant plume, and (c) to minimize remediation costs. In order to meet these objectives, the aquifer at the field site was characterized in detail and numerous delivery grid designs were examined using numerical models. After conducting a cost optimization algorithm, the final design entailed 15 closely spaced re-circulation wells (1-m apart) screened across the entire vertically impacted zone (Hyndman et al., 2000). The wells were used for initial inoculation and weekly aquifer amendments. Installation of the system began in spring 1997 and most downgradient monitoring locations indicated between 95 and 100% CT removal after two to three years of operation (Hyndman et al., 2000 and Dybas et al., 2002).

2.3 THREE-DIMENSIONAL MODEL AQUIFER EXPERIMENT

In order to further understand the bioaugmentation of CT by strain KC, members of MSU's Departments of Civil & Environmental Engineering and Geological Sciences designed a large 3-dimensional model aquifer. This 3-dimensional model aquifer was used to create a carefully controlled set of experiments, designed to simulate the biocurtain at Schoolcraft Plume A (Vidal-Gavilan 2000). This experiment filled a void between the early one-dimensional column studies by Witt et al (1995 and 1999), and the

full-scale biocurtain presented by Hyndman et al (2000) and Dybas et al (2002). Through the use of a three-dimensional aquifer model, many shortcomings of one-dimensional models like edge effects are reduced. Moreover, complete three-dimensional sampling and analyses can be accomplished in a model aquifer, where as costs would be prohibitive to fully characterize a field site in this manner.

3 THREE-DIMENSIONAL LABORATORY MODEL

Column experiments are common practice in hydrogeology and engineering. They allow investigations to take place under controlled conditions, therefore reducing many uncertainties found in the field. In turn these experiments are often used as an intermediate step to evaluate remedial options prior to a field scale application. Furthermore, the data obtained from these experiments can be used to calibrate, and in some cases even develop, reactive transport models. Many hydrogeologists and environmental engineers are discovering that this is a valuable course of action. By decreasing the uncertainty, one can create a conceptual model with fewer assumptions.

This section discusses the development and design specifications of the 3-dimensional model aquifer experiment. Furthermore, it describes the series of tests that were performed to determine specific groundwater flow and aquifer parameters.

3.1 LABORATORY COLUMN DESIGN

The 3-D laboratory model aquifer was composed of a large column representing the Schoolcraft aquifer and a series of stages designed to support the laboratory biocurtain. These stages include pumps, tanks, and a cooling system, to create controls and add amendments to the system. A detailed schematic of the laboratory model is illustrated in Figure 2.

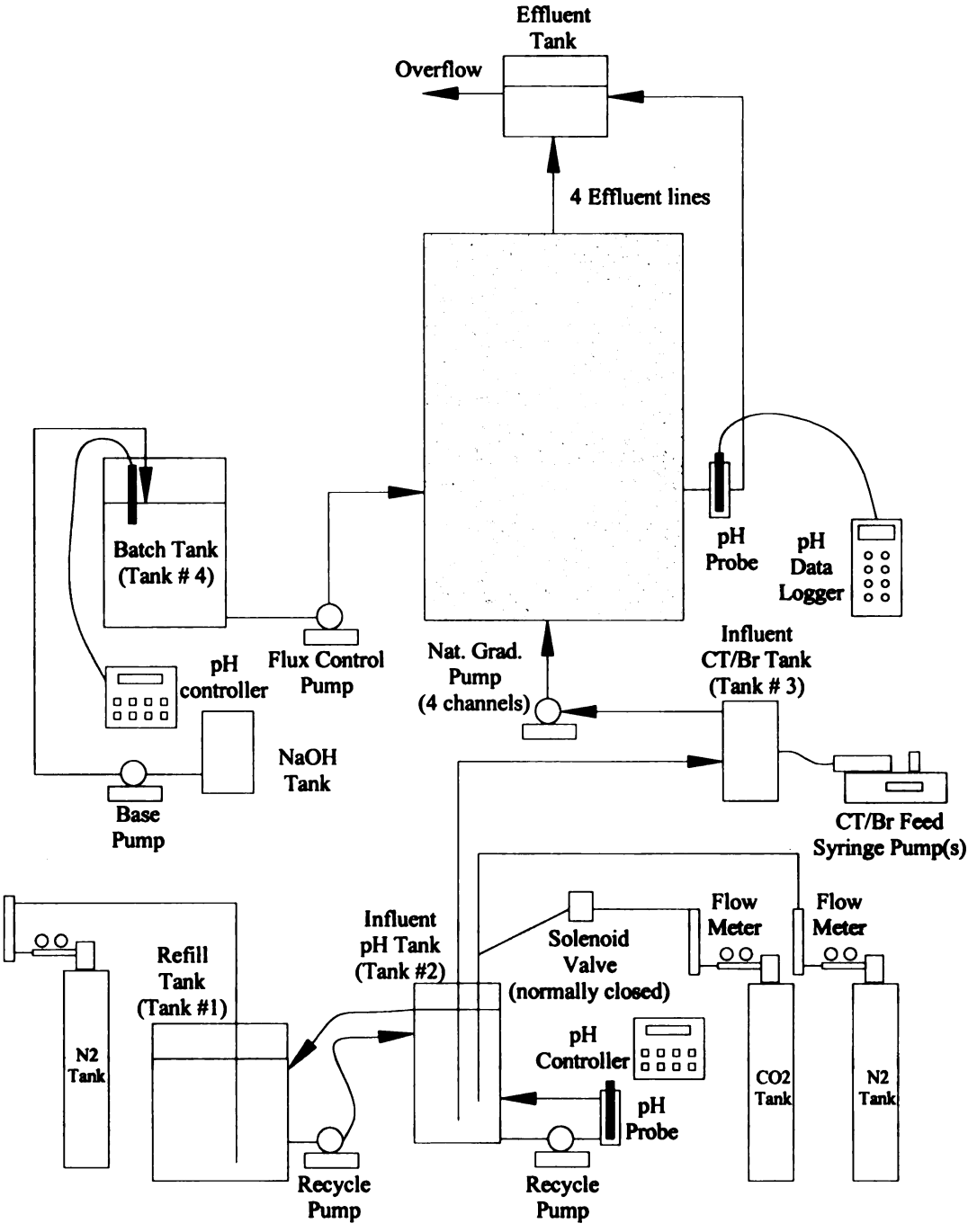

Figure 2. Schematic of laboratory model aquifer experiment, modified from Vidal-Gavilan (2000).

The actual model aquifer was a vertical cylinder 3 feet high by 2 feet in diameter and filled with aquifer soil collected from the site. The sand was mixed to create a homogeneous, isotropic media. The cell was packed by saturating the sand before filling the tank with the wet slurry, and ensuring that the height of water in the tank was always above the surface of the sand, which also aided in the removal of trapped air (Vidal-Gavilan, 2000).

The stainless steel cylinder used for this experiment was both durable and non-reactive. Inflow and outflow lines were placed at the bottom and top of the tank, as well as at the sides. Moreover, 57 sampling ports were installed throughout the cylinder to allow the collection of 3-dimensional data sets (Figure 3) (Vidal-Gavilan, 2000).

The Inflow and outflow lines placed at the bottom and top of the flow cell were used to create conditions similar to natural gradient flow. The system was designed for water to be pumped into the tank through the bottom to guarantee full saturation of the aquifer media. The influent and effluent lines included one center position and six locations that were evenly spaced around the center, at a radius of 8 inches. However, due to improper manufacturing, the top lid did not create a watertight seal with the cylinder, thus the top lid was rotated until a watertight seal was achieved. This resulted in the top lid being rotated clockwise from the desired position by approximately 30 degrees (Figure 4) (Vidal-Gavilan, 2000).

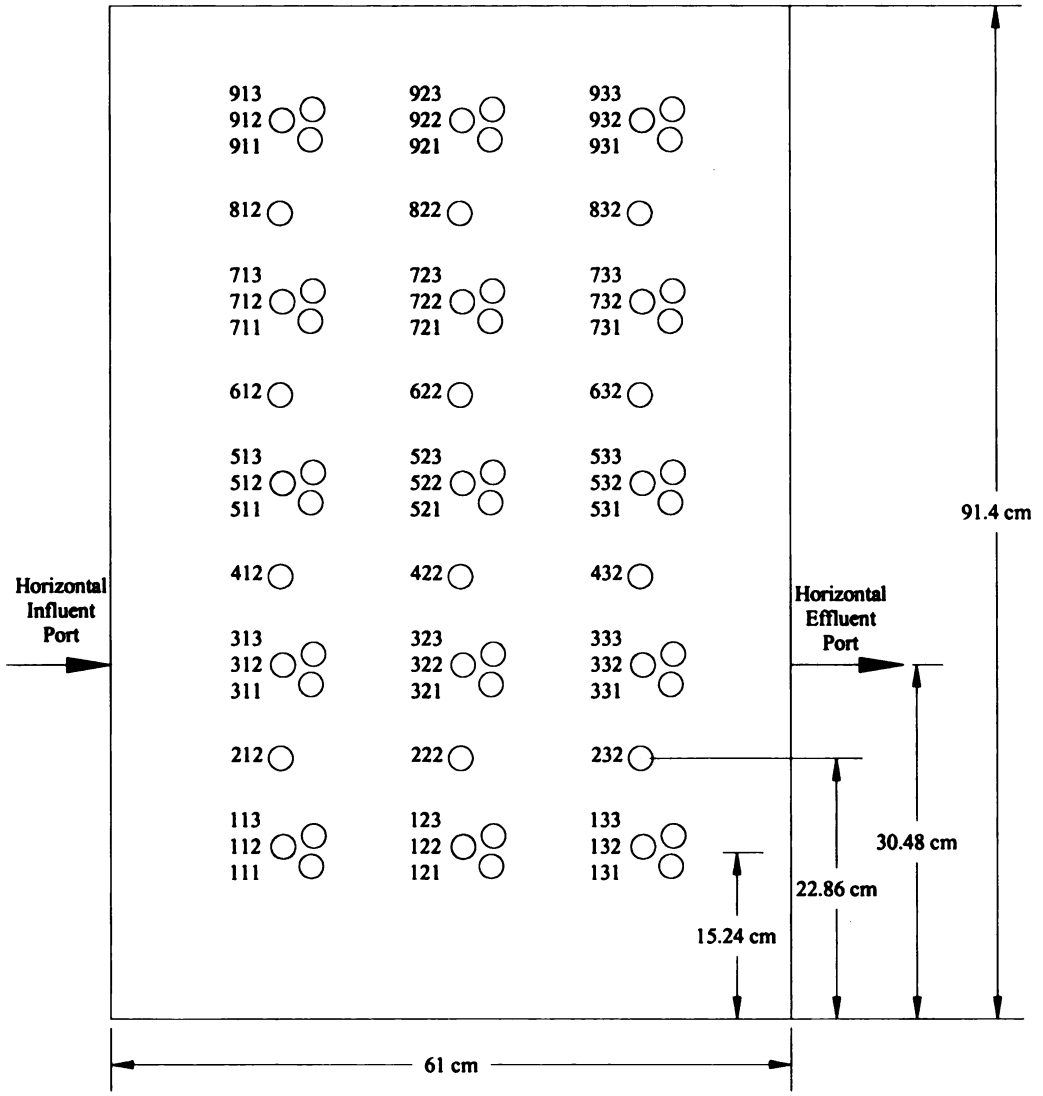

Figure 3. Location of sampling ports, horizontal influent and effluent ports, and model aquifer dimensions, modified from Vidal-Gavilan (2000).

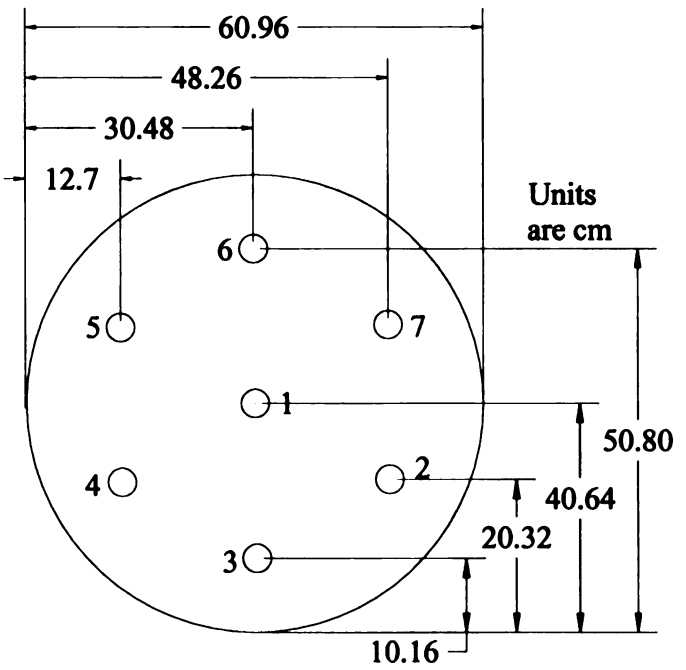

(a) Bottom of the 3-D flow cell.

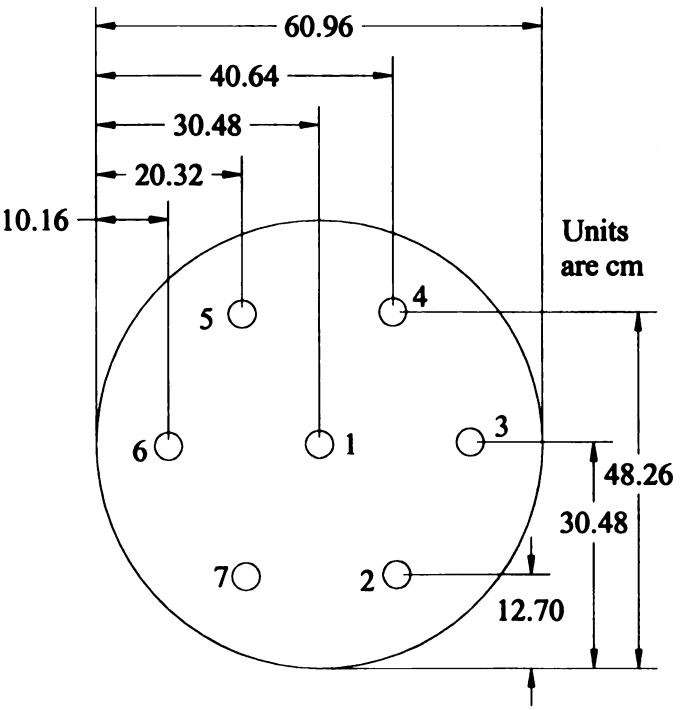

(b) Top of the 3-D flow cell.

Figure 4. Location of vertical influent ports, modified from Vidal-Gavilan (2000).

The horizontal inflow and outflow lines were located 12 inches from the base of the tank on each side. Their purpose was to simulate the lateral flow between a set of injection and extraction wells comprising the Schoolcraft biocurtain. All of the flow lines were attached to the tank via 1/4 inch, stainless steel fittings. The fittings were housed with fine mesh in an attempt to prevent the migration of fine grained sand into the influent and effluent lines.

The 57 sampling ports were positioned throughout the model aquifer and penetrated the aquifer media at various depths. The sampling ports consisted of stainless steel fittings with 1/16 inch stainless steel tubing running through the center of each one. The sampling ports were subdivided into three columns, nine rows and three depths. The center column was perpendicular to the cross flow influent and effluent lines. The other two columns were offset 6 inches from the center. Row number 1 was 6 inches from the bottom of the tank and subsequent rows were 3 inches apart from one another. Odd numbered rows had sampling ports at three separate depths. These depths are assigned 1, 2 or 3, which were equivalent to 6 inches, 12 inches and 18 inches, respectively. Even numbered rows had only one sampling depth at 12 inches. Identification of sampling ports was accomplished through assigning a notation depending on row, column and depth. Sampling ports will herein be referred to as a 3-digit number, where the first number is the row, the second number is the column and the third number is the depth. For example, sampling port 812 is located in row 8, column 1, and depth 2. Refer to Figure 5 and (Vidal-Gavilan, 2000) for details.

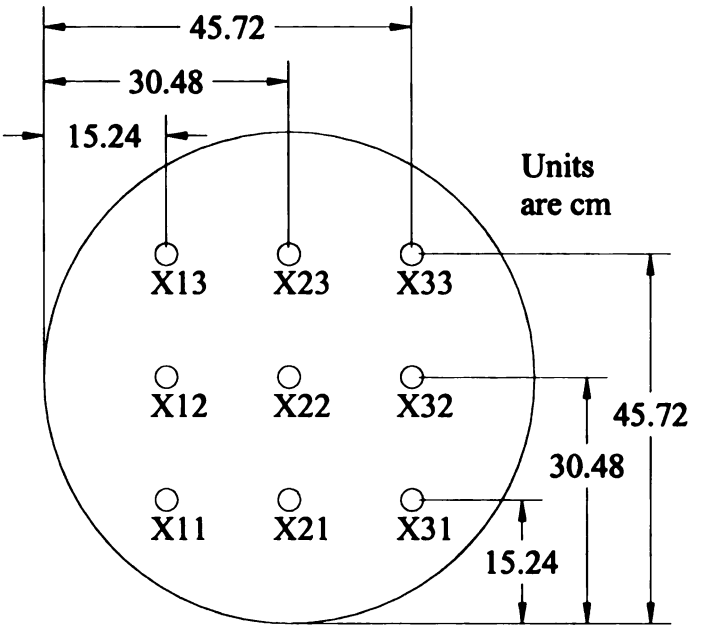

Figure 5. Locations of sampling ports, modified from Vidal-Gavilan (2000).

3.2 SUPPORT SYSTEMS

After the cylinder was fabricated and wet packed with the soil, the support systems were connected to the tank. The design and function of the support systems is as follows (See Vidal-Gavilan (2000) for additional details).

Schoolcraft groundwater was introduced into the laboratory model aquifer system via the refill tank (tank #1). Nitrogen was pumped into the tank at a pressure to just overcome the hydraulic head in order to strip out any dissolved CT. Water from tank #1 was then pumped into the pH adjustment tank (tank #2). An overflow line connected tank #2 to tank #1, thus maintaining a constant hydraulic head in the pH adjustment tank. Nitrogen was also added to tank #2 to strip out any oxygen that may have been added to the water

and create anoxic conditions. Carbon dioxide was added to the water when the pH was above 7.4 to reduce it to 7.2. This was accomplished by means of a pH probe in tank #2 connected to a solenoid that was normally closed. Both of these tanks were housed in a cold room, maintained at the ambient groundwater temperature of Schoolcraft (roughly 12° C).

A gravity feed line was then connected from tank #2 to the amendment tank (tank #3), located outside of the cold room next to the model aquifer. Tank #3 was where chemical species were introduced into the water, i.e. bromide or carbon tetrachloride. This tank had a series of influent ports where syringe pumps could be attached to add a fixed rate of chemical and thus create a constant influent concentration. This tank rested on a magnetic stirring plate with a stir bar mixing the water. A batch tank (tank #4) was used for specific experiments when it was deemed that the engineered support system was unnecessary. Finally the water was fed into the model aquifer either through the bottom of the cell or the side, depending on the nature of the specific experiment. A peristaltic pump provided the vertical flow via connections to the bottom of the model aquifer, while a diaphragm control pump provided the horizontal flow component of the tank.

The effluent lines from the top of the tank converged into a single constant head tank positioned 15 cm above the top of the tank. Prior to the experiments, the vertical influent and effluent lines were decreased to 4 each (influent ports 1, 3, 5, and 7 and effluent ports 1, 2, 4, and 6) due to plugging problems in a few of the other ports observed during the leak testing. The horizontal effluent line discharged to the same constant head tank.

In order to keep water temperature constant and minimize effects of thermal fluctuations on the kinetics of the co-metabolic degradation, the tank was insulated and cooled. Metal tubing was attached to a re-circulating cold water bath kept at 8° C and wrapped around the outside of the tank. Insulation was then adhered to the outside of the tank. Measured model aquifer temperatures matched field conditions and were maintained between 10 and 12° C. Water was sampled through syringes screwed onto the sampling ports and withdrawing 2-5 ml of water for bromide and CT analyses and microbial plate counts, respectively. See Vidal-Gavilan (2000) for details of the design and system operation.

3.3 GROUNDWATER FLOW AND CHEMICAL TRANSPORT EXPERIMENTAL DESIGN

Due to scale differences between the field and the model aquifer, laboratory flow rates varied from those observed on site. Under natural gradient conditions, the average linear velocity of the Schoolcraft aquifer is approximately 14.8 cm/day (Halliburton NUS Environmental Co., 1991). We used approximately 4 times this value for the vertical tracer tests. To achieve this, groundwater was pumped into the 3-D laboratory model aquifer system at a combined flow rate of approximately 33 ml/min. According to Dybas et al (2002), the flow rate of a single injection well is approximately 19 L/min. In order to use flow rates more suitable for a laboratory scale model, this horizontal flow rate was decreased to a value of approximately 280 ml/min. After establishing the flow rates, a series of tracer tests were performed to observe the breakthrough curves and use the data sets to characterize parameters for the numerical modeling, such as porosity and

dispersivity. Following these tests, the soil was titrated with NaOH to raise the pH to a level more suitable for the growth of KC. Lastly, the column was inoculated with KC and the full-scale biocurtain experiment commenced. The target flow rate for the vertical natural gradient flow used in the biocurtain experiment was 14 ml/min.

3.4 HORIZONTAL BROMIDE TRACER TEST

The first tracer test consisted of a conservative tracer breakthrough study performed between the single horizontal influent and effluent lines without the presence of a vertical flow component. The primary objective of this test was to experimentally determine the amount of time required to achieve breakthrough in the delivery zone and observe if any preferential flow paths existed. Additional objectives were to collect a data set that could be used with numerical models in order to estimate the porosity and dispersivity of the model aquifer.

Bromide was chosen as the tracer for its ease of analyses with a bromide probe. Sodium bromide was mixed with nitrogen stripped Schoolcraft groundwater in tank #4 to create a bromide solution of 114.5 mg/L. This concentration was assumed constant throughout the experiment. The bromide solution was pumped into the column at a flow rate of roughly 280 ml/min, however flow measurements taken from the effluent water stream indicated that the rate varied between 260 and 300 ml/min. These variations were attributed to the flexible tubing inside the peristaltic pump, or partial plugging of flow lines.

Based on preliminary calculations, using an estimated porosity of 37% and flow rate, full tracer breakthrough was expected after 3 hours. A Cole-Parmer bromide electrode was connected to a Jenco model 6091 data logger and placed in-line with the effluent stream. Data was recorded at 5-minute increments for the duration of the test (204 minutes). A sampling schedule was prepared in accordance with the breakthrough estimate for a selected number of internal sampling ports. The schedule was created to capture the tracer progressively as it traveled through the tank. In turn, samples were collected at 90, 120, 150, and 180 minutes after the start of the test. 2-3 ml samples were collected from these sampling ports and later analyzed with the bromide probe upon test completion.

3.5 VERTICAL BROMIDE TRACER TEST AND CARBON TETRACHLORIDE SORPTION STUDY

Following the conservative horizontal tracer test, a combined conservative (bromide) vertical tracer test and Carbon Tetrachloride sorption test was performed. The objectives of this experiment were to (a) determine the amount of time required to achieve breakthrough in the vertical dimension, (b) compare the breakthrough curves of Br and CT and calculate the retardation value of the CT, and (c) utilize the data to determine physical parameters for the numerical model. This test was performed without the influence of the horizontal delivery system.

Carbon Tetrachloride and bromide were mixed in tank #3. Two syringe pumps delivered the chemicals into tank #3 where they were combined with gravity drained groundwater

from tank #2. The syringe pumps were set to inject a specified concentration of each chemical constituent at a constant flow rate in order to create constant influent concentrations. The target concentration of bromide was 80 ppm and the target concentration of CT was 50 ppb. Influent concentrations were analyzed several times over the course of the experiment. Results indicated that the influent bromide concentration varied between 62.0 and 74.6 ppm with an average concentration of 68.9 ppm, and the CT influent concentrations varied between 36.7 and 64.5 ppb with an average of 49.4 ppb (Vidal-Gavilan, 2000). It was later realized that the variations in concentration were the result of changes in water level in tank #3 from the gravity feed line.

The target flow rate for this experiment was 33 ml/min. Flow rates were collected several times over the course of the experiment and measured from the combined effluent, located 15 cm above the top of the tank. Though the vertical flow system had been tested prior to this experiment, fluctuations in flow rate were observed between 22 and 36 ml/min. Over the course of the 42-hour bromide tracer test, the flow rate averaged 34.3 ml/min. During the 10 day CT portion of the experiment the flow rate averaged 32.7 ml/min.

Water samples were collected from the combined effluent at 15-minute intervals once the bromide tracer front was observed nearing the effluent. Bromide samples were collected from selected internal sampling ports at 16, 24, 30, 31, 32, 33, 34, 35, and 36 hours. All samples were analyzed with the bromide electrode. Water was sampled for CT analyses

at 16, 24, 48, 72, 96, 120, 138, 146, 161, 184, and 241 hours. CT was analyzed by gas chromatography, as described by Vidal-Gavilan (2000). CT addition continued through the model aquifer for an additional two days to try and homogenize the distribution of solute in the model aquifer.

3.6 SOIL TITRATION

Upon completion of the vertical bromide tracer and CT sorption tests, the pH of the model aquifer was adjusted through a soil titration process. The goal of this procedure was to elevate the pH of the delivery zone from the naturally occurring pH of 7.2 to approximately 8.2, where Pseudomonas strain KC flourishes. In turn, the adjustment of the delivery zone was accomplished by injecting CT spiked Schoolcraft groundwater with an approximate CT concentration of 45 ppb and an elevated pH of 8.2. Water was injected into the horizontal influent port at an approximate flow rate of 280 ml/min and flowed out of the horizontal effluent port into the constant head discharge tank over a 16-hour period. Data was collected in-line at 5-minute increments from the effluent port and analyzed with a Jenco model 6091 pH meter and a Hanna Instruments pH probe.

3.7 INOCULATION AND HORIZONTAL BROMIDE TRACER TEST 2

Once the pH of the delivery zone was optimized for the growth of strain KC, the model aquifer was ready to be inoculated. To replicate the field application, the goal was to set-up a population of strain KC in the delivery zone, thus creating the biocurtain.

A 57 L fermenter was prepared with filter-sterilized Schoolcraft groundwater and strain KC cultures, and amended with acetate to a concentration of 800 ppm, 70 ppm nitrate, roughly 40 ppb CT, phosphate to a concentration of 10 ppm, trace metals, and base to a pH of 8.2 (refer to Vidal-Gavilan (2000) for a complete description of the strain KC culture preparation). The final inoculum concentration was approximately 8.8×10^7 cfu/ml. The fermenter was spiked with bromide, to a concentration of roughly 64 mg/L, and connected to the model aquifer via a diaphragm pump. The inoculation and tracer test lasted for approximately 3 hours. The flow rate was measured several times and averaged 272 ml/min. Samples for bromide and mobile phase KC analyses were collected at 30-minute intervals from the horizontal influent, ports 312, 322, 332, and the horizontal effluent during the duration of the test. Dissolved CT was measured from the horizontal influent as well; however, concentrations did not hold steady and fell to below detectable limits by the first hour. Upon completion of the inoculation, the vertical flow was initiated and the horizontal flow ceased. Moreover, sampling of rows 1, 3, and 5 for bromide and mobile phase KC immediately followed the commencement of the inoculation/tracer injection. All bromide samples were analyzed with the bromide electrode, as previously described, and biomass concentrations were determined by Vidal-Gavilan (2000) through plate counting on R2A agar dishes.

3.8 BIOCURTAIN EXPERIMENT

After the inoculation event, the bioaugmentation phase of this study began. The goal of this experiment, and the true impetus of this study, was to simulate the biocurtain at the Schoolcraft site. As mentioned above, the horizontal flow component was terminated once the inoculation event was finished and the vertical flow system was activated, simulating the natural gradient flow. The experiment lasted two weeks and was broken up into three stages. The first bioremediation phase lasted 6 days, after which point the vertical flow was temporary shut off, and a 3 hour feeding event took place between the horizontal flow system, followed by another 7 days of natural gradient flow.

Schoolcraft groundwater was pumped into the model aquifer at a flow rate of approximately 14 ml/min. Flow readings were recorded from the combined effluent on a daily basis and indicated that the flow fluctuated between 13 and 14 ml/min. Carbon tetrachloride was added to the water in tank #3 via a syringe pump. Influent concentrations of CT were monitored on a daily basis. The average influent concentration was 37.9 ppb, however fluctuated between 16.8 and 61.7 ppb. Samples were collected from the combined effluent on a daily basis and analyzed for CT. Samples were collected from the odd numbered internal sampling ports at three different times during the experiment, 1.5 hours, 5 days, and 12 days after the start of the experiment. CT was analyzed by gas chromatography, as described in Vidal-Gavilan (2000).

The feeding event occurred on the 6th day of the biocurtain experiment. The vertical flow rate was temporarily turned off and the horizontal flow system was activated. The model aquifer was injected with amended Schoolcraft groundwater with a pH of 8.2, acetate (100 mg/L), nitrate (70 mg/L), carbon tetrachloride (53 μg/L), and trace metals. The feeding event lasted approximately 3 hours. The flow rate was monitored every 30 minutes from the horizontal effluent port and averaged 287 ml/min, though fluctuated between 265 and 301 ml/min. In the field case the natural gradient flow continues during the feeding event in the field, however this difference from the field situation was deemed insignificant due to the difference in magnitude of the horizontal and vertical flow rates. After the feeding event, the horizontal flow system was terminated and the natural gradient flow resumed.

The experiment continued for another 6 days at which point it was determined that several problems existed with the experiment and that the resulting data was becoming less meaningful. This will be discussed in detail in Chapter 7. See Vidal-Gavilan (2000) for details of the collected data.

4 3-D LABORATORY MODEL AQUIFER EXPERIMENTAL RESULTS

The following chapter presents the results and analyses of the 3-D laboratory aquifer model experiment. Where appropriate, geostatistical techniques were employed to aid in the visualization of the data. These and other images in this thesis are presented in color.

4.1 HORIZONTAL BROMIDE TRACER TEST – LABORATORY RESULTS

The results of the horizontal bromide tracer test are listed in Appendix A. The data was normalized by dividing the observed concentration by the influent concentration (C/C_0). Resulting from the slight fluctuation of influent concentrations and errors associated with the analyses of the bromide, values of C/C_0 were occasionally greater than 1.0. When this occurred they were set to 1.0 and denoted with asterisks in the Appendix. As was mentioned in Chapter 2, data was collected from the internal sampling ports at 90, 120, 150, and 180 minutes after the start of the experiment. Figure 6 illustrates the 3-D data sets in the context of the 3-D model aquifer. The dots indicate the location where the sample was collected and are shaded in accordance to the concentration gradient listed next to each figure.

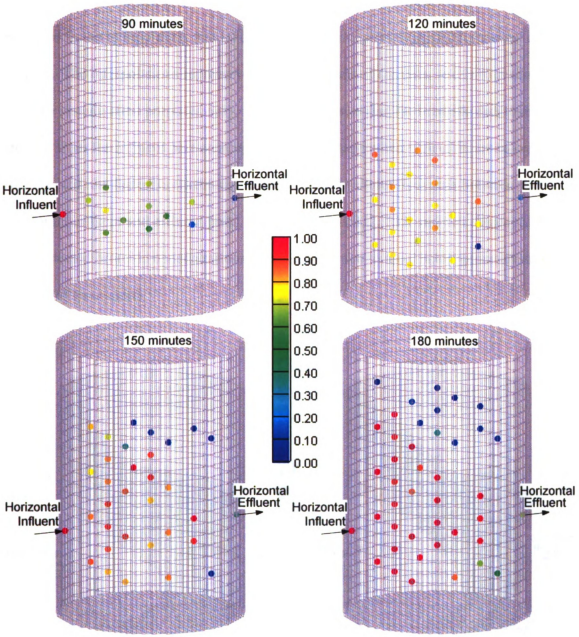

Figure 6. Distribution of bromide concentrations, in C/C_0, for the horizontal bromide tracer test (90, 120, 150, and 180 minutes).

Adequate samples were collected at 150 and 180 minutes to create 3-D geostatistical plots. Shaded iso-surfaces were generated from these interpolations to aid in the visualization of the bromide tracer front (Figure 7). Interpolations were performed inside

of Groundwater Modeling System (GMS) 4.0 using kriging. The 3-D finite difference grid used in the interpolation will be discussed in the numerical modeling section of this chapter. The interpolations represent statistical models of the data, and in turn should be used for visualization purposes only. The data indicates that the bromide distribution radiates from the influent port creating a parabolic shape when viewed in cross-section. As expected, the fastest breakthrough occurs along the direct flow path between the horizontal influent and effluent ports. Sampling ports 232, 132, and 131 displayed less than expected bromide concentrations. This may be due to local heterogeneities in the vicinity of those ports.

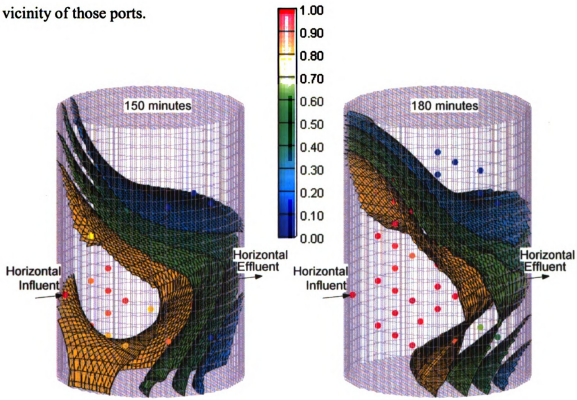

Figure 7. Iso-surfaces generated from kriging bromide concentrations, in C/C_0, for the horizontal conservative tracer test (150 and 180 minutes).

Data was also collected from the horizontal effluent port at 5-minute intervals. In turn, this represents the most complete dataset to observe the tracer breakthrough. A graph of C/C_O versus time (Figure 8) suggests some instability in the readings from the bromide

electrode. However, since the data was primarily used to look at the slope of the breakthrough curve and the center of mass arrival time, a little instability in the readings was acceptable. The maximum normalized concentration reached at the effluent was 0.78, thus indicating that full breakthrough had not been achieved by the end of the experiment. The center of mass, or 50% breakthrough, arrived at approximately 154 minutes. The data obtained from this experiment was used to calibrate the numerical groundwater flow model. This will be discussed in detail in the numerical modeling section of this thesis.

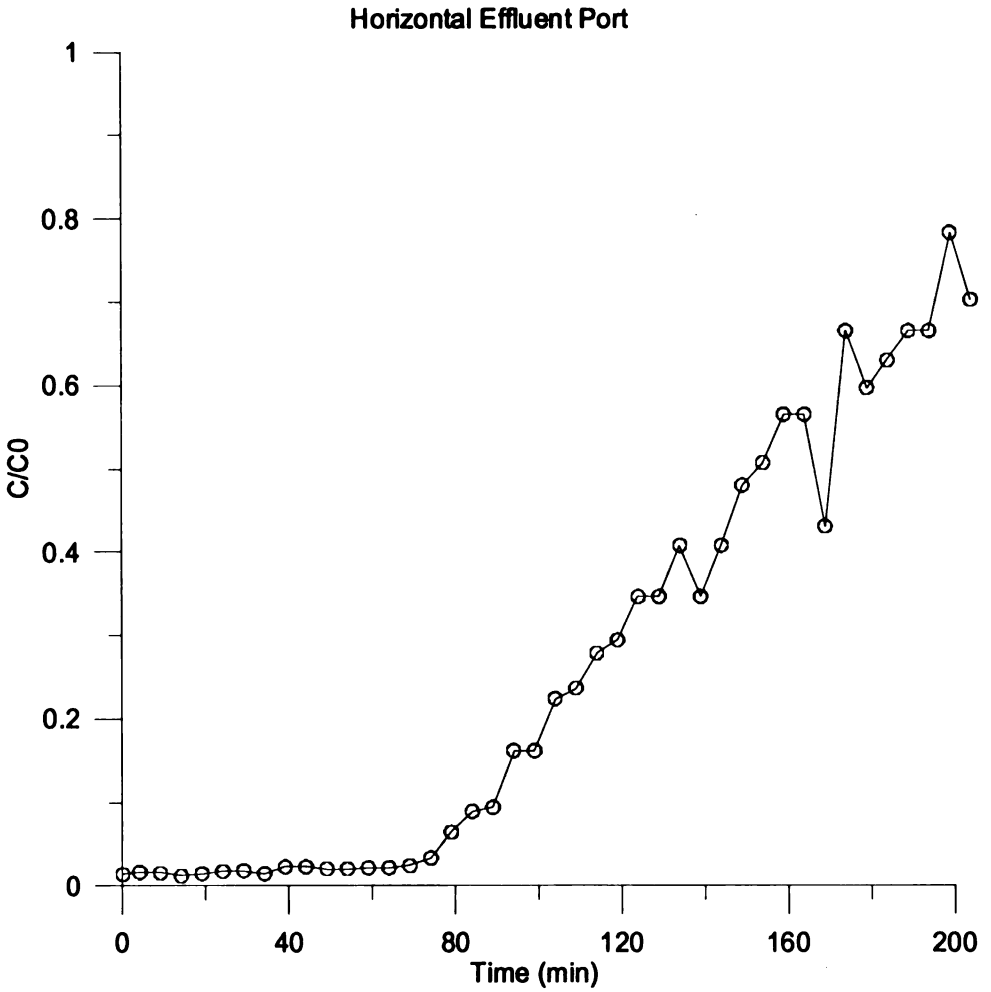

Figure 8. Effluent bromide concentrations, in C/C_0, for the horizontal conservative tracer test.

4.1.1 Vertical Bromide Tracer Test and Carbon Tetrachloride Sorption Study

The data from the vertical bromide tracer test and carbon tetrachloride sorption study are included in Appendix B. Since these two experiments were run simultaneously, the data needed to be normalized, so that direct comparisons could be made. Once again, if C/C_0 was greater than 1.0, it was set to 1.0 and indicated in the appendix. This fluctuation in influent concentrations resulted in more than half of the sampling ports exhibiting

concentrations above 1.0 after full breakthrough occurred. The maximum normalized concentration observed during this test was 1.16.

4.1.1.1 Vertical Bromide Tracer Test

In order to effectively characterize the bromide breakthrough, the data was broken into three distinct data sets, illustrating the 3-dimensional movement of the tracer, the 2-dimensional breakthrough of the tracer as it passed through the plane represented by row 9, and the 1-dimensional breakthrough of the combined vertical effluent ports. Sufficient 3-dimensional data was collected at 16 and 24 hours to observe the bromide front as it traveled up through the model aquifer. Once again, geostatistical techniques were utilized inside GMS 4.0 to aid in the visualization of these two data sets. Figure 9 shows the 3-D data sets in the context of the model aquifer and the shaded iso-surfaces that were generated from interpolating the data using inverse distance weighting with a quadratic nodal function. As was noted earlier, these interpolations should be used for visualization purposes only. In general, the iso-surfaces illustrate a roughly radial tracer front moving up from the influent ports at the bottom of the tank. However, several locations within the model aquifer indicated less than expected bromide concentrations. This is further elucidated in the series of 2-D plots of collected data.

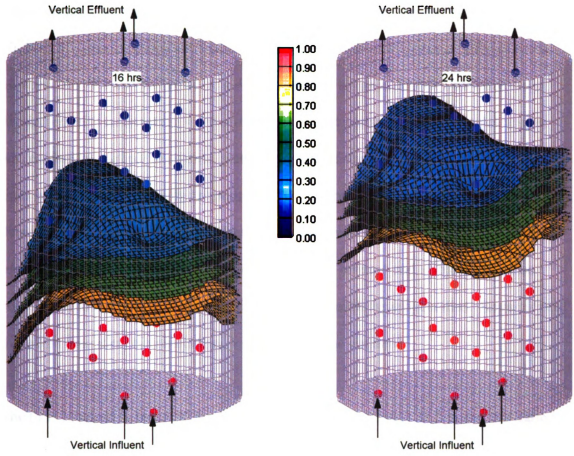

Figure 9. Distribution of bromide concentrations in C/C_0 and corresponding iso-surfaces generated from interpolation using inverse distance weighting, for the vertical conservative tracer test (16 and 24 hours).

In order to observe the breakthrough as the bromide approached the vertical effluent ports of the model aquifer, samples were collected and analyzed from all of the row 9 sampling ports at the following times, 30, 31, 32, 33, 34, 35, and 36 hours. This data was brought into GMS 4.0 and interpolated in two-dimensional cross sections using kriging (Figure 10). The data and subsequent interpolations, illustrate a non-uniform breakthrough as the bromide passes row 9. The portion of the model aquifer near sampling port 923 displays the fastest breakthrough. Sampling port 922, which represents the centerline of the

column as it passes through row 9, displays the second fastest breakthrough. The slowest breakthrough was observed near sampling ports 913 and 921. As can be seen in Figure 10, both of these locations are located near the same x, y coordinates as influent ports, however are 76.2 cm higher in the z dimension. It was assumed that flow rates were divided equally amongst the 4 influent and 4 effluent ports and that the model aquifer was uniformly packed. However, partial plugging of some of the influent and effluent lines was observed during this experiment. Direct comparison with the CT breakthrough data indicated that this plugging effectwas partially responsible for the non-uniform breakthrough. However, the rotated positions of the influent and effluent ports also contributed to the non-uniform flow field, as did possible heterogeneities. Regardless of these less than ideal circumstances, valuable data was obtained.

The time required to reach 50% breakthrough in row 9 averaged 32.3 hours, but varied between 30.2 and 35.1 hours. These arrival times were calculated through linear interpolations between time series observations. Using this average for the center of mass arrival time and the height of row 9 (76.2 cm), an average linear groundwater velocity of 2.36 cm/hr was determined (Vidal-Gavilan, 2000).

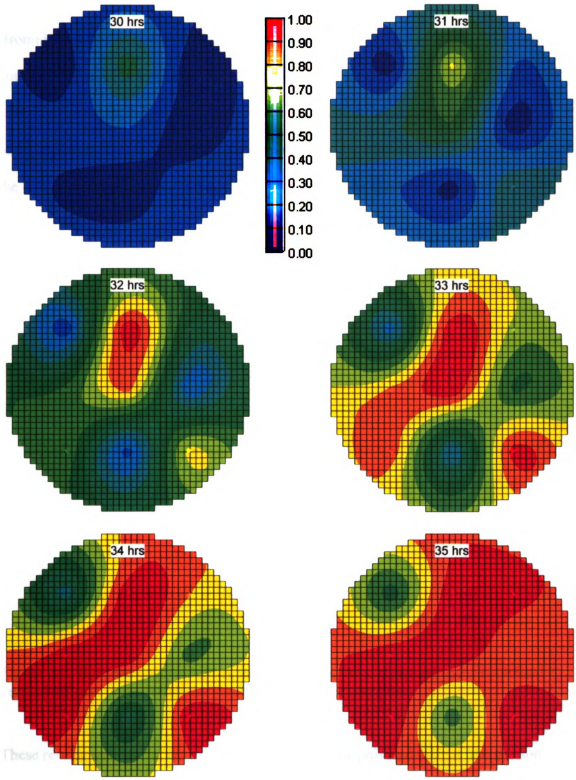

Figure 10. Distribution of bromide concentrations, in C/C_0, in row 9 sampling ports and shaded contours generated through kriging for the vertical conservative tracer test (30, 31, 32, 33, 34, and 35 hours).

Bromide samples were also analyzed from the combined vertical effluent of the model aquifer. Figure 11 is a graph of the breakthrough curve. It is apparent that the sample collection schedule did not fully characterize the bromide breakthrough. Fortunately, adequate samples were collected to determine the center of mass arrival time at the top of the column (approximately 39 hours) and the slope of the breakthrough curve.

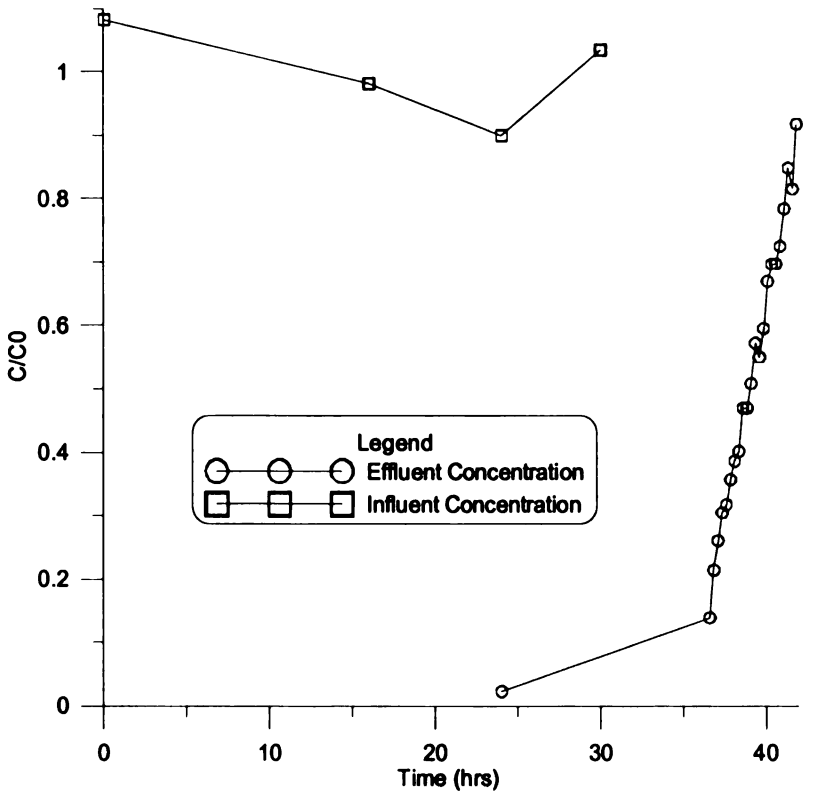

Figure 11. Bromide concentrations, in C/C_0, versus time, measured at the combined vertical effluent ports during the vertical conservative tracer test.

These results were useful for many reasons. First, they provided insight into the non-uniform nature of the vertical groundwater flow in the model aquifer. Secondly, they were used to estimate the retardation coefficient of carbon tetrachloride, as will be

discussed in the next section. Lastly, the data sets obtained from this experiment were again used in the calibration of the numerical groundwater flow model.

4.1.1.2 Carbon Tetrachloride Sorption Study

The results of the carbon tetrachloride sorption study were useful to visualize the movement of contaminant in the model aquifer and to determine the retardation factor. As noted earlier, the CT influent concentrations varied between 36.7 and 64.5 ppb, averaging 49.4 ppb (refer to Figure 12a for a graph of the normalized influent concentrations). The 50% breakthrough of CT in row 9 occurred at approximately 79.6 hours, arriving as early as 60.5 hours at port 923 and as late as 120.9 hours at port 921. These arrival times were calculated in the same manner as the vertical bromide arrival times. Furthermore, utilizing the same technique as was done to determine the average linear groundwater velocity; one arrives at an average CT velocity of 0.96 cm/hr. Refer to Appendix C for the data.

Retardation is often determined by dividing the velocity of a retarded chemical species by the average linear velocity (Fetter, 1988). Since both the average linear velocity and the CT velocity were determined at the same height in the model aquifer, and knowing that velocity equals distance divided by time, the retardation equation was re-written in terms of arrival times. Utilizing the Solver feature inside of Microsoft Excel, the optimal retardation value was calculated. This was accomplished by dividing the 50% CT arrival time data by the retardation value and minimizing the root mean squared residual

between the Br and adjusted CT data sets by solving for the optimal retardation value. This approach yielded a retardation value of 2.61. This is consistent with CT isotherm studies performed on Schoolcraft soil, which yielded a retardation factor of 2.64 (Zhao et al., 1999). This study also indicated that there was a kinetic component or multi-rate behavior to the sorption.

Figure 12. Bromide and carbon tetrachloride breakthrough curves.

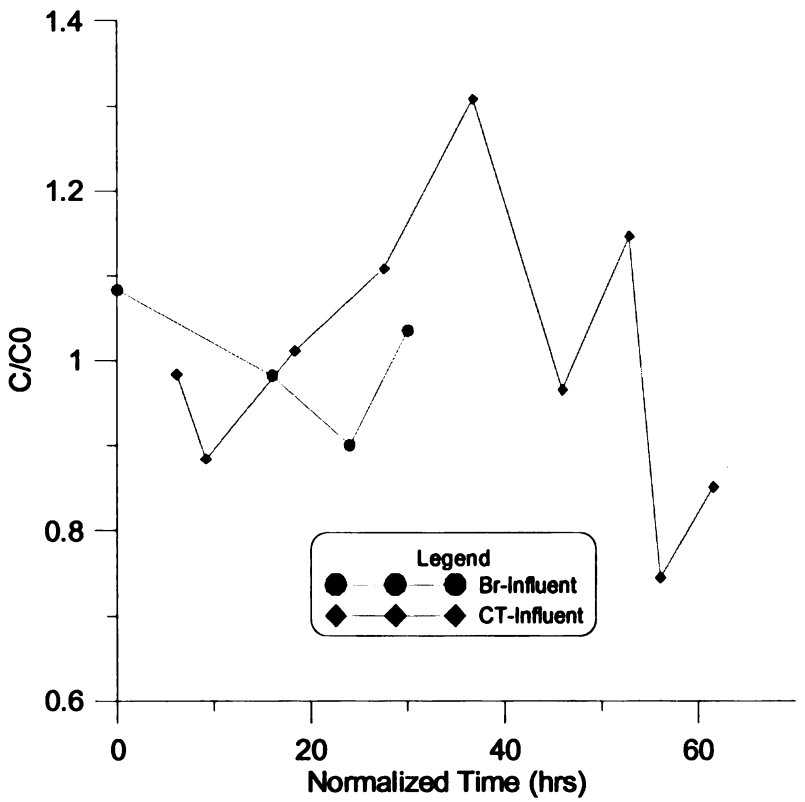

Figure 12a. Influent concentrations versus time for Br and CT.

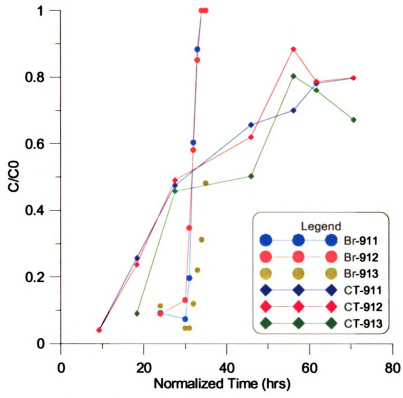

Figure 12b. Br and CT breakthrough curves at row 9, column 1, all three depths.

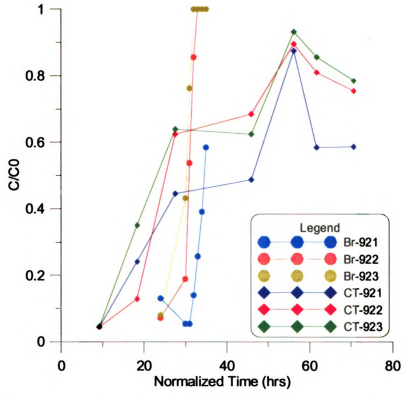

Figure 12c. Br and CT breakthrough curves at row 9, column 2, all three depths.

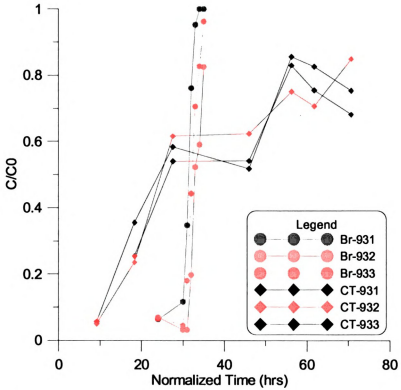

Figure 12d. Br and CT breakthrough curves at row 9, column 3, all three depths.

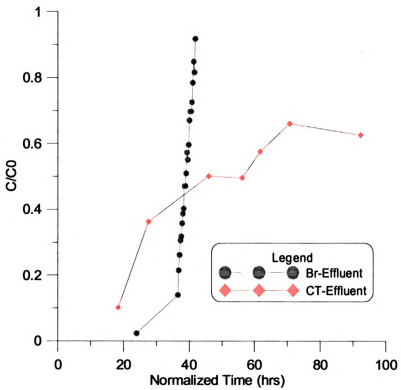

Figure 12e. Br and CT breakthrough curves at the combined effluent port.

CT concentrations were plotted versus time, along with the corresponding Br concentrations, to create a series of breakthrough curves at the influent port, all row 9 sampling ports and the combined vertical effluent port (Figure 12). This data was originally presented in Vidal-Gavilan (2000). In order to visualize the breakthrough of CT and Br on the same plot, the CT time was divided by the retardation factor. Notice that the 50% breakthroughs of the row 9 sampling ports and the effluent port are roughly the same, however the slopes of the curves are different due to the non-equilibrium or multi-rate nature of the sorption. This experiment was simulated using a two-site numerical sorption model as described in section 5.6.

4.1.2 Soil Titration

Data was obtained by X. Zhao at the horizontal effluent port and recorded at 5-minute intervals. Figure 13 is a plot of pH versus time. The starting pH of the model aquifer was roughly 7.4. The pH of the influent water was 8.2 and at the end of the 14.5-hour titration, the effluent pH was 8.0. Thus full titration of the model aquifer was not quite achieved, illustrating the high buffering capacity of the soils. However, KC flourishes when the pH is between 7.8 and 8.3.

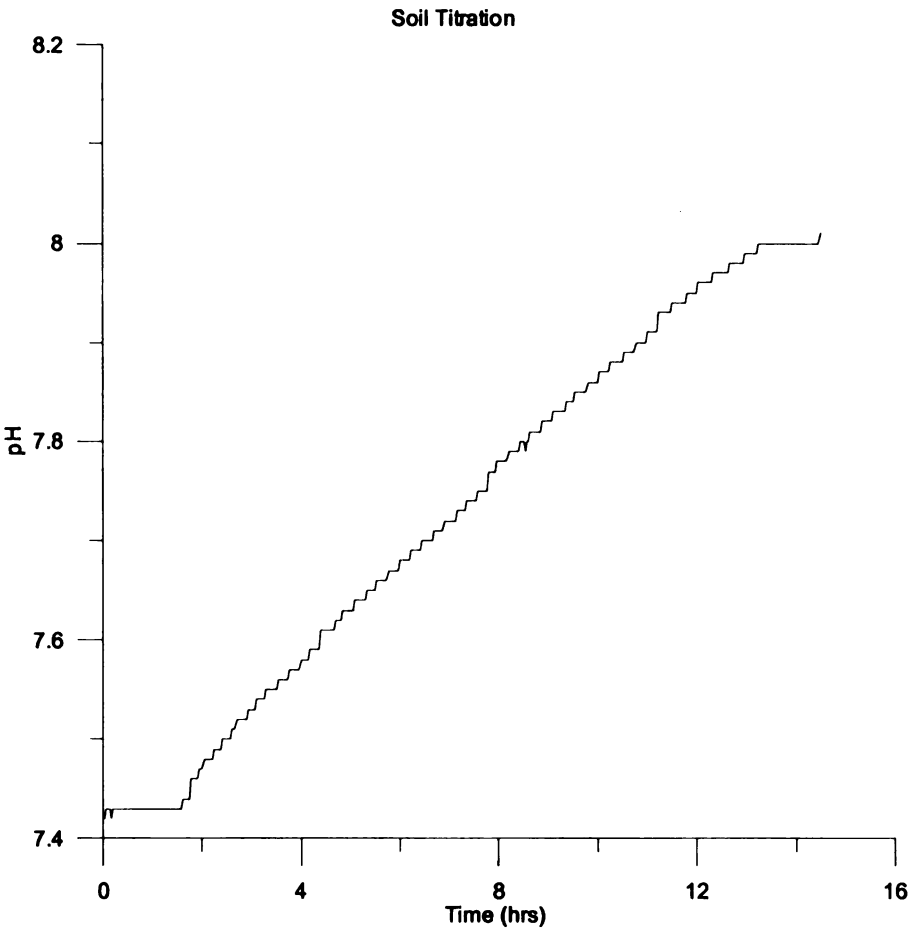

Figure 13. pH versus time measured from the horizontal effluent port during the soil titration.

4.1.3 Inoculation

The results of the combined inoculation and bromide tracer test are listed in Appendix D. Time series data sets of the liquid phase biomass and bromide were collected at sampling ports 312, 322, 332, and the horizontal effluent. Once again, the data sets were normalized so that direct comparisons could be made. The C_0 for bromide was measured once during this experiment and assumed to be equal to 63.8 ppm throughout the duration of the test. The influent liquid phase biomass was measured several times over the course of the experiment and averaged 8.8×10^7 cfu/ml. Once again, values of C/C_0 were

occasionally greater than 1.0. When this occurred they were set to 1.0 and indicated with an asterisks in the appendix.

Figure 14 shows the breakthrough of the liquid phase biomass and tracer. Over the course of the 3-hour experiment, full breakthrough of the bromide and liquid phase biomass was achieved at sampling ports 312, 322, and 332. Concentrations decreased after full breakthrough occurred, due to fluctuations in the influent concentrations. Because the flow rate for this test matched the first horizontal tracer test, full breakthrough was not anticipated at the horizontal effluent for either bromide or liquid phase biomass. As expected, all of the sampling ports show a lag between the bromide arrival time and the liquid phase biomass. This could be due to a portion of the liquid phase biomass attaching to the aquifer media or a retardation of the mobile phase KC. This differential breakthrough is further illustrated in the data sets that were collected at the end of the inoculation event. Samples were collected from rows 1 – 5 and analyzed for bromide and liquid phase biomass. The data was brought into the 3-D finite difference grid and interpolated using kriging. Once again, iso-surfaces were generated for visualization purposes (Figure 15).

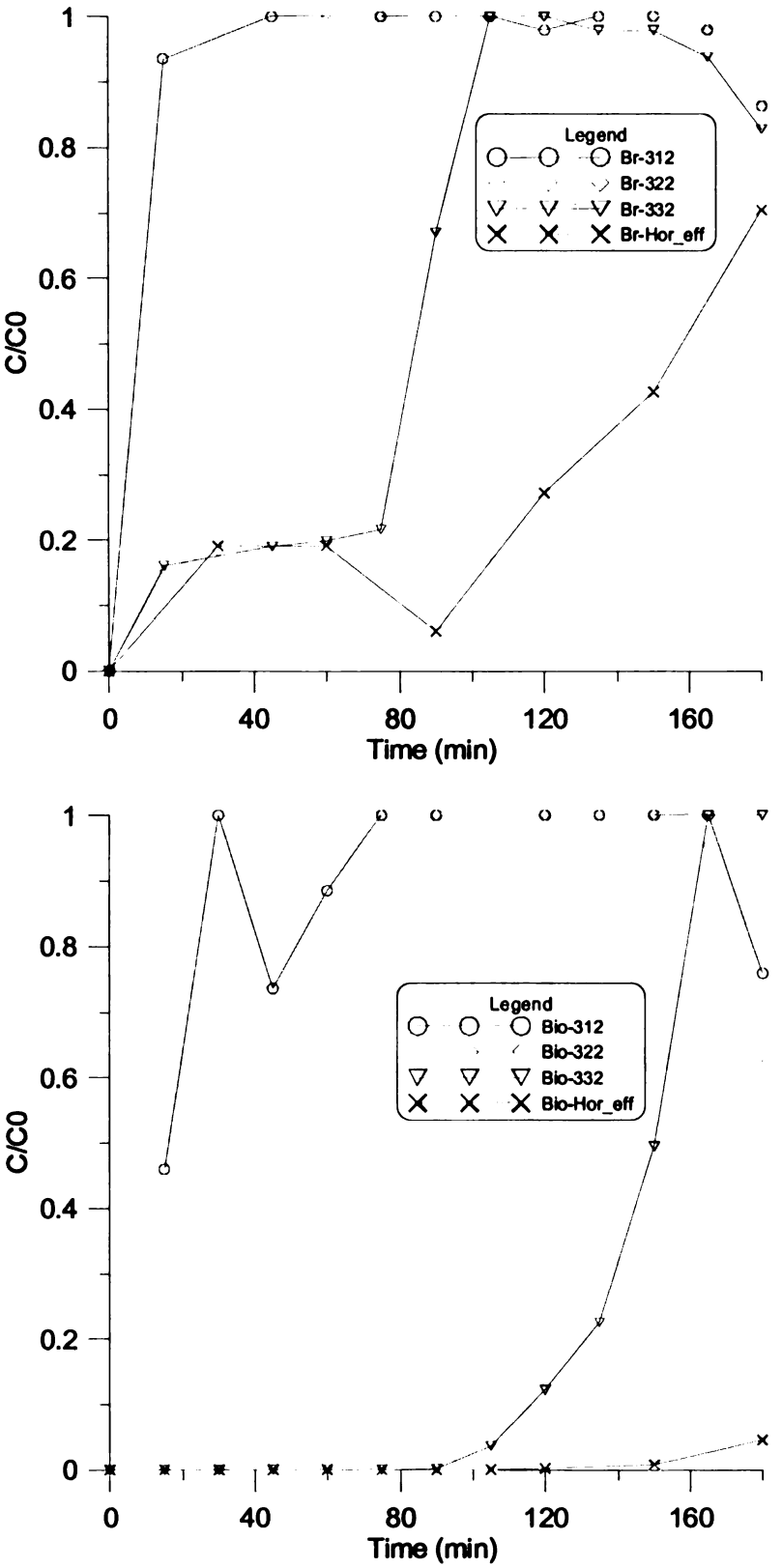

Figure 14. Bromide (top) and liquid phase biomass (bottom) breakthrough curves during the inoculation event (modified from Vidal-Gavilan, 2000).

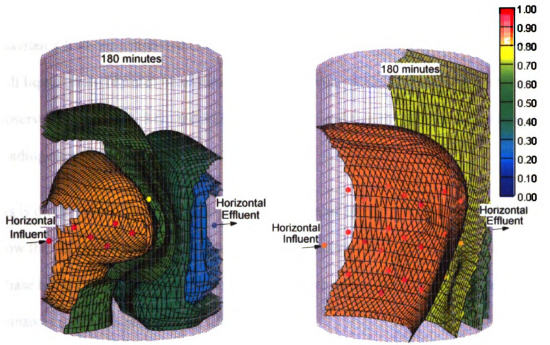

Figure 15. Iso-surfaces generated from kriging bromide (left) and liquid phase biomass (right) concentrations, in C/C_0, at the end of the inoculation event (180 minutes) (Modified from Vidal-Gavilan, 2000).

As can be seen, both the tracer and biomass show parabolic breakthroughs emanating from the horizontal effluent port. These figures also clearly display the lag time between the tracer and liquid phase biomass. More importantly, the spatial distribution of the liquid phase biomass is visualized. A concentration gradient was established with higher concentrations of liquid phase biomass near the influent port and very low concentrations at the horizontal effluent port.

The immobile phase biomass was not measured during this experiment. However, when using this dataset, Vidal-Gavilan (2000) applied the clean-bed filtration theory to estimate the amount of solid phase biomass remaining in the model aquifer. The parameters used in the filtration theory were previously determined from a 1-D column study investigating

the soil loading capacity of KC in Schoolcraft soil (Radabaugh, 1998). In general, Vidal-Gavilan's findings stated that once KC reached a concentration of $3x10^7$ cfu/g in the soil, full liquid phase biomass breakthrough was observed. Since 100% breakthrough was observed at ports 312, 322, and 332, it can be assumed that the soils have reached their loading capacity.

As is discussed in the next section, the distribution of biomass is key to understanding how the CT was degraded during the biocurtain experiment. Furthermore, the mobile phase biomass data was useful to test the predictive capability of a user-defined reactive transport model, as presented in Chapter 6.

4.1.4 Biocurtain Experimental Results

Although the simulated biocurtain was monitored through the analyses of dissolved carbon tetrachloride, acetate and nitrate, liquid phase biomass, and pH, only limited dissolved phase CT data was available for use in this thesis. This sparse dataset made it difficult to analyze the bioremediation experiment. Dissolved phase CT data was obtained from the vertical combined effluent ports at 1.5 hours, 2.2 days, 3.2 days, 5 days, and 12 days, the odd numbered internal sampling ports at 1.5 hours, 5 days, and 12 days, and the horizontal effluent port during the feeding event (Appendix E).

Resulting from the limited data and experimental oversights, the results are difficult to interpret. The results suggest that the simulated biocurtain was actively degrading carbon tetrachloride. Based entirely on the concentrations of CT in rows 7 and 9 and the

combined vertical effluent, it appears as if the laboratory biocurtain was actively degrading CT, for those sampling ports all show a decrease in concentration over time. A graph illustrating this decrease has been prepared for row 7 (Figure 16). Recalling the distribution of liquid phase biomass at the end of the inoculation, it was expected that maximum CT removal would occur closer to the horizontal influent and decrease near the horizontal effluent. This may be evident in the data obtained from the row 7 ports.

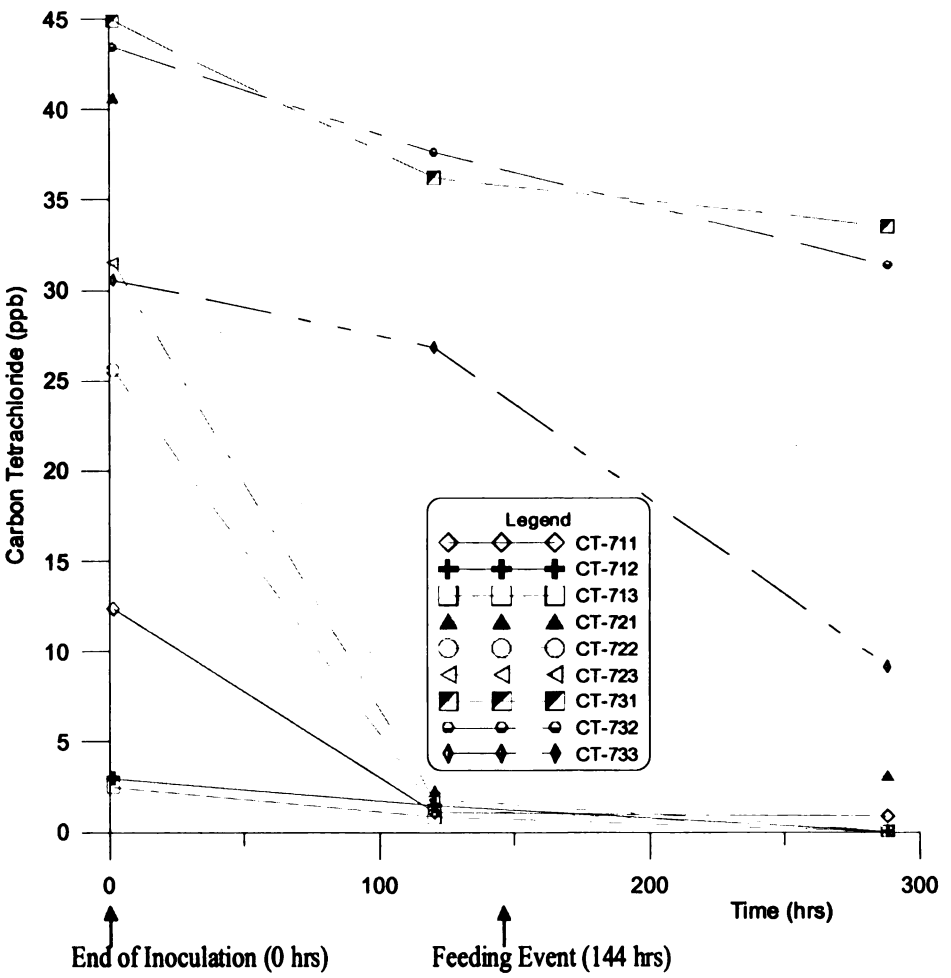

Figure 16. Carbon tetrachloride concentrations in row 7 sampling ports during the biocurtain experiment.

Rows 1 – 5 exhibit mixed results, with many of the sampling ports indicating increases in CT concentrations over time. This could be a result of the initial distribution of CT in the model. Since the CT included in the inoculum was degraded within an hour of the onset of the inoculation event, initial concentrations of CT between the horizontal influent and effluent ports were low. Once again, 3-D interpolations were generated using kriging inside of GMS 4.0 to illustrate the CT distributions after 1.5 hours and 12 days (Figure 17). Figure 17a, illustrates the CT distribution 1.5 hours after the end of the inoculation event and the beginning of the CT spiked natural gradient flow. As can be seen in Figure 17a, the CT distribution looks like the inverse of the biomass distribution at the end of the inoculation (Figure 15b) with the lowest CT concentration near the horizontal influent port. Figure 17b illustrates the distribution of the CT after the biocurtain has been operating for 12 days. As can be seen in this figure, concentrations are elevated near the vertical influent ports and towards the horizontal effluent port. Concentrations are less in row 7, primarily on the side proximal to the horizontal influent port. This suggests that either the biocurtain was most active near row 5 and that the bioactive zone migrated from the delivery zone due to the natural gradient flow vertically transporting the microbes or that the low CT concentrations in that portion of the column were a result of the low concentration CT zone that developed during the inoculation event migrating vertically. Based entirely on advective flow, the low concentration CT zone emanating from the horizontal influent port should have migrated to the top of the tank within 3 days. Therefore, the data suggests that the majority of the CT decrease over time was the result of biodegradation.

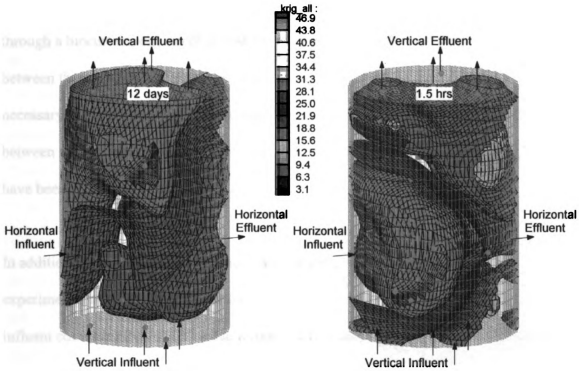

Figure 17. Carbon tetrachloride concentrations (ppb) 1.5 hours and 12 days into the biocurtain experiment.

Based on analytical results from row 7, the average decrease in concentration as contaminant moved through the biocurtain was 31% at 1.5 hours, 68% at 5 days, and 77% at 12 days. However, using the median of the analytical results from row 7, the decrease in CT concentrations is 19% at 1.5 hours, 95% at 5 days, and 98% at 12 days. The median values are more representative when determining the remediation percentages, for they are not influenced by outliers or in the case the ports proximal to the horizontal effluent where it was already shown that the biomass concentrations were much lower. These results compare favorably to what was observed in the field (Dybas et al., 2002).

Moreover, the results indicate that in order to uniformly treat a contaminant as it moves through a biocurtain, one needs to make certain that the biomass is evenly distributed between the injection and extraction wells comprising the biocurtain. It is therefore necessary to ensure that full breakthrough of the liquid phase biomass has occurred between the injection and extraction wells and that heterogeneities in the aquifer material have been accounted for.

In addition to the sparse dataset, many unforeseen problems occurred during the experiment that compromised portions of the data. In particular, the highly variable influent concentrations of CT added a complexity to the experiment, as did the lack of pH control. pH dropped significantly over the course of the experiment; according to Gavillan (2000), one week after the feeding event, the pH decreased to roughly 7 in the biocurtain, at which point a second titration of the model aquifer occurred. This titration lasted 72 hours and required 1,214 liters of re-circulated pH adjusted groundwater to bring the pH up to 8.2 at the horizontal effluent. Based on these problems, the research team decided to end the experiment early. Fortunately sufficient data was collected to utilize the results in a series of numerical reactive transport models aimed at simulating portions of the laboratory biocurtain experiment.

5 NUMERICAL MODELING RESULTS

Groundwater Modeling System (GMS) 4.0 and 5.0, the numerical modeling software used in this project, includes modules for geostatistics, site characterization, groundwater flow modeling, reactive transport modeling, calibration, and visualization. GMS possesses common numerical modeling programs, of which MODFLOW 2000 (Harbaugh et al., 2000) was selected for the finite-difference flow model and RT3Dv2.5 (Clement, 1997) was chosen for the finite-difference reactive transport modeling. Inside MODFLOW 2000, layer property flow (LPF) was selected as the flow package with the preconditioned conjugant gradient (PCG2) solver. The following packages were utilized in RT3D: the advection package with hybrid method of characteristics (HMOC), dispersion, source sink mixing, the generalized conjugate gradient solver (GCG, to implicitly solve the dispersion and source/sink portions of the reactive transport equation), and the user-defined reaction module. The user-defined reaction module allows users a great deal of flexibility to describe site specific reactions, including in-situ chemical oxidation and bioremediation. Given the broad application of this model, researchers at Michigan State University utilized RT3D to create a numerical model that accounts for the CT bioaugmentation associated with the Schoolcraft project.

5.1 MICROBIAL TRANSPORT AND CARBON TETRACHLORIDE DEGRADATION MODEL BACKGROUND

The extensive research associated with the Schoolcraft Plume A resulted in increased understanding on biodegradation processes and rates. This understanding of the processes

allowed for the creation of a three dimensional microbial transport and biodegradation model. This model is unique to the co-metabolic degradation of CT by strain KC that occurs under denitrifying conditions with nitrate as the electron acceptor and acetate as the electron donor. The model is comprised of seven, partial differential, coupled mass balance equations that account for the primary reactions involved in the transport, sorption, and biotransformation of CT. Specifically, the modeled processes include the transport of CT, nitrate, acetate, bromide, and mobile phase strain KC with considerations to advection, dispersion, sorption, and chemical reaction, as well as, microbial growth, decay, attachment and detachment (Phanikumar et al., 2002a, Phanikumar et al., 2002b, Phanikumar and Hyndman, 2003, Phanikumar et al., 2005).

This model was first applied to one-dimensional column studies conducted at Michigan State University, which investigated microbial transport and CT degradation in two intermittently fed aquifer columns (Phanikumar et al., 2002a). Utilizing starting parameters gleaned from literature and independent experiments, the authors conducted a series of parameter optimizations whose resulting solution provided reasonable fits to CT, nitrate, acetate, and early time mobile KC data. The modeling results indicated that the CT degradation rate for a small lab column was an order of magnitude less than what was estimated from a batch study. Furthermore, the modeling suggested that another source of nitrate consumption was present through the existence of indigenous flora in the 1-D columns.

The model was then applied to data obtained from the one-dimensional column study to explore the interaction of sorption and bioavailability with pulsed nutrient injections (Phanikumar and Hyndman 2003). The results indicated the strong influence of bioavailability on degradation and the necessity to include degradation terms for sorbed phase mass, without which retardation is an insensitive parameter. Moreover, the authors demonstrate that using a pulsed nutrient injection strategy is much more efficient than continual pumping. These observations have wide application to the field of reactive transport modeling and remedial system design.

Most recently, Phanikumar et al. (2005) utilized the reactive transport model to predict solute concentrations across the Schoolcraft site prior to and during the biocurtain operation using the optimized parameters obtained from the one-dimensional column study (Phanikumar et al., 2002a). The results fit the observed acetate and nitrate concentrations well; however they over predict the amount of CT degradation using the lab optimized parameters. In order to better predict the CT concentrations, the authors decreased the CT degradation rate by half and suggested that the difference in laboratory rates and field rates may be due to limitations in electron acceptor availability. The study also provided insight into the dynamics of the field biocurtain and the influence of heterogeneities and pumping on microbial transport and solute concentrations.

5.1.1 Multi-Component Reactive Transport Model

As described above, the multi-component reactive transport model is comprised of seven mass balance equations accounting for the primary reactions involved in the transport,

sorption, and biotransformation of CT. Equations (1) through (6) are coupled to account for the dependency of the substrate utilization, growth and decay of strain KC, and bioavailability. Equation (1) relates the transport and degradation of aqueous phase CT with sorption. Equation (2) accounts for the growth, decay, and attachment of mobile strain KC cells and the detachment of immobile strain KC cells, while Equation (3) describes the coupled processes for the immobile phase strain KC cells. Equation (4) describes the utilization of the electron donor (acetate) and equation (5) describes the utilization of the electron acceptor (nitrate). Equation (6) accounts for the concentration of sorbed CT, based on a two-site sorption model. Equation (7) describes the transport of the non-reactive tracer (bromide) (Phanikumar et al., 2005).

(1) Carbon tetrachloride concentration

$$R\frac{\partial C_{CT}}{\partial t}=\frac{\partial}{\partial x_i}\left(D_{ij}\frac{\partial C_{CT}}{\partial x_j}\right)-\frac{\partial}{\partial x_i}(v_i C_{CT})-kX_m C_{CT}-\frac{\rho k}{\theta}[(1-f)K_d C_{CT}-S_{CT}]+Q^S C_{CT}{}^S$$

(2) Mobile-phase strain KC concentration

$$\frac{\partial X_m}{\partial t}=\frac{\partial}{\partial x_i}\left(D_{ij}\frac{\partial X_m}{\partial x_j}\right)-\frac{\partial}{\partial x_i}(v_i X_m)+\left[\mu_{\max}\frac{C_a}{C_a+K_{sa}}\frac{C_n}{C_n+K_{sn}}-b_{KC}\left(1-\frac{C_a}{C_a+K_{sa}}\right)-K_{at}\right]X_m$$
$$+K_{de}\left(1-\frac{C_a}{C_a+K_{sa}}\right)X_{im}+Q^S X_m{}^S$$

(3) Immobile-phase strain KC concentration

$$\frac{\partial X_{im}}{\partial t}=\left[\mu_{\max}\frac{C_a}{C_a+K_{sa}}\frac{C_n}{C_n+K_{sn}}-b_{KC}\left(1-\frac{C_a}{C_a+K_{sa}}\right)-K_{de}\left(1-\frac{C_a}{C_a+K_{sa}}\right)\right]X_{im}+K_{at}X_m+Q^S X_{im}{}^S$$

(4) Acetate concentration

$$\frac{\partial C_a}{\partial t} = \frac{\partial}{\partial x_i}\left(D_{ij}\frac{\partial C_a}{\partial x_j}\right) - \frac{\partial}{\partial x_i}(v_i C_a) - \frac{\mu_{\max}}{Y_a}\frac{C_a}{C_a + K_{sa}}\frac{C_n}{C_n + K_{sn}}(X_m + X_{im}) + Q^S C_a{}^S$$

(5) Nitrate concentration

$$\frac{\partial C_n}{\partial t} = \frac{\partial}{\partial x_i}\left(D_{ij}\frac{\partial C_n}{\partial x_j}\right) - \frac{\partial}{\partial x_i}(v_i C_n) - \frac{\mu_{\max}}{Y_n}\frac{C_a}{C_a + K_{sa}}\frac{C_n}{C_n + K_{sn}}(X_m + X_{im})$$
$$-\left[\frac{b_{KC}}{Y_{nb}}\left(1 - \frac{C_a}{C_a + K_{sa}}\right) + \gamma\frac{C_n}{C_n + K_{sn}}\right](X_m + X_{im}) + Q^S C_a{}^S$$

(6) Sorbed phase CT concentration

$$\frac{\partial S_{CT}}{\partial t} = k[(1-f)K_d C_{CT} - S_{CT}] - kX_{im}S_{CT}$$

(7) Bromide tracer concentration

$$\frac{\partial C_{Br}}{\partial t} = \frac{\partial}{\partial x_i}\left(D_{ij}\frac{\partial C_{Br}}{\partial x_j}\right) - \frac{\partial}{\partial x_i}(v_i C_{Br}) + Q^S C_{Br}{}^S$$

Refer to the Table 1 for a complete description of the above symbols. The variables on the left hand of the equations are the concentrations of all of the species being modeled. C_{CT}, X_m, X_{im}, C_n, C_a, S_{CT}, and C_{Br} are the dissolved concentrations of carbon tetrachloride, mobile phase strain KC, immobile phase strain KC, acetate, nitrate, sorbed CT, and dissolved bromide, respectively. The term R in equation (1) is the retardation factor which is determined through $R = 1 + (\rho f K_D/\theta)$, where K_D is equal to the partition coefficient. This equation has been modified from the original retardation equation, as presented in Freeze and Cherry (1979) to include the fraction of equilibrium sites (f), as described in Zhao et al (1999), which limits the amount of equilibrium sorption that occurs (Phanikumar et al., 2005).

The first group of terms in the equations for CT, mobile phase KC, acetate, nitrate and bromide account for the transport of solute based on dispersion, where the dispersion coefficient (D) is equal to α^*U and U is equal to the average linear velocity and α is the longitudinal and transverse dispersivities. The second group of terms in the CT, mobile phase KC, acetate, nitrate and bromide equations account for the transport of solute based on advection. When used alone, these two groups of terms account for the basic advection-dispersion equation as described in Freeze and Cherry (1979). The third group of terms in equation (1) accounts for the degradation of dissolved CT by means of the mobile phase KC and a second order reaction rate. The fourth group of terms in equation (1) accounts for the degradation of dissolved CT on the equilibrium sorptive sites. The concentration of sorbed phase CT is controlled by the kinetic sorption, as described in equation (6). The fifth term in equation (1) is the CT source term resulting from recirculation. This term was necessary for the field application of the model, since the extracted groundwater contained solutes, which were re-injected into the subsurface (Phanikumar et al, 2005). This process did not occur in the laboratory column study; therefore, all of the source terms denoted with Q^S are zero.

The third group of terms in equation (2) accounts for the growth, decay and attachment of the mobile phase biomass. These terms are related through the acetate and nitrate (substrate) concentrations in the form of Monod terms. The fourth set of terms in equation (2) accounts for the detachment of immobile phase biomass. Equation (3)

functions similarly to equation (2), except that it describes the linked processes of the immobile phase strain KC.

The third group of terms in equations (4) accounts for the depletion of the electron donor (acetate) through the growth of mobile and immobile phase biomass. Again growth is dictated by Monod terms. A similar process is described in the nitrate utilization equation, equation (5), which describes the nitrate sink that results from the transfer of electrons from donor to acceptor and prompts microbial growth. The fourth group of terms in equation (5) accounts for nitrate that is consumed during processes such as microbial decay and utilization by indigenous flora or endogenous respiration. Readers are encouraged to refer to Phanikumar et al. (2002a, 2002b, 2003, and 2005) for additional information pertaining to the reactive transport model.

5.2 LABORATORY COLUMN STUDY NUMERICAL MODEL CONCEPTUALIZATION

The first step in the model development was to create the finite difference grid representing the laboratory model aquifer. The 3-D grid consisted of 25 layers, and 41 cells in the x and y dimensions. Cells were de-activated outside of the 61 cm diameter tank to create the cylindrical shape of the model aquifer. Once the 3-D grid was created, the fore mentioned interpolations were completed inside the geostatistics module.

The laboratory aquifer was modeled as a confined aquifer since the potentiometric surface was always greater than the top of the tank. The influent ports were modeled as

wells. Furthermore, since all of the effluent ports were connected to tubing that discharged to the same reservoir, they were modeled as constant head cells. Even though the laboratory column showed signs of heterogeneities, sufficient hydraulic head and permeability data was not available to account for this. Therefore, for the purposes of the numerical modeling, the laboratory column was assumed to be homogenous. The hydraulic conductivity was held constant at 0.027 cm/sec. The hydraulic conductivity of the Schoolcraft aquifer was characterized using constant head permeameter tests on hundreds of aquifer samples obtained from cores collected across the delivery zone (Zhao et al., 2005; Dybas et al., 2002; Hyndman et al., 2000).

5.3 CALIBRATION OF GROUNDWATER FLOW AND CONSERVATIVE TRACER TRANSPORT MODEL

Traditionally, the calibration process involves varying input parameters, such as hydraulic conductivity, and repeatedly running the model until the residual error between observed and computed hydraulic heads and fluxes are within an acceptable level of accuracy (Anderson and Woessner, 1992). In addition to minimizing residual error it is often necessary to examine the hydraulic gradient, groundwater flow direction, and water mass balance (Mandle, 2002). The calibrated parameters for the tracer test model were vertical anisotropy, porosity, and dispersivity. In this case, the calibration process entailed minimizing the residual error between simulated and observed conservative tracer test data collected at the effluent port. Hydraulic conductivity did not need to be calibrated. In accordance with Darcy's Law, since the fluxes were held constant during numerical simulations, changing the hydraulic conductivity would result in an equal

change in the gradient, thus creating no net change in the flux. In order to alter the rate of transport for the simulation, one needs to adjust the effective porosity. This is seen in the relationship describing the average linear velocity, where:

$$v = (K\partial h/\partial l)/\theta$$

Therefore, decreasing the porosity would effectively increase the simulated average linear velocity, which is what dictates the advective portion of solute transport.

Prior to calibrating the model, a working MODFLOW simulation was generated. Simulations were created that modeled the vertical and horizontal conservative tracer tests. The first calibration was performed on a model that simulated the horizontal conservative bromide tracer test. The average measured flow rate was used as a positive flux into the well representing the horizontal influent port. Starting heads were uniformly assigned as 115 cm across the grid. A steady state MODFLOW model was then run. Once the flow field had been solved, the RT3D simulation was set-up. A single stress period was created that matched the duration of the horizontal tracer test. All of the input parameters were assigned uniformly across the model domain. This included values for porosity, dispersivity, the ratio of transverse dispersivity to longitudinal dispersivity, the ratio of vertical dispersivity to longitudinal, and the effective molecular diffusion coefficient. Since temporal three-dimensional data was sparse for this particular experiment, residuals were determined at the horizontal effluent port. Parameters were varied over a range of values and successive model iterations were simulated and their corresponding residuals were recorded. The resulting calibration can be visualized in the graph of simulated versus observed concentrations at the horizontal effluent port (Figure 18).

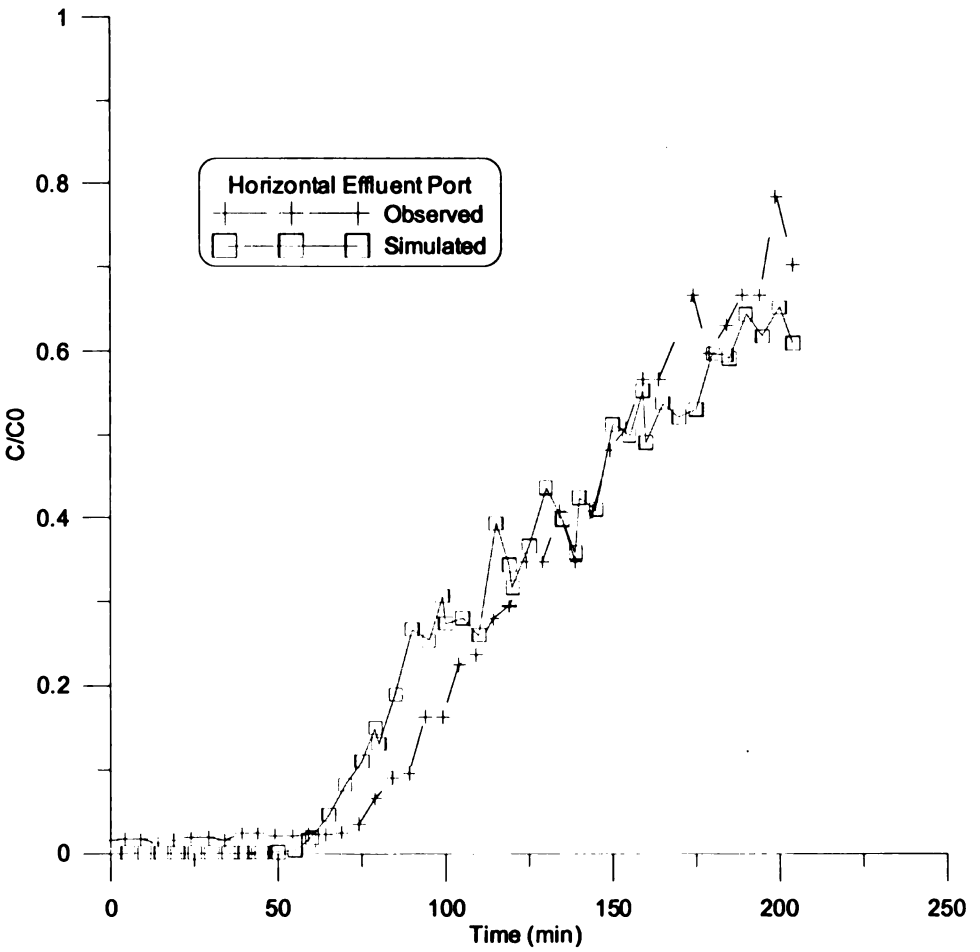

Figure 18. Simulated versus observed bromide tracer concentrations during the horizontal tracer test.

As can be seen in Figure 18, the slope of the simulated cross flow tracer test is similar to the slope of the observed data. The slope of the breakthrough curve is primarily controlled by dispersivity. A steeper slope would demand a lower dispersivity value or a reduction in the amount of numerical dispersion. Dispersivity was tested over a wide range of values (0.001-10 cm) during the calibration process. Decreasing the dispersivity below 0.1 cm did not improve the fit between simulated and observed much, as this value is likely in a range to numerical dispersion. This less than perfect fit could have been

attributable to one of a number of reasons, including heterogeneities in the model aquifer, varying influent concentrations and flow rates, and numerical dispersion. During the calibration process attempts were made to decrease the numerical dispersion by decreasing the Peclet number from 15 to 10, an acceptable value according to Huyakorn et al (1983). This was accomplished by increasing the number of grid cells, however little change was observed in the goodness of fit between simulated and observed. Moreover, increasing the grid cells drastically slowed down simulation times, which extends the times necessary to calibrate the model.

The vertical anisotropy was also varied during the calibration process and the results were visually noted. As mentioned earlier there was inadequate spatiotemporal data to compare the simulated and observed at most locations; however, data was available that allowed for the comparison of the bromide distribution at the end of the tracer test. It was noted that if vertical anisotropy was ignored (Kh/Kv=1), a slightly better visual fit existed between simulated and observed data in rows 8 and 9; however, the goodness of fit between the simulated and observed horizontal effluent data decreased. Since the data obtained at the horizontal effluent represents the average concentration of solute leaving the model aquifer it was determined that maintaining the goodness of fit between the simulated and observed values at this location was more important. This was achieved when the vertical anisotropy was equal to (Kh/Kv=2).

Other factors that may have contributed to the less than ideal fit between the simulated and observed breakthrough curve include, the number of particles in the numerical

advection package, the type of numerical advection package used, the fluctuations in the influent concentrations and flow rates, and heterogeneities in the model aquifer. The number of particles in the numerical advection package was increased to try and decrease the amount of numerical dispersion; however, this did not improve the goodness of fit between simulated and observed, nor did using a different numerical advection package, such as method of characteristics (MOC). Attempts were made to simulate fluctuations in the influent concentrations and flow rates, however insufficient data was available to adequately describe these variations and the resulting simulations were not an improvement. Once a set of values had been estimated that created the minimum residual error, the parameters were used in a model mimicking the vertical conservative tracer test.

The vertical tracer test was set-up with 4 wells, representing the influent ports, which were assigned a quarter of the average observed flow rate. 4 constant head cells (115 cm) were established at the top of the model aquifer, representing the effluent ports. Once again, vertical anisotropy, porosity, and dispersivity were tested over a range of values and the residuals were recorded for each simulation. In this case, the residuals and breakthrough curves were calculated and compared to the average row 9 concentrations. The simulated breakthrough curves were also compared to the measurements for each of the row 9 sampling ports. The starting parameters that were solved for the horizontal tracer simulation resulted in reasonable fits between for the vertical tracer simulation; however, minor changes improved the match between simulated and observed values. Specifically, a slightly lower porosity was required.

Calibration was achieved once a set of parameters had been identified that created low residual error for both the horizontal and vertical simulations. In order to match the slope of the observed vertical breakthrough curves, both the dispersivity and the vertical anisotropy (K_h/K_v) were tested. It was discovered that increasing the vertical anisotropy resulted in a better goodness of fit between the simulated and observed values and that the slope of the observed values could not be achieved by altering the dispersivity alone, supporting what was determined during the horizontal bromide tracer calibration. While packing the physical model with sand, efforts were taken to homogenize the aquifer media, however, it is possible that settling occurred, creating layers of lower conductivity and heterogeneities in the model aquifer. The calibrated values for vertical anisotropy (K_h/K_v), porosity, and dispersivity are 2.0, 0.31, and 0.1 cm, respectively.

Graphs of simulated versus observed concentrations have been generated for the vertical tracer models (Figures 19-20). Figure 19 illustrates the simulated versus observed breakthrough curves for the average row 9 concentrations. The fit between these two data sets is very good. Figure 20 shows the plots of simulated versus observed values for all of the row 9 sampling ports. These fits are also reasonable, however the breakthrough of the simulated bromide appears to be consistently a little ahead of the observed breakthrough for ports 913, 921, and 933. These ports are proximal to the x, y coordinates of the influent ports, however 76 cm higher. In turn, the numerical simulation appears to be over predicting the hydraulic head in the vicinity of the influent ports. Attempts were made to develop a better fit in ports 913, 921, and 933, by increasing the amount of transverse dispersion and adjusting the relative flow through the

influent ports (i.e. weighting certain influent ports while maintaining a constant influent flow rate), however the model appeared to be fairly insensitive to adjustments in the influent flow rates and changing the transverse dispersivity resulted in worse fits for the other sampling ports.

The observed breakthrough curves for ports 911, 923, and 931 are all ahead of the simulated breakthrough curves. The observed data suggests that more flow went through this region of the model aquifer. This is visible in the series of 2-dimensional interpolations that were presented in Figure 10. Again, attempts were made to try and weigh the amount of flow entering through certain influent ports, however this did not provide a solution.

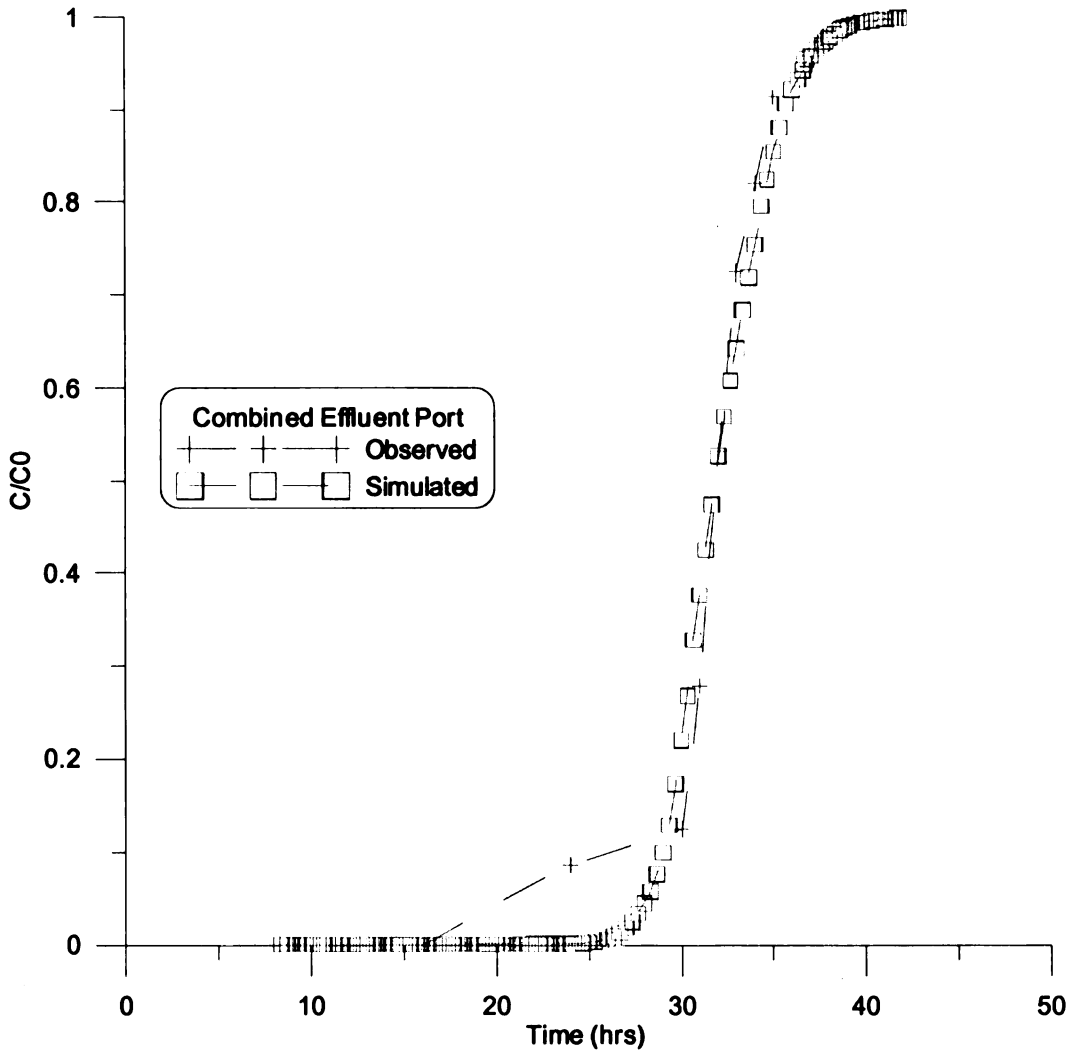

Figure 19. Simulated versus observed vertical bromide tracer test results for the combined vertical effluent port.

Figure 20. Simulated versus observed RT3D simulation of the vertical bromide tracer test at row 9 sampling ports

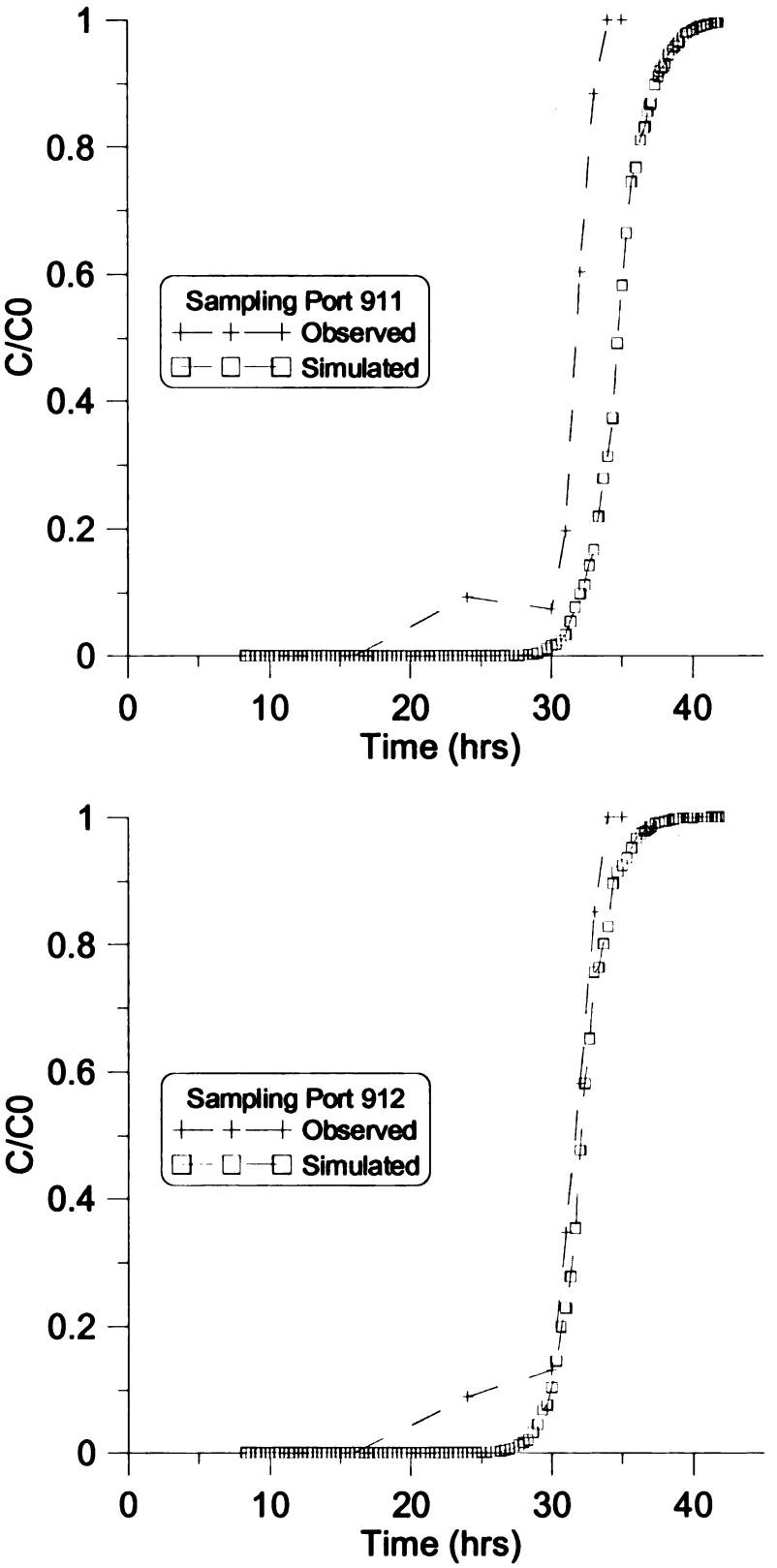

Figure 20 (continued)

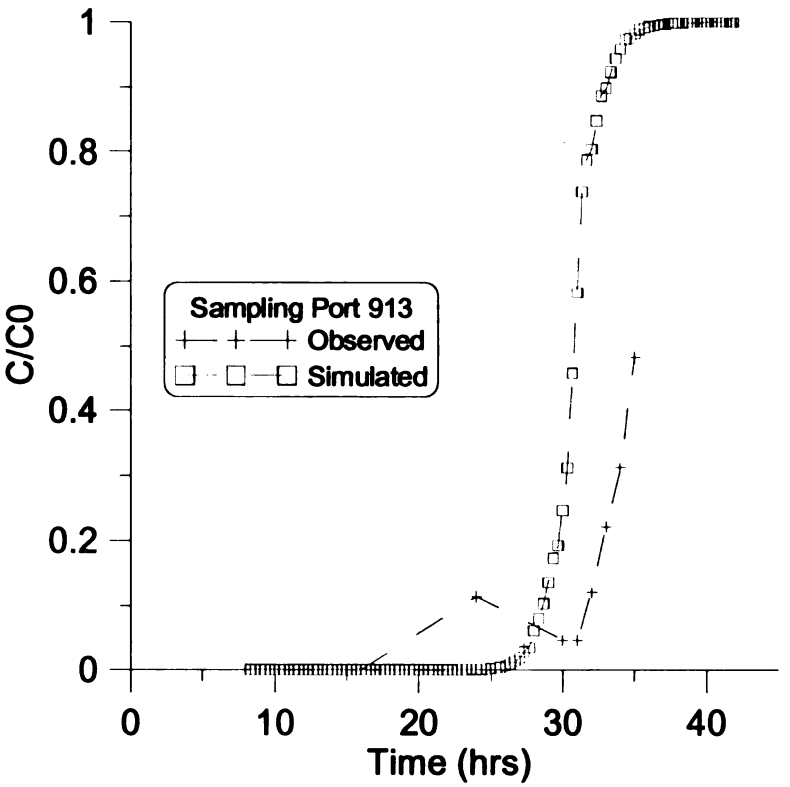

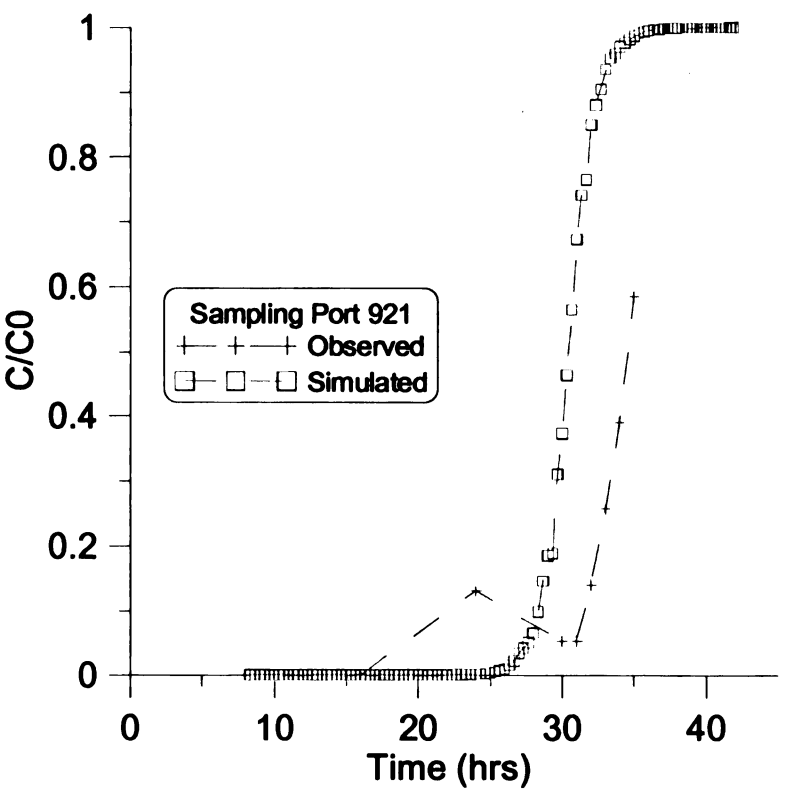

Figure 20 (continued)

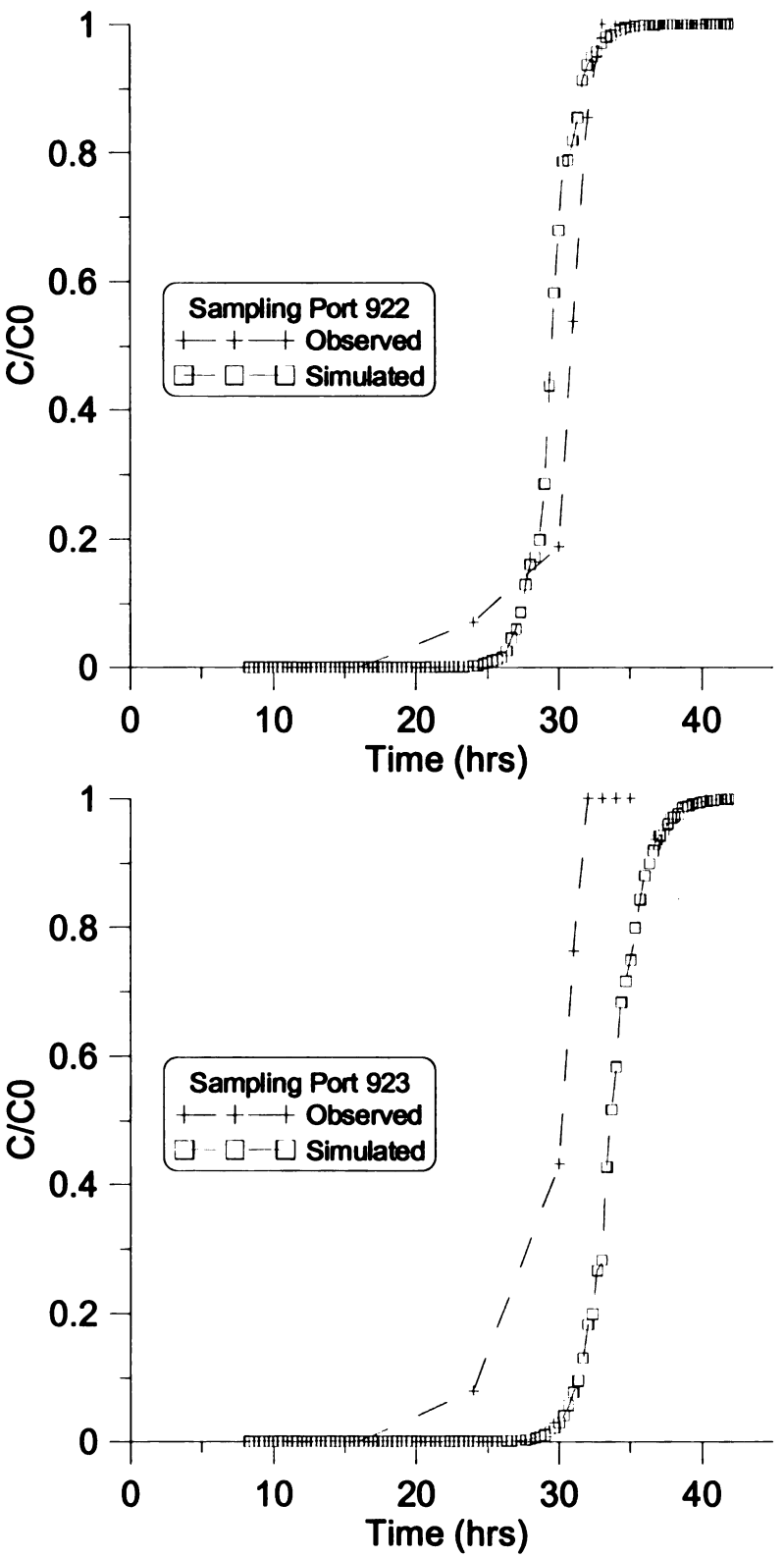

Figure 20 (continued)

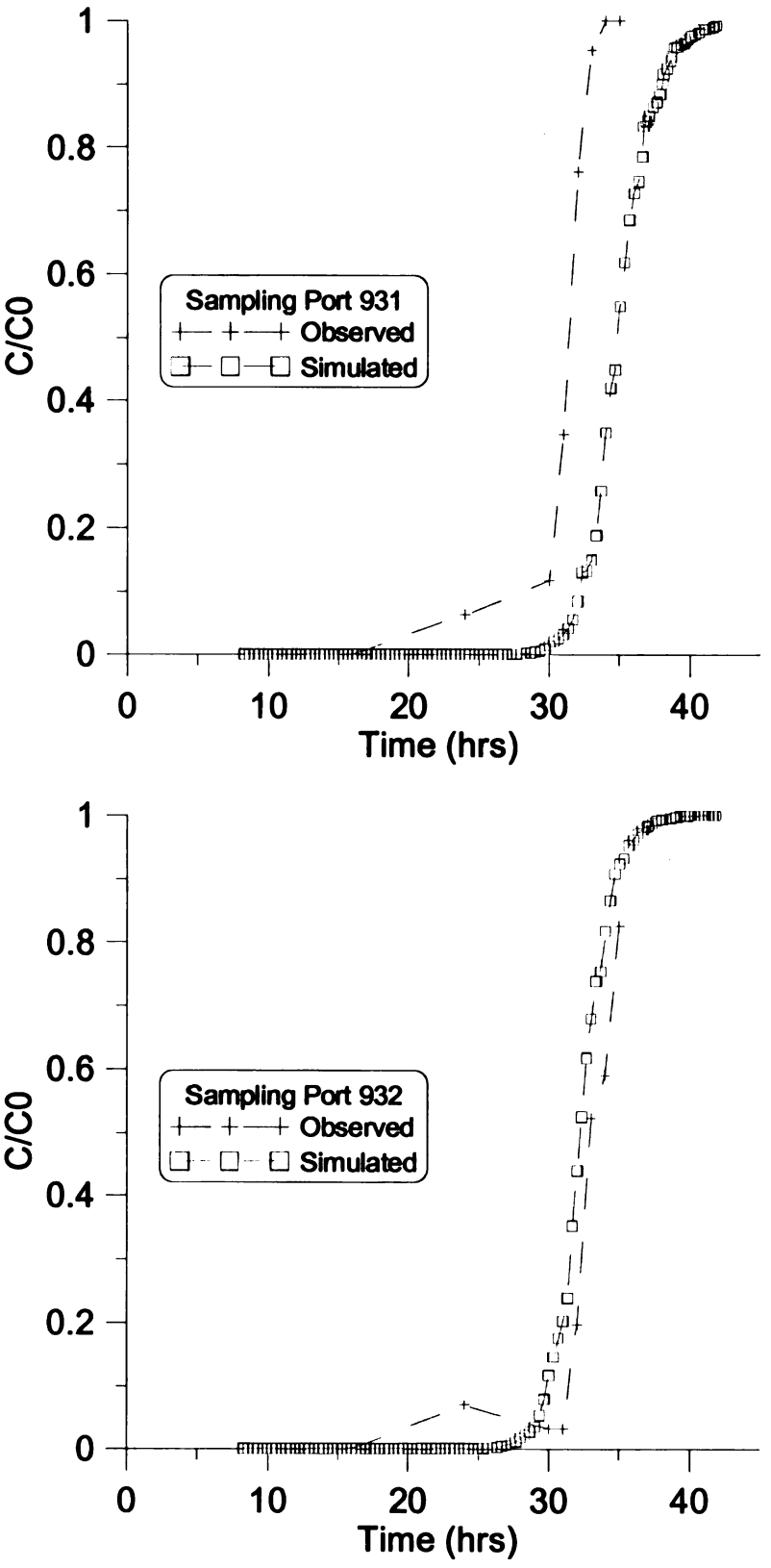

Figure 20 (continued)

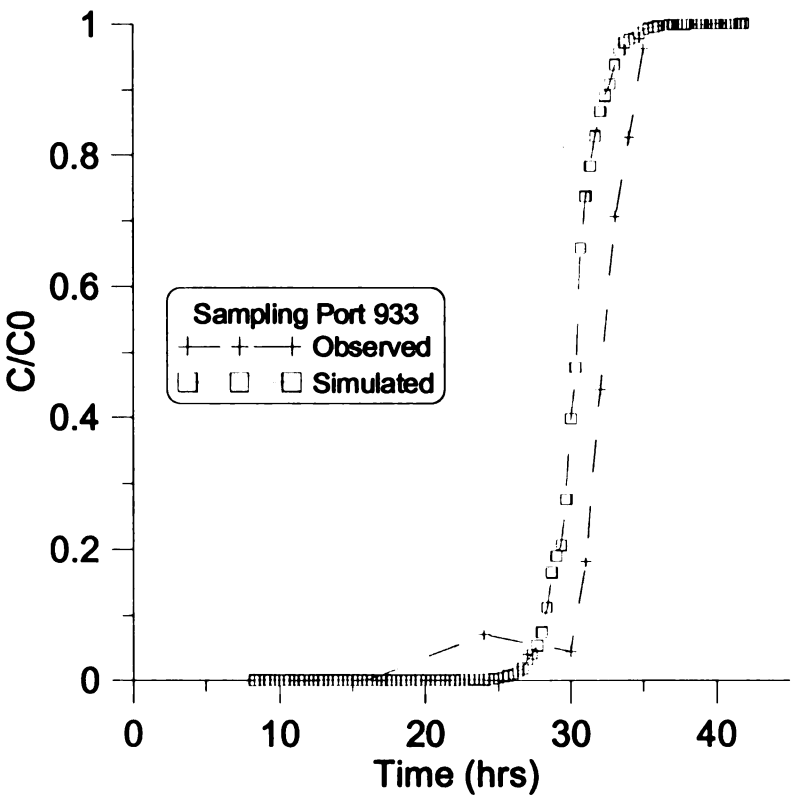

Iso surfaces were also generated for the horizontal and vertical simulated tracer tests (Figures 21 and 22) to compare them to the interpolated iso-surfaces created from the observed data (Figures 7, 9). Figure 21 illustrates the iso-surfaces of the simulated cross-flow tracer test at 150 and 180 minutes. Figure 22 illustrates iso-surfaces of the simulated vertical tracer test at 16 and 24 hours. As can be seen from both of these figures, the simulated iso-surfaces exhibit an idealized distribution of chemical mass with greater transport occurring proximal to the influent port(s) then what was observed in the laboratory model. The observed iso-surfaces suggest more spreading of the tracer fronts as they move towards the effluent port(s). This could be in part attributable to the interpolations used to create the iso-surfaces or heterogeneities in the model aquifer.

However, as was previously mentioned, there was not enough data to account for possible heterogeneities in the column.

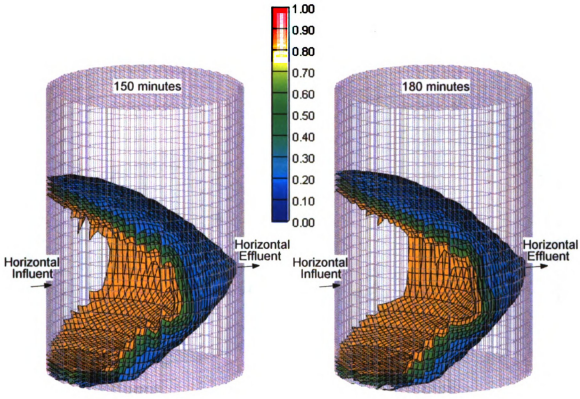

Figure 21. Iso-surfaces generated from the RT3D simulation of the horizontal bromide tracer test at 150 and 180 minutes, compare to Figure 7 for the observed iso-surfaces at the same times.

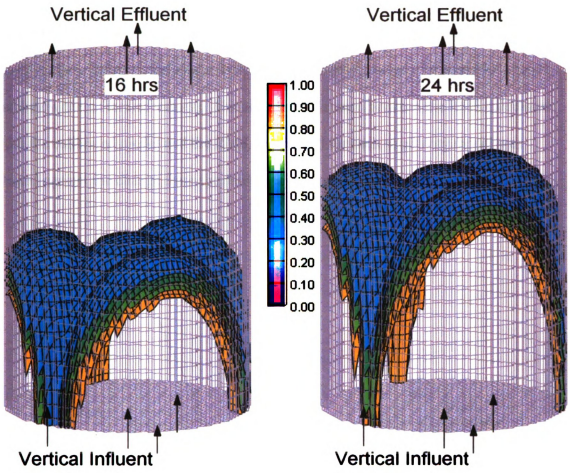

Figure 22. Iso-surfaces generated from the RT3D simulation of the vertical bromide tracer test at 16 and 24 hours. Compare to Figure 9 for the iso-surfaces generated from the observed data sets.

5.4 SENSITIVITY ANALYSES

The objective of a sensitivity analyses is to demonstrate the uncertainty in a calibrated model by varying the input parameters over a reasonable range of values (Anderson and Woessner 1992). The evaluation often entails noting the change in average hydraulic head from the calibrated model. In this case, parameter sensitivity was evaluated by looking at the root mean squared error (RMS) between simulated and observed bromide

concentrations at the horizontal effluent port of the cross-flow tracer test and the resulting simulated versus observed breakthrough curves for the horizontal and vertical bromide tracer studies. Porosity and dispersivity were tested over a range of values (50% above and below the calibrated values). The absolute difference between the RMS calculated from the calibrated model and the RMS determined for each sensitivity model was plotted against the change from the calibrated parameter (Figure 23).

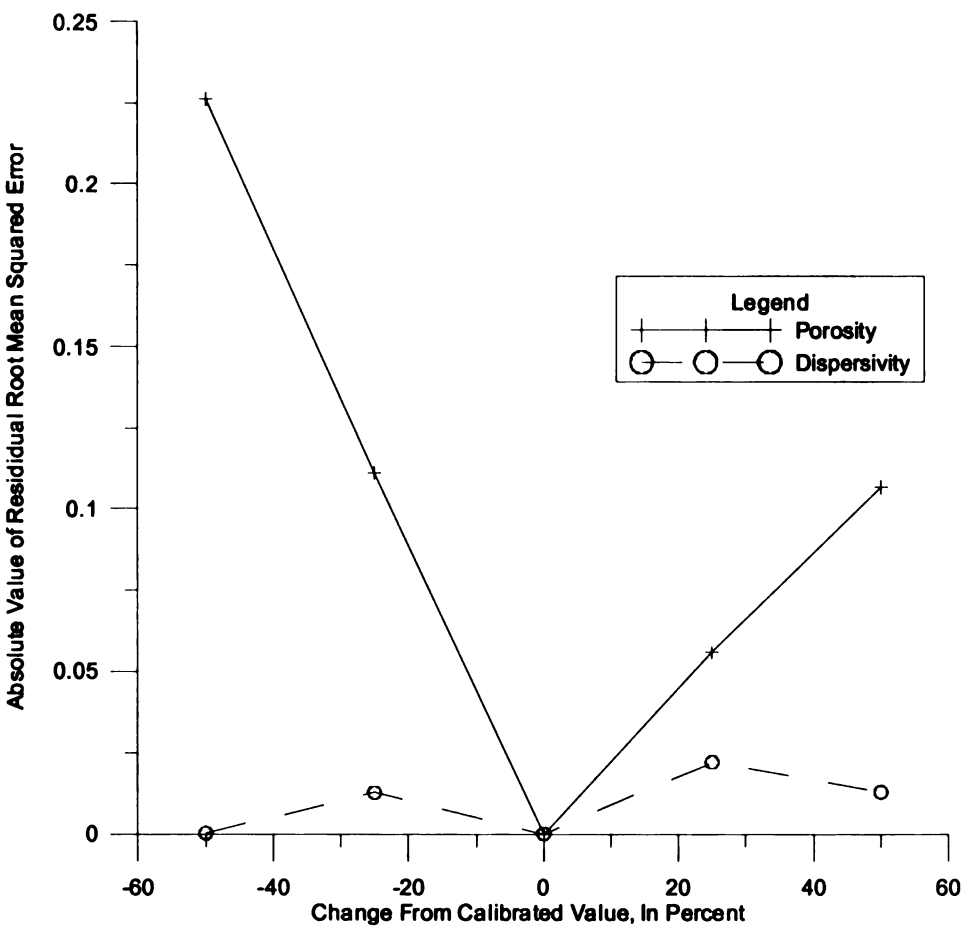

Figure 23. Sensitivity analyses of porosity and dispersivity in the horizontal bromide tracer study.

As can be seen, porosity is the more sensitive parameter in the horizontal bromide tracer study. This observation prompted an additional sensitivity analyses to determine if dispersivity was as insensitive in the vertical tracer study as it was in the horizontal tracer study. Dispersivity was tested over a wide range of values (0.1 – 3.0 cm); however instead of calculating the RMS error between the two simulations, comparisons were made between the resulting breakthrough curves (Figure 24a and b). The resulting curves indicate that dispersivity is fairly insensitive in the horizontal tracer study, yet very sensitive in the vertical tracer study. This is discussed further in the next section. The sensitivity analyses supports the estimated value of dispersivity of 0.1 cm, arrived at during the calibration.

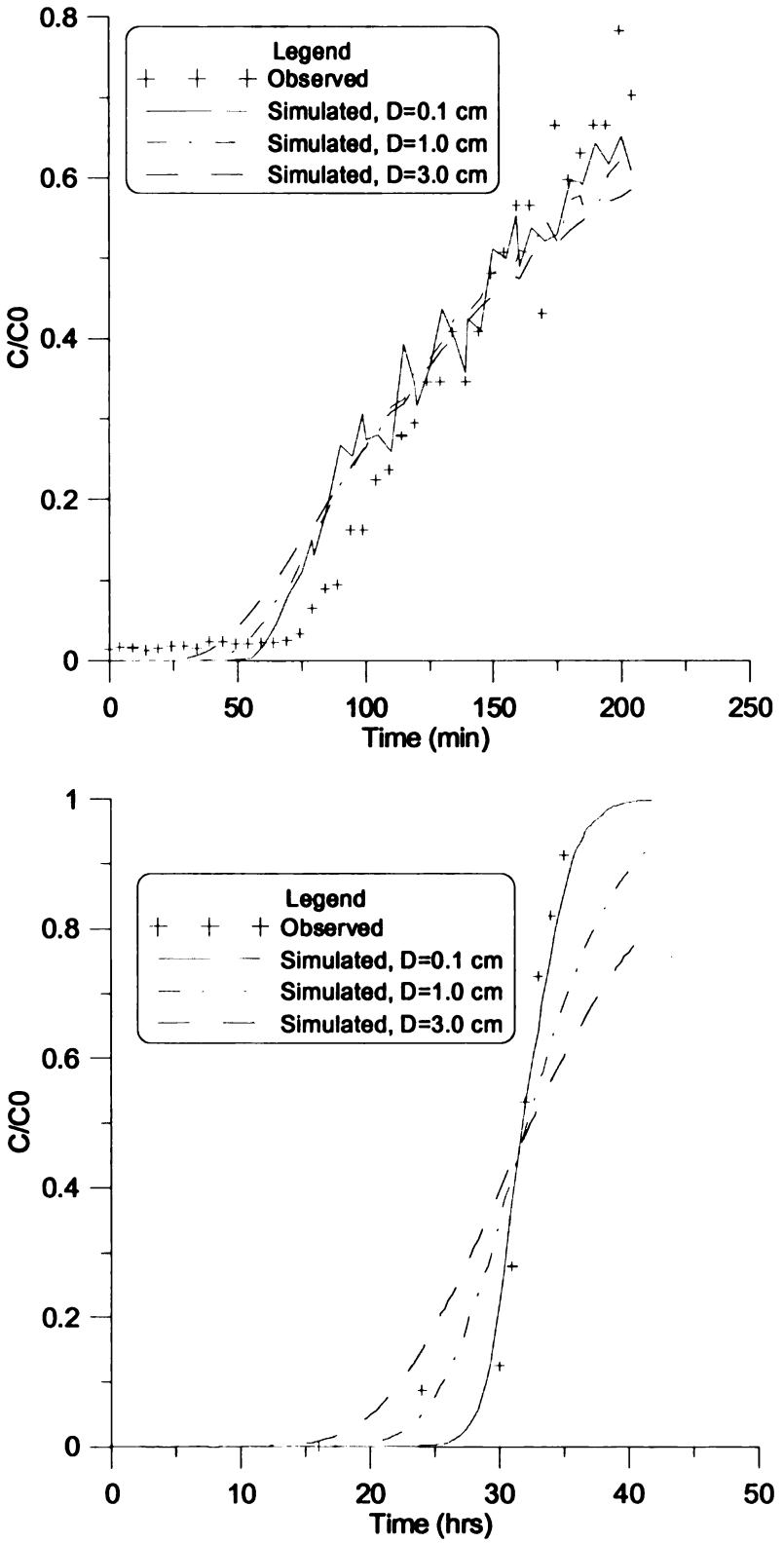

Figure 24. Sensitivity analyses exhibiting the effects of varying dispersivity on the horizontal (top) and vertical (bottom) breakthrough curves.

5.5 CONSERVATIVE TRACER TEST DISCUSSION

The modeling of the conservative tracer tests provided insight into the nature of solute transport through the model aquifer. Values of porosity, dispersivity and vertical anisotropy were estimated based on the groundwater transport model. These parameters are critical for development of a reactive transport model. Often times environmental professionals use generic parameters as input into numerical models, which in turn create solutions that have no bearing on reality. Since the basic flow and transport parameters have been estimated through the bromide tracer tests, these parameters can be used with more confidence in the biocurtain numerical model simulations. An additional benefit of using a numerical model is that it is very easy to adjust parameters and observe the effect, helping the user to understand the connectivity of different processes. For example, adjusting the porosity and observing how it affects the breakthrough curve.

The modeling of the conservative tracer indicated that the physical aquifer model was more complicated than expected. It is clear that treating the aquifer media as homogenous and pumping rates equal in each of the injection/extraction ports is an oversimplification; however, as was previously mentioned accounting for heterogeneity was outside of the scope of this work. The numerical modeling results also indicated that the numerical model was more complicated than expected. The results exhibited more chemical mass proximal to the influent port(s) than what was observed in the laboratory model. More importantly though were the observations drawn from the sensitivity analyses. The results indicated that dispersivity is relatively insensitive in the horizontal flow regime; however, very sensitive in the vertical flow. This insensitivity may be a

result of numerical dispersion. The cause of the enhanced numerical dispersion in the horizontal test could be due to the divergent, convergent flow that occurs between the single horizontal injection and extraction ports. The resulting velocity field produces hydraulic gradients that are diagonal to the finite difference grid cells, along with higher local velocities than in the vertical test. Having identified these shortcomings, one expects the data generated from the carbon tetrachloride sorption simulation, inoculation, and biocurtain simulations to also exhibit these characteristics.

5.6 CARBON TETRACHLORIDE SORPTION SIMULATION

The carbon tetrachloride sorption simulation was set-up in the same manner as the vertical bromide tracer simulation, with 4 wells representing the influent ports, which were assigned a quarter of the average observed flow rate, and 4 constant head cells (115 cm) assigned to the effluent ports at the top of the tank. The simulation utilized the calibrated parameters from the bromide tracer tests. Concentrations of CT were assigned at each influent port and set at the average observed influent concentration entering the laboratory model. Concentrations of the other reactive species were left at zero since they were not included in the laboratory experiment, with the exception of bromide, which was modeled separately and presented earlier.

Parameter	Description	Value(s)	Source
α_L	longitudinal dispersivity, cm	0.1, 3.0	calibration of bromide tracer tests, CT sorption study
$\alpha_T:\alpha_L$	ratio of transverse to longitudinal dispersivity	0.3	calibration of bromide tracer tests
$\alpha_V:\alpha_L$	ratio of vertical to longitudinal dispersivity	0.1	calibration of bromide tracer tests
θ	sediment porosity	0.31	calibration of bromide tracer tests
K	hydraulic Conductivity, cm sec^{-1}	0.027	Dybas et al.(2002) and Hyndman et al. (2000)
b_{kc}	microbial decay rate, day^{-1}	0.13	Phanikumar et al. (2005)
f	fraction of exchange sites	0.437	Phanikumar et al. (2005)
γ	nitrate utilization coefficient, day-1	18.89	Phanikumar et al. (2005)
K_{at}	attachment rate, day-1	0.9	Phanikumar et al. (2005)
K_d	distribution coefficient, L/mg	3.9×10^{-7}	Zhao et al. (1999)
K_{det}	detachment rate, day -1	0.04	Phanikumar et al. (2005)
K_{sa}	half-saturation coefficient for acetate, mg/L	1.0	Phanikumar et al. (2005)
K_{sn}	half-saturation coefficient for nitrate, mg/L	12.0	Phanikumar et al. (2005)
k'	second-order CT reaction rate, L/mg-day	0.12	Phanikumar et al. (2005)
κ	first order kinetic (de) sorption rate, day -1	0.36	Phanikumar et al. (2005)
$\mu_{\xi\alpha\mu}$	maximum specific growth rate, day -1	3.11	Phanikumar et al. (2005)
ρ_b	soil bulk density, mg/L	1.63×10^6	Phanikumar et al. (2005)
Y_a	yield for acetate, mg cells/mg substrate	0.4	Phanikumar et al. (2005)
Y_n	yield for nitrate, mg cells/mg substrate	0.25	Phanikumar et al. (2005)
Y_{nb}	yield for biomass, mg cells/mg substrate	0.46	Phanikumar et al. (2005)

Table 1. List of numerical model input parameters.

Recalling equations (1) and (6) it was necessary to define a set of reaction parameters for this simulation, specifically values for bulk density (ρ), first order kinetic (de) sorption rate (κ), fraction of exchange sites at equilibrium (f), and the distribution coefficient (K_d). The initial parameters were gleaned from the recent work conducted by the Departments of Geological Science and Civil and Environmental Engineering (Phanikumar et al., 2005), in which they applied their biodegradation model to the Schoolcraft site (refer to Table 1 for parameters). A simulation was executed and the

results were compared to the observed data. Figure 25 illustrates the average row 9 simulated versus observed data utilizing the initial parameters. As can be seen, the 50% breakthrough of the simulated CT matches fairly well with the 50% breakthrough of the observed data. This was also the case with the vertical effluent port. Moreover the simulated CT breakthrough curves reach asymptotic values of C/C_0, which were fairly consistent with the observed data. However, the slopes of the simulated and observed breakthrough curves do not agree. Therefore, a sensitivity analysis was performed on parameters thought to have an effect on the slope of the breakthrough curves. Values of κ, f, and K_d were perturbed from their initial conditions and the effects were noted.

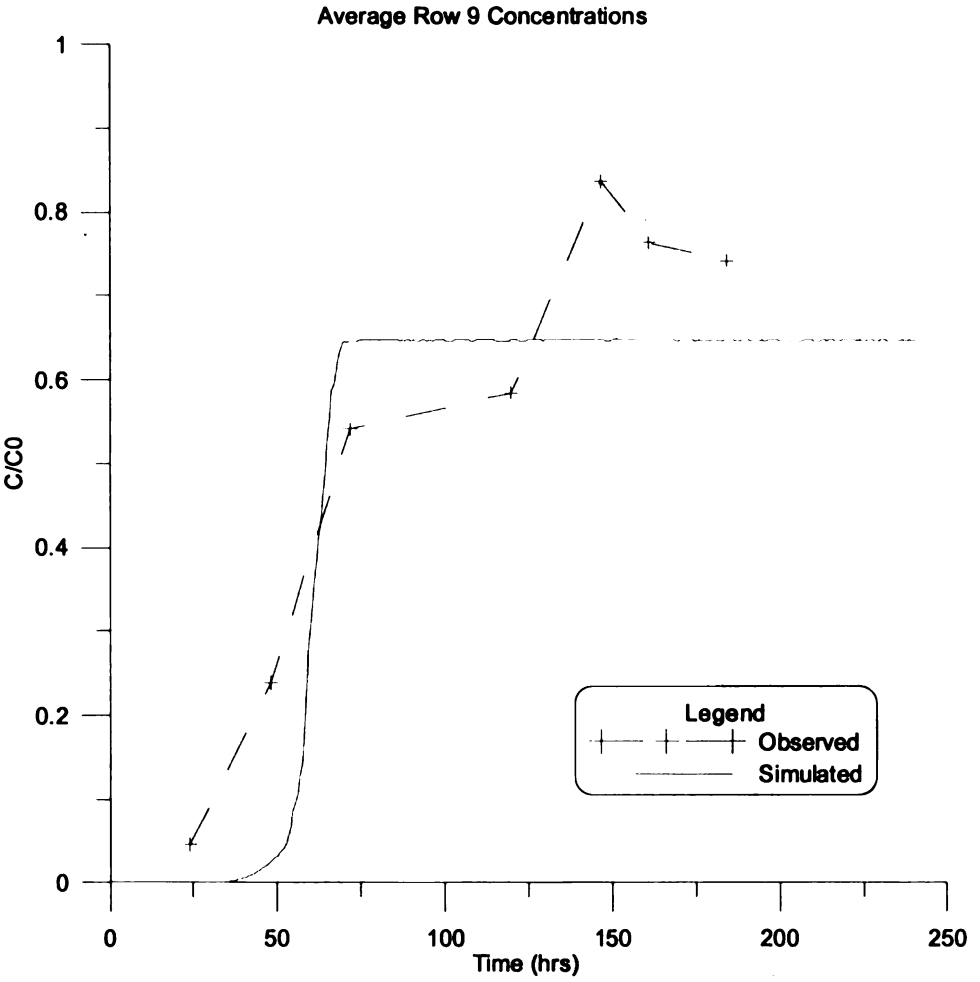

Figure 25. Simulated versus observed concentrations at row 9 using the initial reaction parameters from Phanikumar et al. (2005) and the calibrated parameters from the tracer simulations.

5.6.1 CT Sensitivity Analysis

The first parameter that was adjusted in an attempt to better fit the observed the breakthrough curve was the first order kinetic (de) sorption rate. This parameter was reduced to a fifth of its initial value and the simulation was run. The effect of decreasing κ appears to increase the asymptotic value of the dissolved phase CT; however, does not have an effect on the slope of the breakthrough curve (Figure 26). Conversely increasing this parameter decreased the asymptotic value of C/C_0. All of the following simulations

were terminated prematurely for the sake of time, when it was evident that the parameter perturbation did not produce the desired effect.

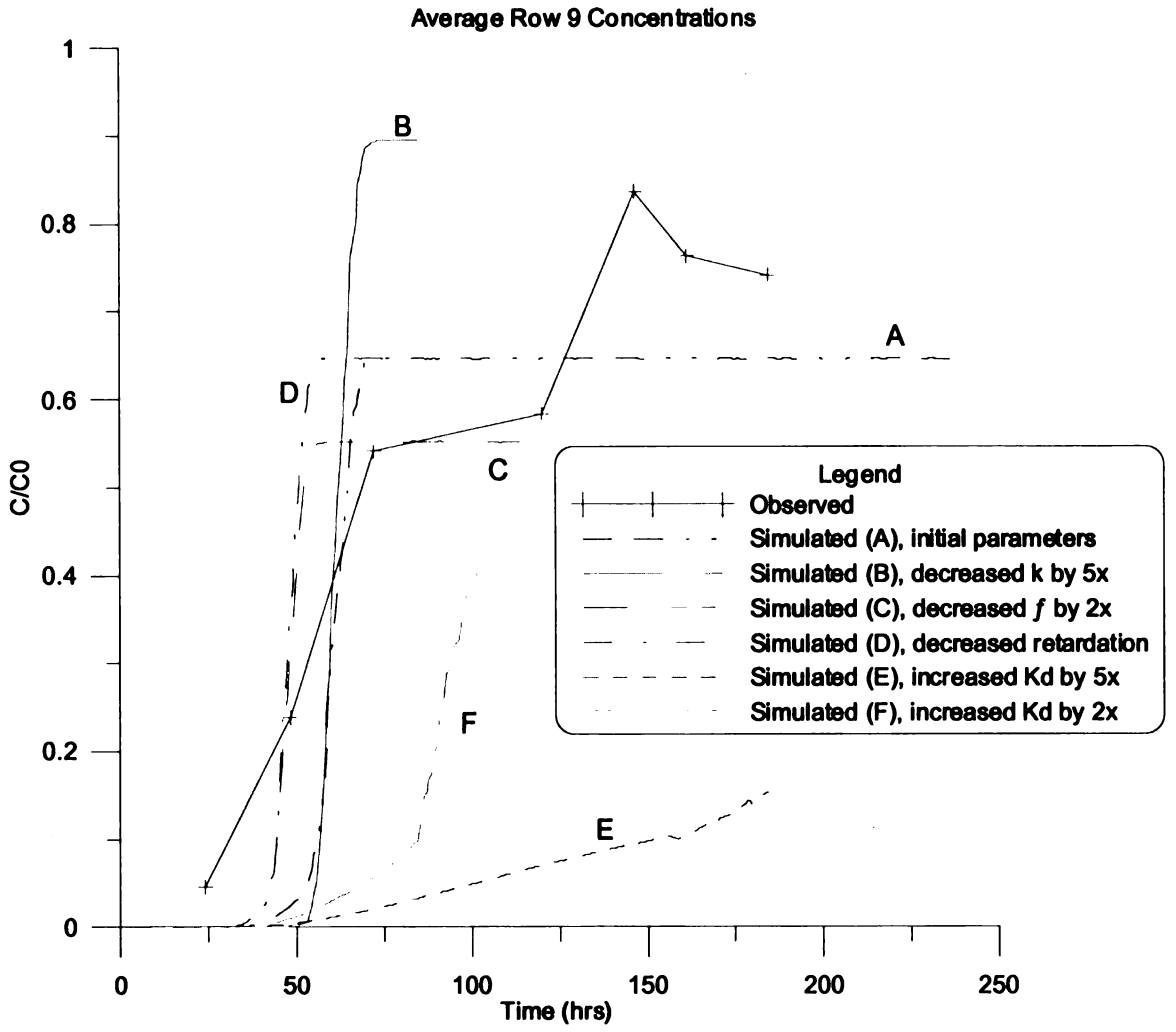

Figure 26. Simulated CT breakthrough curves resulting from perturbations to sorption parameters.

The second parameter that was perturbed was the fraction of exchange sites at equilibrium. This parameter was reduced by half, thus reducing the retardation value from 1.89 to 1.45 as well, since *f* is also a term in the determination of R. The effect of this perturbation was that it reduced the time required to achieve breakthrough and decreased the asymptotic value of C/C_0; however, no change to the slope was observed

(Figure 27). A simulation was also run that utilized the initial parameters, but reduced the retardation value to 1.45. The result indicated that a reduction in the retardation translates the breakthrough curve to arrive earlier without affecting the slope or the asymptotic value of C/C_0 (Figure 26).

The third parameter that was investigated was the distribution coefficient. According to Dybas et al. (2002) values of K_d vary over three orders of magnitude in the field, therefore there is a great deal of uncertainty in this parameter and thus perturbations to this parameter are justified by field data. The first simulation increased K_d by a factor of five and thus the retardation value was increased to 5.48. The effect of this change was that it drastically decreased the slopes of the breakthrough curves and never achieved asymptotic values (Figure 26). The results looked favorable though, since this was the first parameter perturbation that resulted in a change of slope. Therefore, additional simulations were run using increased values of K_d (2x and 1.4x the initial value); however, neither simulation produced the desired effect. In both cases the slope of the breakthrough curves increased dramatically and did not match the observed data, the center of mass arrivals were late, and the asymptotic values of C/C_0 were too low. Simulations were also explored that varied several parameters at the same time and set-up multiple stress periods corresponding to the observed fluctuations in influent concentrations and flow rates; however, none of these simulations resulted in better fits between the simulated and observed. Therefore, one last parameter was investigated that is known to affect the shape of a solute breakthrough, that being dispersivity.

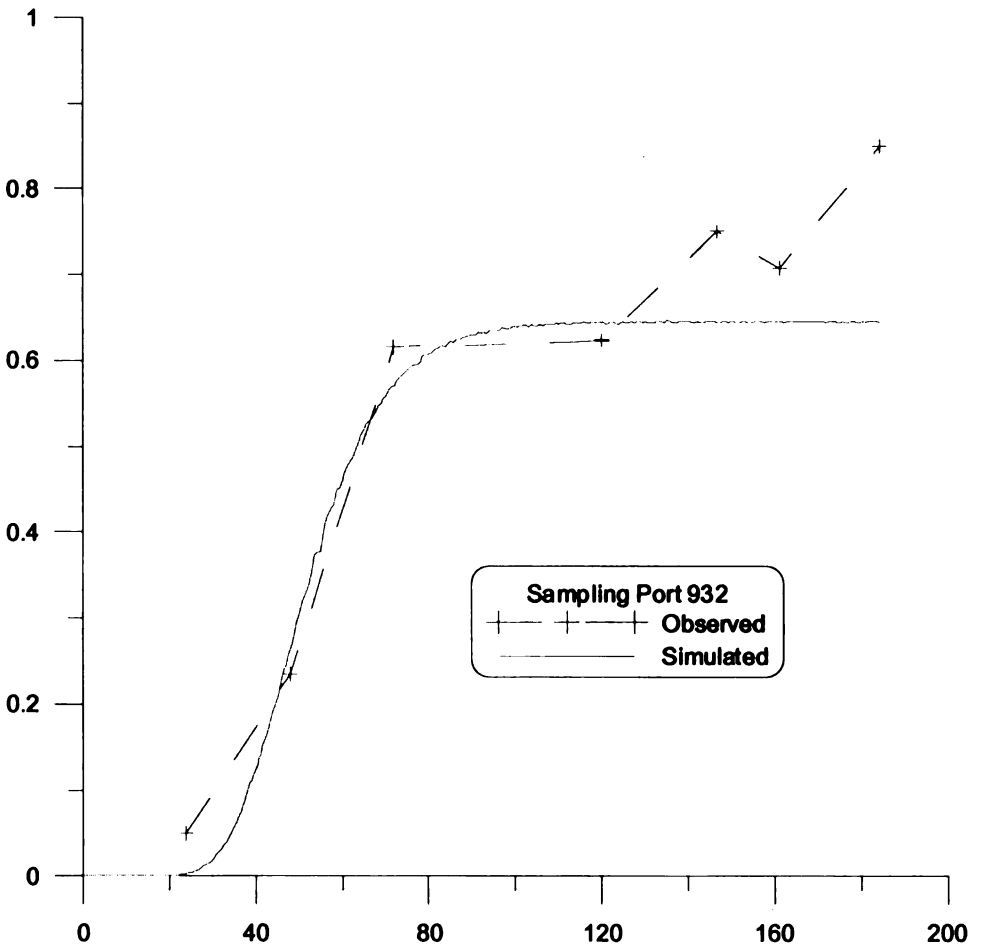

Figure 27. Simulated versus observed carbon tetrachloride concentrations during the CT sorption study at sampling port 932.

Recall that dispersivity was calibrated during the horizontal and vertical bromide tracer simulations; however, this parameter was re-visited to determine if increasing its value would create the desired effect on the slope of the CT breakthrough curves. Utilizing the initial reactive transport parameters that resulted in acceptable fits between the simulated and observed center of mass arrival times and the asymptotic values reached by the CT breakthroughs, several simulations were run with increased values of dispersivity. The results indicated that a dispersivity of 3 cm creates the desired affect on the slope of the CT breakthrough curves and that a decrease in the retardation value to 1.58 was required

to match up the arrival time of the breakthroughs. Moreover, the initial reaction parameters appear to adequately describe the CT transport and sorption. Refer to Figure 27 for an example of simulated versus observed at sampling port 932 and Table 1 for the reaction parameters used in this simulation.

5.6.2 CT Sorption Simulation Discussion

The results of the CT sorption simulation sensitivity analyses were very informative in regard to the nature of the two-site sorption model developed by Zhao et al (1999) and incorporated into the RT3D model developed by Phanikumar et al (2002a, 2002b, 2003, and 2005). The expectation was that by adjusting the first order kinetic (de) sorption rate, fraction of exchange sites at equilibrium, or the distribution coefficient, one would achieve a better fit between the simulated and observed CT breakthroughs. This was not the case when the parameters were independently adjusted; however, if a multi-parameter optimization was performed one may arrive at a better fit. In order to produce a better fit between the simulated and observed an adjustment of the dispersivity and retardation was required. Conceptually this approach was flawed, for though adjusting the dispersivity created the desired effect; in general the amount of dispersion is often considered the same for a non-reactive solute as it is for a reactive solute. Unless diffusion or size exclusion plays a significant role in the amount of dispersion, then differential tracer breakthroughs can be expected, as indicated during microcosm studies conducted at M.S.U. (Ewer, 1997; Brennan, 2004). However, neither of these factors should have influenced the CT transport.

Another possibility is that the current model does not adequately account for the kinetics of the CT sorption. Observing the laboratory CT breakthrough curves it is apparent that changes in the slope of the curves occurred that are inconsistent with the bromide breakthrough curves. This could be an effect of the uncertainty in the dataset (fluctuating influent concentrations and flow rates) or a factor that was unaccounted for in the sorption model, like spatial variability in the CT sorption rate. Exploring the idea of a multi-rate sorption model has been explored by Haggerty and Gorelick (1995) and may require additional work through the use of 3-dimensional sorption studies.

An additional, and perhaps more plausible explanation for the observed CT breakthrough curves, is that there is a spatial distribution to the distribution coefficient. The packing of the column likely caused an uneven distribution of fraction organic carbon, for as sediment was wet packed into the model and fell through the column of water, the coal particles may have settled out more slowly, based on their grain size and density. Evidence of this can be seen in the initial arrival times of bromide and CT. If there were an equal amount of retardation throughout the column, then the initial arrival of bromide and CT would not match. The fact that it does, suggest that fastest flow path within the column may not have had any fraction organic carbon to allow sorption to occur. In turn, by varying the distribution coefficient throughout the model and utilizing inverse modeling techniques, one may arrive at a solution that more closely agrees with the observed data.

The numerical modeling exercise moved forward utilizing the initial CT sorption reaction parameters with the adjusted retardation value and increased dispersivity. The next simulation conducted was the inoculation of the laboratory model.

5.7 INOCULATION SIMULATION

The inoculation simulation was set-up in the same manner as the horizontal bromide tracer study. A horizontal flow rate was established at the horizontal influent port that matched the average flow rate observed during the inoculation. Concentrations of bromide, acetate, nitrate, and liquid phase strain KC matched the measured influent concentrations used in the laboratory study, refer to section 4.7. CT was not included as an injected species since concentrations were negligible due to CT degradation in the inoculum prior to inoculation. Concentrations were simulated in the units of mg/L. According to Phanikumar et al. (2002), one cfu/mL of strain KC is roughly equal to 1.67 x 10^{-7} mg/L; therefore, the measured biomass concentrations were converted to ppm. The simulation lasted approximately 3 hours and utilized all of the initial reaction parameters as presented in Phanikumar et al (2005), with the exception of the retardation value, which was altered based on the CT sorption simulation results. The model was also run with the increased dispersivity value, as determined through the CT sorption study and the porosity, as determined through the bromide tracer tests. Refer to Table 1 for a complete list of all of the reactive transport parameters.

The results indicate a poor agreement between simulated and observed mobile strain KC concentrations (Figures 28). Both the simulated mobile strain KC and bromide exhibit early breakthroughs along the centerline sampling ports (312, 322, and 332). This was expected based on the results of the horizontal bromide tracer simulation, in which the flow and non-reactive transport model was calibrated to the horizontal effluent concentrations. Recall that this approach was chosen to try and match the average solute concentrations leaving the laboratory model aquifer in lieu of attempting a calibration to the sparse data collected from the internal sampling ports. Though the simulated concentration histories appear far earlier than the observed, the slopes of the breakthrough curves at 312 and 322 are reasonable; however, the slope of the simulated breakthrough curve at 332 is too gradual. Comparisons were not made at the horizontal effluent, since mobile strain KC was only just starting to arrive at the end of the inoculation.

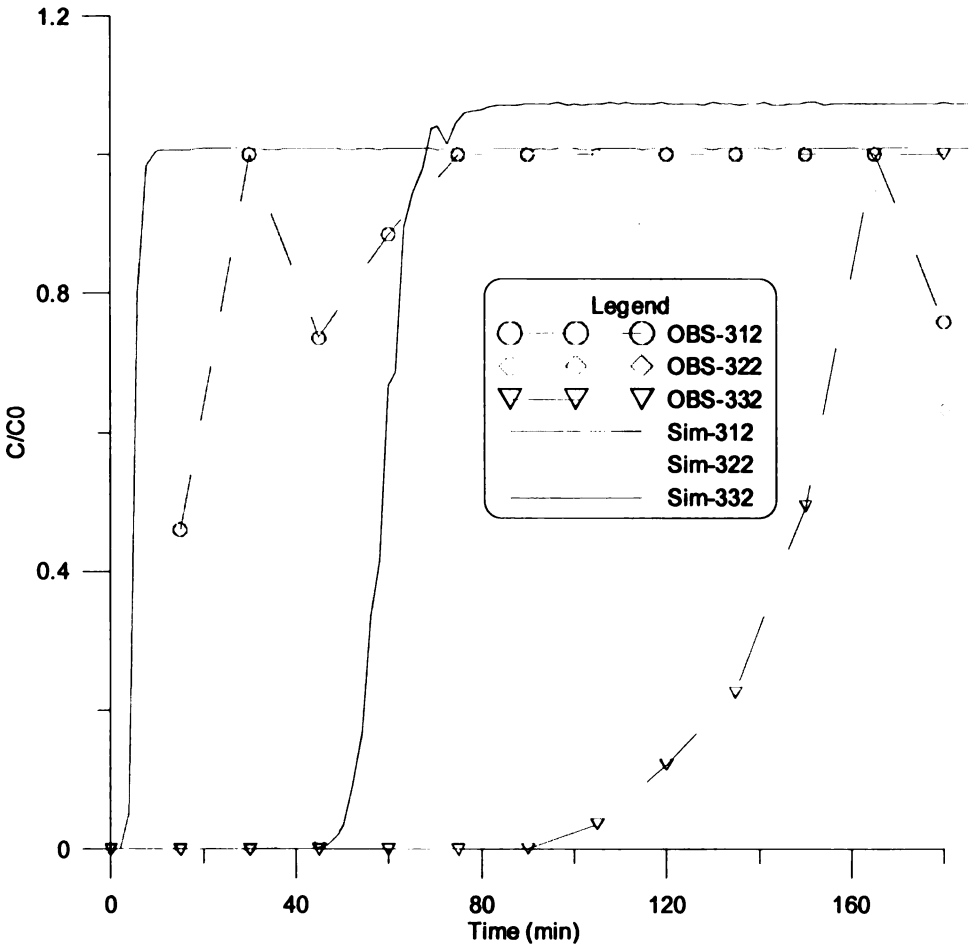

Figure 28. Comparison of simulated versus observed mobile strain KC concentrations during the inoculation event.

The most important observation to come from this simulation involved the relative timing of breakthroughs. As was discussed in Section 5.1.3 there was a significant lag time between the mobile strain KC and the bromide breakthrough curves; however, this differential breakthrough did not occur in the inoculation simulation. Instead, the simulated breakthrough curves exhibit almost simultaneous arrivals of Br and mobile phase KC (Figure 29). This simultaneous arrival had previously been observed during past model applications (Phanikumar et al., 2002a, Phanikumar et al., 2005). The only difference was that instead of seeing mobile phase KC and bromide breakthroughs

occurring together, the authors displayed graphs of mobile phase KC and acetate concentrations versus time. In fact in the application of the model to the one-dimensional column studies (Phanikumar et al., 2002a), the simulated mobile phase KC is transported faster than acetate. The comparison between mobile strain KC and acetate and mobile strain KC and bromide can be made, since in the above referenced articles, the authors noted that acetate and bromide exhibit similar transport patterns.

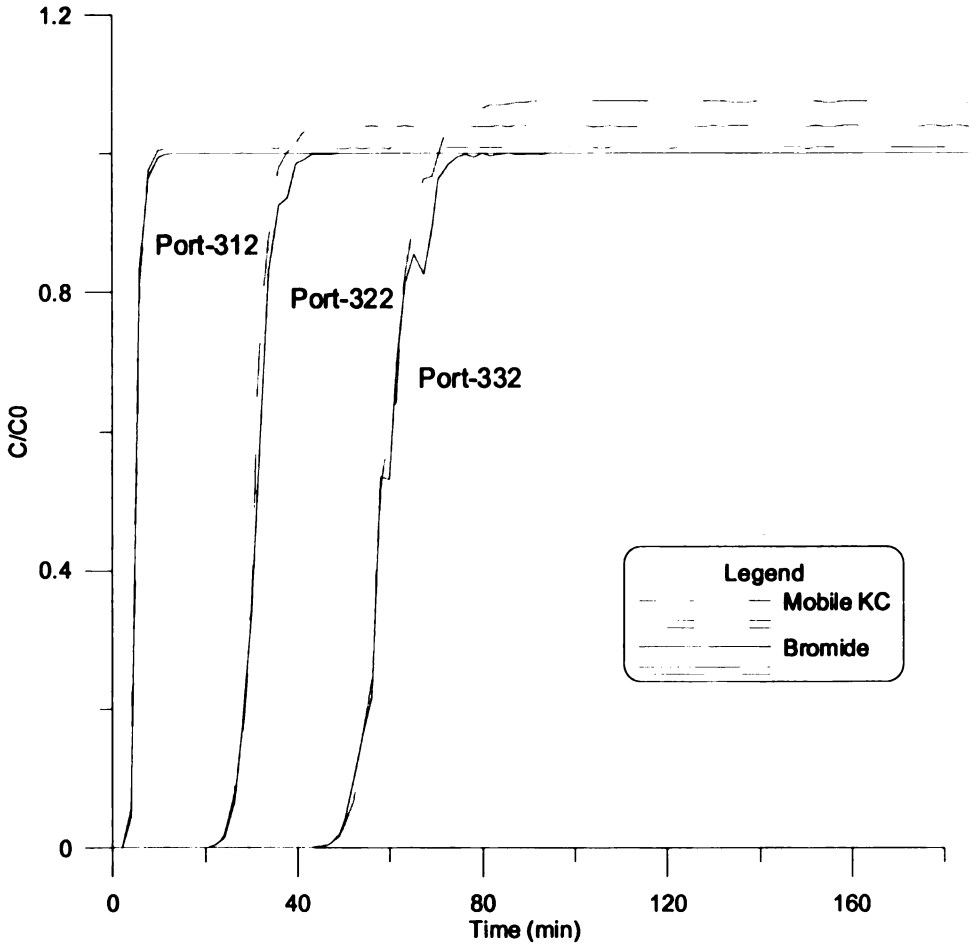

Figure 29. Comparison of bromide and mobile strain KC during the inoculation event.

Previous studies (Murphy et al., 1997; Johnson et al., 2001; Phanikumar et al., 2005) have noted the effect of aquifer heterogeneities on the timing of microbial transport.

Though the laboratory model may have contained small-scale heterogeneities, due to settling of sediments during wet packing, they would have existed as layers parallel to the centerline sampling ports between the horizontal influent and effluent. Therefore, the velocity field established directly between the horizontal influent and effluent should not have been affected by the occurrence of possible heterogeneities. Another factor must be responsible. A simulation was run with an increased attachment rate (K_{at}) to see if increasing that parameter would delay the transport of strain KC. This idea had been used previously by Phanikumar et al. (2005) to account for the increased attachment rate due to the inoculation of a flocculated culture; however, the perturbation only increased the asymptotic value reached during the breakthrough. Another simulation was run utilizing the optimized reaction parameters solved for in the one-dimensional column study (Phanikumar et al., 2002a). This simulation utilized a higher value for the microbial decay rate; however, no change was observed in the mobile strain KC breakthrough curves or the relative breakthroughs of the mobile strain KC and bromide. Therefore, the data suggests that there is an additional factor controlling the lag time between the mobile KC and a conservative tracer, perhaps something similar to a retardation factor. Evaluating an additional reaction parameter is beyond the scope of this thesis; though should be considered as microbial transport models continue to evolve.

5.8 NUMERICAL BIOCURTAIN SIMULATION

The biocurtain simulation was designed to mimic the 3 stages of the laboratory model biodegradation study following the inoculation event, as described in Section 4.8. This

included the first biodegradation period, the feeding event, and the second biodegradation event. The reactive parameters used in this simulation were the same as were utilized in the recent model application to the Schoolcraft site (Phanikumar et al., 2005), with the exception of porosity and dispersivity. Refer to Table 1 for a complete list. Starting concentrations of acetate, nitrate, dissolved CT, sorbed CT, mobile phase biomass, and immobile phase biomass were established that corresponded with the concentrations at the end of the inoculation event. It was the hope to utilize the results of the inoculation simulation as the starting concentrations for the biocurtain simulation; however, ensuing from the poor fit between simulated and observed the author decided to use the available laboratory data instead. The only exception was for the initial concentrations of the immobile phase biomass, which did utilize the concentrations from the end of the inoculation simulation, for a good analog did not exist.

The observed bromide data, which had previously been kriged to the finite difference grid (Figure 15), was used as a proxy for the distribution of the starting acetate and nitrate concentrations by multiplying the C/C_0 Br values in each cell by the injected concentrations of nitrate and acetate. The kriged mobile strain KC at the end of the inoculation was input as the starting concentrations for this simulation. The kriged CT concentrations at 1.5 hours after the start of the biocurtain study (Figure 17) were utilized as the starting concentration of dissolved CT in each grid cell. The starting sorbed phase CT concentration in each grid cell used the above distribution of the dissolved phase CT concentrations and assumed equilibrium sorption. Therefore, the value in each grid cell was multiplied by the distribution coefficient and the fraction of exchange sites.

Results of the biocurtain simulation indicate a high degree of CT degradation throughout the column. The simulated CT concentrations exhibit a much higher degree of mass removal than what was observed; however, given the numerous difficulties in both the laboratory model (fluctuating CT concentrations over time, decrease in pH versus time, etc.) and the numerical model, a quantitative analyses of these results would be entirely speculative. Instead, it is more appropriate to observe general distributions of mass and relative timing of species transport in qualitative terms.

In order to observe the relative timing of species transport at two locations in the column, graphs of the concentrations of each of the main reactive components have been prepared for sampling ports 312 and 722 (Figure 30). Sampling Port 312 was selected to illustrate concentrations proximal to the horizontal influent port along the centerline of the horizontal velocity field. Sampling port 722 was chosen to exhibit concentrations towards the top of the column along the centerline of the vertical velocity field.

Figure 30. Comparison of simulated concentrations for sampling ports 312 (top) and 722 (bottom) during the biocurtain experiment.

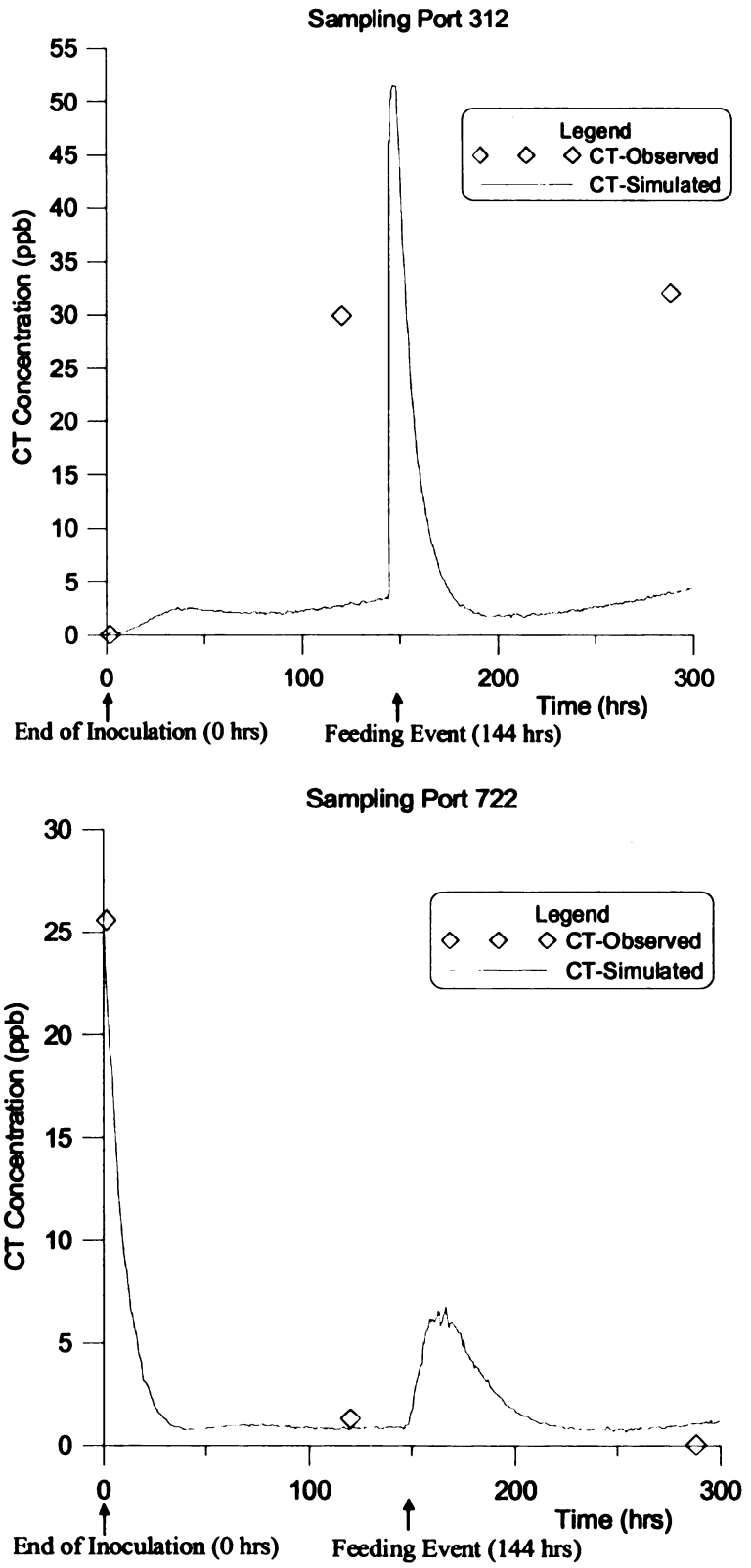

Figure 30 (continued)

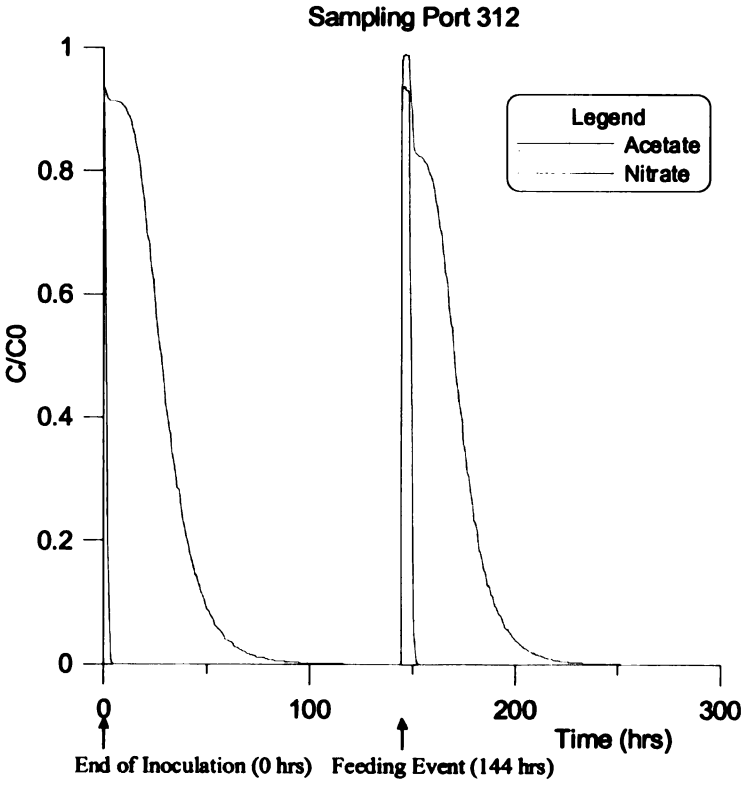

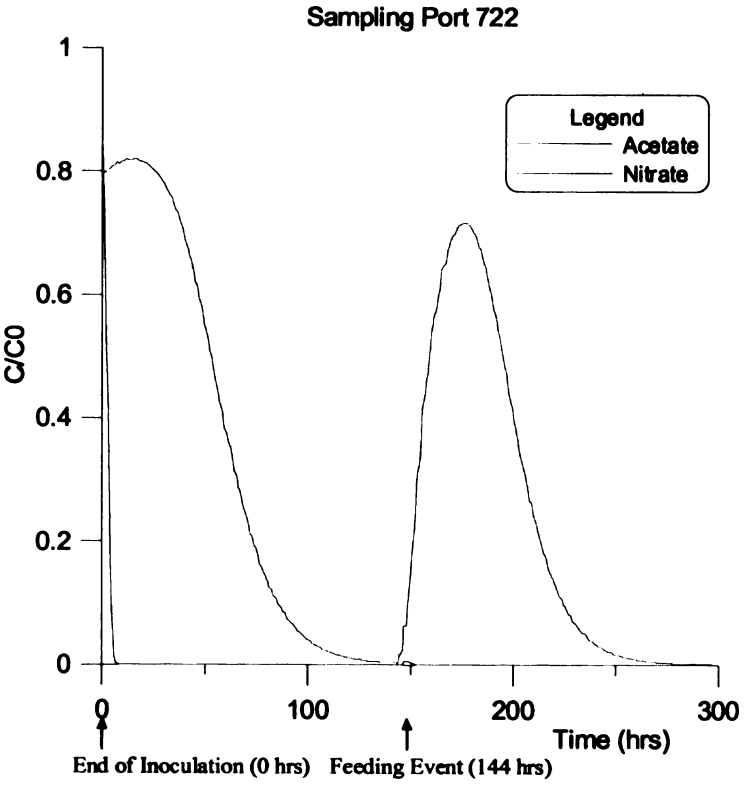

Figure 30 (continued)

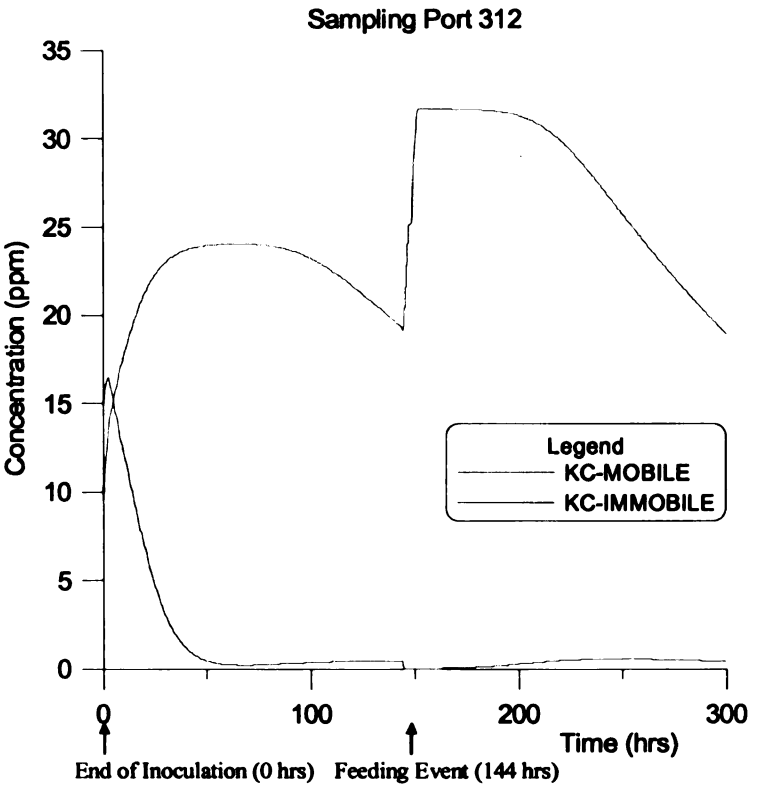

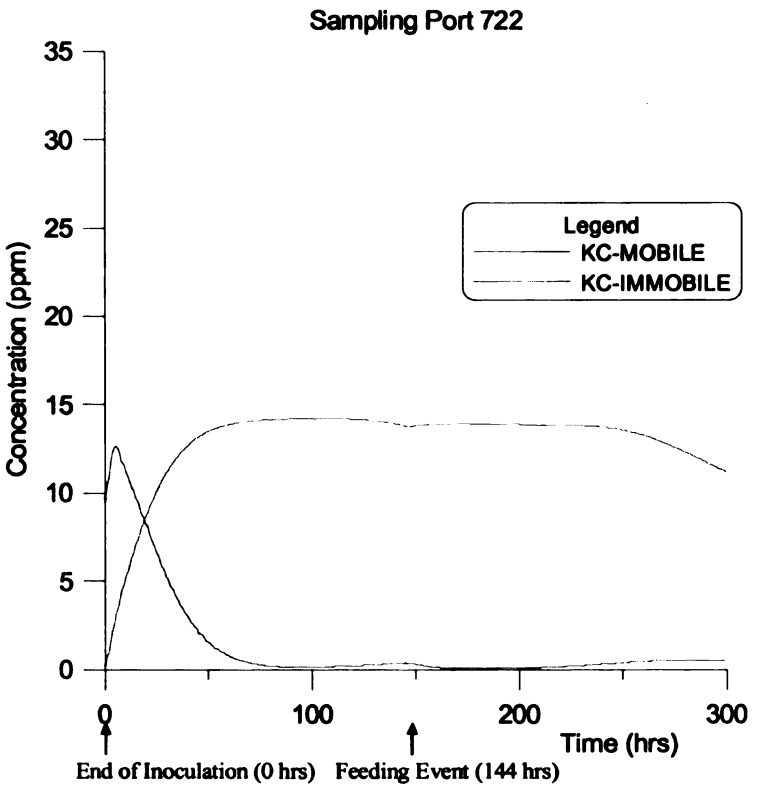

Nitrate and acetate concentrations were normalized by the initial concentrations for each phase, so that they could be viewed together. CT concentrations were expressed in ppb and strain KC was expressed in ppm. Based on the CT concentrations at port 312 and 722, the model predicts a high degree of CT degradation, which occurred very quickly, as indicated by the mass removal of CT after the inoculation event. Concentrations of acetate exhibit a decline that corresponds with the growth of immobile strain KC. The electron donor was completely consumed after 100 hours of the experiment; at which point the immobile strain KC concentrations began to decrease, indicating microbial decay. The nitrate concentrations exhibit a sharp decline soon after the inoculation and feeding event. In the case of sampling port 722, the simulation exhibits almost no nitrate reaching this location after the feeding event. This almost instantaneous decline in nitrate has also been noted in the field (Dybas et al., 2002, Phanikumar et al., 2005). Based on these model results, it appears as if this electron acceptor is a rate-limiting factor. And though the model still demonstrated CT mass removal without nitrate in the system, the microbial population was declining, which would eventually halt the ability to transform CT except near the upgradient source from the bottom of the column. If nitrate data was available for use during this thesis, one may find that a decrease in the nitrate utilization coefficient, that accounts for indigenous microbial activity or a decrease in the growth rate, is appropriate. Lastly, the simulated microbial concentrations support what has previously been noted by Dybas et al. (2002) and Phanikumar et al. (2005), that the immobile microbes exhibit much higher concentrations than the mobile microbes. Furthermore, the sharp decline in the concentration of mobile microbes is coincident with the sharp decline in the nitrate concentrations.

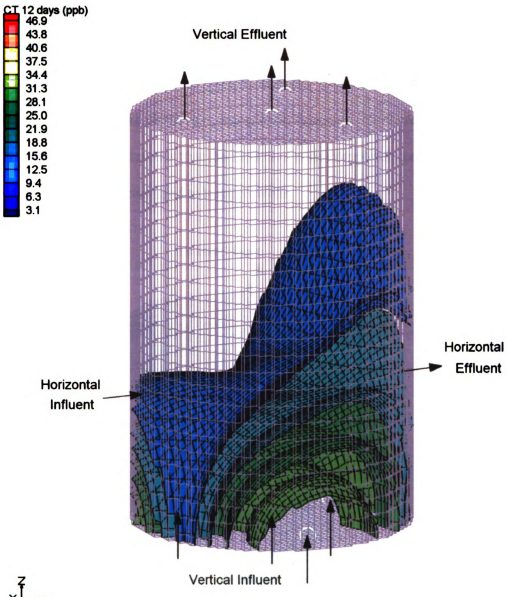

Figure 31. Concentrations of CT represented by iso-surfaces at day 12 of the simulation.

A plot of iso-surface concentrations was prepared illustrating the CT concentrations at the end of the 12 days (Figure 31). The distribution of CT remaining in the column agrees with the general observed distribution of CT, as indicated in Figure 17. Recall that when

evaluating the observed data it was speculated that the greater degree of degradation near the horizontal influent port resulted from a more biologically active zone. This agrees with the simulation, as illustrated by iso-surface plots of the simulated mobile and immobile strain KC after 12 days (Figure 32 and 33). Therefore, as stated earlier, in order to create an effective biocurtain, it is critical to ensure that there is a sufficient enough distribution of microbes that the bioactive zone completely covers the region of the aquifer between injection and extraction wells.

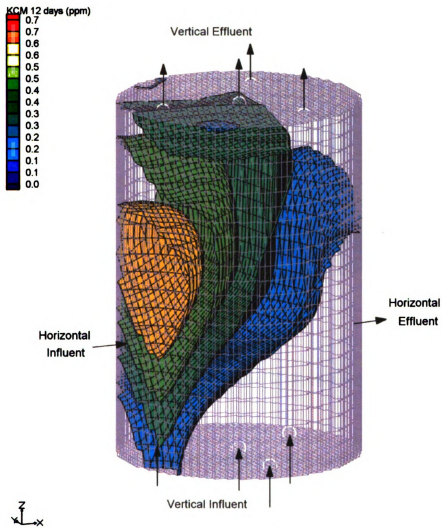

Figure 32. Concentrations of mobile strain KC represented by iso-surfaces at day 12 of the biocurtain simulation.

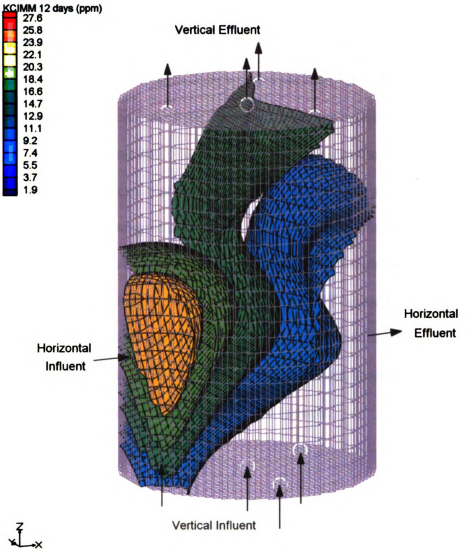

Figure 33. Concentrations of immobile strain KC represented by iso-surfaces at day 12 of the biocurtain simulation.

Though there was inadequate data for a more complete comparison between simulated and observed reactive species, the application of the 3-D flow and transport model to the laboratory biocurtain experiment provided insight into the nature of the remediation of Schoolcraft Plume A. The interdependence of nitrate, acetate, mobile and immobile

biomass, on the degradation of dissolved and sorbed carbon tetrachloride was made clear through the numerical modeling. Unfortunately, due to issues with the laboratory experiment and the difficulties in calibrating the numerical flow and transport model, a detailed analysis of the reaction parameters was not possible. Therefore, one cannot state if the parameters formerly optimized for the one-dimensional column studies by Phanikumar et al. (2002a and 2003) are applicable for this three-dimensional laboratory model. The results do indicate that the numerical simulation over predicted the amount of CT degradation, which suggest that a decrease in the second order CT reaction rate may be appropriate. When this model was applied to the field-scale biocurtain, Phanikumar et al. (2005) also noted an over prediction of CT degradation, though an acceptable prediction of acetate and nitrate. They found that reducing the CT degradation term by half produced a much better fit between simulated and observed. Again, this was not investigated here, given the inadequacies in the datasets.

6 DISCUSSION

The three-dimensional model aquifer experiment was designed to mimic the Schoolcraft biocurtain and serve as a link between spatially limited one-dimensional column studies and the field scale application. The specific goals of this thesis were to (a) improve our understanding of how well *Pseudomonas stutzeri* KC was transported in the subsurface, (b) to visualize the spatial distribution of biomass after an inoculation event, and (c) to conduct a case study utilizing the user-defined reactive transport model developed by the Departments of Geological Sciences and Civil and Environmental Engineering at Michigan State University that accounts for the three-dimensional microbial transport and biodegradation associated with the Schoolcraft project. Although there were many problems encountered during the study, the three-dimensional model aquifer experiment did produce several sets of useful data to evaluate the effectiveness of microbial transport and to examine the user-defined reactive transport model.

The laboratory model aquifer study began with a series of tests designed to characterize the aquifer media and gain insight into parameters effecting the flow and transport of dissolved species. Horizontal and vertical conservative tracer tests were conducted, as was a CT sorption study. The results of these tests were evaluated and later modeled using MODFLOW and a user defined RT3D model accounting for the three-dimensional reactive transport. The numerical model provided estimates for the porosity and dispersivity, which were later used in the inoculation and biocurtain simulations. Of key importance was the discovery of sensitivity of dispersivity in the vertical velocity field, but not in horizontal flow direction. This may be the result of the unique velocity field

generated by the divergent/convergent flow between the horizontal influent and effluent ports. This flow regime exhibited signs of numerical dispersion, resulting from the primarily non-orthogonal flow across the finite difference grid cells. Discovering this problem through the conservative tracer test simulations was important, for this phenomenon would be present in the inoculation and biocurtain simulations as well; however, would have been more difficult to identify since there are many more parameters to consider when modeling these scenarios. The indication of a directional insensitivity to dispersivity should be further investigated if multi-directional flow and transport models continue to be utilized.

Another interesting aspect of this project was the CT sorption study. Based on the comparison between the bromide and CT breakthrough curves there appears to be a process that is currently not accounted for in the reactive transport model. As noted earlier, there may be a need to investigate a multi-rate sorption model or a model that accounts for a spatial variability of the distribution coefficient.

The inoculation event was perhaps the most important aspect of this model aquifer experiment, for according to the literature there is a lack of spatiotemporal microbial transport data. Our data clearly demonstrates that strain KC can be effectively distributed through saturated porous media; though, the results indicate that transport is slower than a conservative tracer. This is an important distinction to note, since the effectiveness of bioaugmentation depends largely on the distribution of the microbes, therefore when designing a biocurtain, engineers and scientists should be mindful of the biomass

concentrations and not assume complete coverage of a bio-active zone through the detection of a conservative tracer.

The inoculation data also provided the opportunity to test how well the user-defined microbial transport and biodegradation model predicted the transport of strain KC. Simulations predicted an almost simultaneous arrival of the conservative tracer and mobile phase biomass using past reactive transport parameters gleaned from the literature, which was clearly not the case for the observed data. This suggests that there is an additional factor controlling the observed lag time between the mobile strain KC and a conservative tracer, such as a retardation factor. This observation should be considered as microbial transport models continue to progress.

The laboratory biocurtain study demonstrated successful mass removal of carbon tetrachloride and provided an interesting case study for application of the microbial and biodegradation model. Resulting from the scarcity of available datasets for comparative purposes and the problems encountered during the laboratory study, in-depth qualitative analysis of the biocurtain simulation was not possible. Instead the simulated biocurtain was used to provide insight into the rates and processes involved with bioaugmentation. The interdependence of the reactive species, as described by the coupled partial differential equations, is clearly visualized in the results of the simulated biocurtain. Furthermore, the simulation demonstrates the need for effective distributions of electron acceptors and donors, as well as microbial concentrations to maintain successful bioaugmentation. Though there is little data to compare the simulation to, the results do

suggest an over-prediction, which would suggest the need to decrease the CT degradation rate.

Many problems arose during the laboratory experiment and subsequent numerical modeling. The first problem encountered involved the ill-fitting top of the flow cell, which required a 30 degrees rotation to create a watertight seal, thus contributing to the non-uniform velocity field in the vertical flow direction. A second problem encountered was the inability to maintain constant influent flow rates. This was due to occasional partial plugging of influent lines and tubing wear during peristaltic pump use. More problematic though, were the fluctuating influent concentrations caused by changes in the volume of water within the solute amendment tank. Lastly, the lack of pH control during the biocurtain experiment proved to be the problem that truly ended the laboratory study. Many of these problems could be prevented in future three-dimensional laboratory aquifer studies, as described in Vidal-Gavilan (2000). Specifically additional attention should be placed on measuring and maintaining flow rates, measuring hydraulic heads across the velocity field to generate groundwater flow gradients, utilization of pumps instead of reliance on gravity, placement of finer screens in influent and effluent ports, closed-loop recirculation, etc.

APPENDICES

APPENDIX A

Horizontal Tracer Test
Bromide Concentrations at Internal Sampling Ports (C/C_0)

Location	X	Y	Z	30 min	60 min	90 min	120 min	150 min	180 min
111	15.24	15.24	15.24				0.77	0.80	0.97
112	15.24	30.48	15.24				0.79	0.80	1.00*
113	15.24	45.72	15.24				0.79	0.87	1.00*
121	30.48	15.24	15.24				0.77	0.84	0.86
122	30.48	30.48	15.24						
123	30.48	45.72	15.24				0.74		0.96
131	45.72	15.24	15.24					0.10	0.45
132	45.72	30.48	15.24				0.09		0.66
133	45.72	45.72	15.24						
212	15.24	30.48	22.86	0.80	0.67	0.66	0.77	0.87	1.00*
222	30.48	30.48	22.86		0.57	0.59	0.83	0.80	1.00*
232	45.72	30.48	22.86			0.23	0.77	0.93	0.96
311	15.24	15.24	30.48	0.90	0.80	0.66	0.77	0.91	1.00
312	15.24	30.48	30.48	0.96	0.70	0.75	0.83	0.91	0.97
313	15.24	45.72	30.48	0.78	0.78	0.72	0.77	0.84	1.00*
321	30.48	15.24	30.48		0.20	0.61	0.79	0.84	1.00*
322	30.48	30.48	30.48		0.75	0.69	0.77		1.00*
323	30.48	45.72	30.48						
331	45.72	15.24	30.48			0.07	0.19	0.93	0.96
332	45.72	30.48	30.48			0.72	0.86	1.00	0.96
333	45.72	45.72	30.48						
412	15.24	30.48	38.1	0.78	0.78	0.66	0.83	0.91	0.93
422	30.48	30.48	38.1		0.78	0.72	0.83	0.80	1.00*
432	45.72	30.48	38.1						1.00*
511	15.24	15.24	45.72				0.77	0.87	0.86
512	15.24	30.48	45.72				0.79	0.84	0.93
513	15.24	45.72	45.72				0.86	0.77	1.00*
521	30.48	15.24	45.72					0.83	
522	30.48	30.48	45.72				0.86	0.93	1.00*
523	30.48	45.72	45.72				0.83	0.97	0.89
531	45.72	15.24	45.72						
532	45.72	30.48	45.72						
533	45.72	45.72	45.72						
612	15.24	30.48	53.34					0.84	1.00*
622	30.48	30.48	53.34					0.90	
632	45.72	30.48	53.34						

Location	X	Y	Z	30 min	60 min	90 min	120 min	150 min	180 min
711	15.24	15.24	60.96					0.37	1.00*
712	15.24	30.48	60.96					0.73	0.93
713	15.24	45.72	60.96					0.80	1.00*
721	30.48	15.24	60.96					0.05	0.09
722	30.48	30.48	60.96					0.10	0.34
723	30.48	45.72	60.96					0.09	0.09
731	45.72	15.24	60.96					0.06	0.05
732	45.72	30.48	60.96					0.05	0.04
733	45.72	45.72	60.96						
812	15.24	30.48	68.58						0.96
822	30.48	30.48	68.58						0.04
832	45.72	30.48	68.58						0.03
911	15.24	15.24	76.2						0.10
912	15.24	30.48	76.2						
913	15.24	45.72	76.2						0.03
921	30.48	15.24	76.2						0.03
922	30.48	30.48	76.2						0.02
923	30.48	45.72	76.2						
931	45.72	15.24	76.2						
932	45.72	30.48	76.2						
933	45.72	45.72	76.2						
Hor_Influent	0	30.48	30.48	1.00*	1.00*	1.00*	1.00*	1.00*	1.00*
Hor_Effluent	60.96	30.48	30.48	0.02	0.02	0.09	0.28	0.41	0.67

Horizontal Tracer Test
Bromide Concentrations at Effluent Sampling Port (C/C_0)

Time (min)	Horizontal Effluent Port
0	0.014
4	0.017
9	0.016
14	0.012
19	0.015
24	0.017
29	0.018
34	0.015
39	0.023
44	0.023
49	0.021
54	0.021
59	0.022
64	0.022
69	0.024
74	0.033
79	0.064
84	0.089
89	0.094
94	0.162
99	0.162
104	0.224
109	0.237
114	0.279
119	0.294
124	0.347
129	0.347
134	0.408
139	0.347
144	0.408
149	0.480
154	0.507
159	0.565
164	0.565
169	0.431
174	0.665
179	0.597
184	0.630
189	0.665
194	0.665
199	0.783
204	0.702

APPENDIX B

Vertical Tracer Test
Bromide Concentrations at Internal Sampling Ports (C/C_0)

	0 hr	16 hr	24 hr	30 hr	31 hr	32 hr	33 hr	34 hr	35 hr	36 hr
111		1.00*	1.00*							
112		1.00*	0.90							
113		1.00*	0.97							
121		1.00*	0.94							
122		1.00*	0.90							
123		1.00*	0.94							
131		1.00*	0.99							
132		1.00*	0.99							
133		0.98	0.94							
212										
222										
232										
311		1.00*	0.97							
312		1.00*	1.00*							
313		0.52	0.94							
321		0.88	0.94							
322		1.00*	0.90							
323		1.00*	0.97							
331		0.98	0.94							
332		0.92	0.94							
333		0.95	0.94							
412										
422										
432										
511		0.22	1.00*							
512		0.14	0.97							
513		0.09	0.74							
521		0.21	0.80							
522		0.73	0.97							
523		0.82	0.94							
531		0.32	0.99							
532		0.14	0.94							
533		0.12	0.94							
612										
622										
632										

Location	0 hr	16 hr	24 hr	30 hr	31 hr	32 hr	33 hr	34 hr	35 hr	36 hr
711			0.14							
712			0.17							
713			0.12							
721		0.16	0.13							
722		0.09	0.57							
723		0.07	0.83							
731			0.51							
732			0.22							
733			0.10							
812					0.70	0.96	1.00*	1.00*	1.00*	
822				0.80	0.95	1.00*	1.00*	1.00*	1.00*	
832				0.51	0.73	1.00	1.00*	1.00*	1.00*	
911			0.09		0.20	0.60	0.88	1.00*	1.00*	
912			0.09		0.35	0.58	0.85	1.00*	1.00*	
913							0.22	0.31	0.48	0.70
921			0.13	0.05	0.05	0.14	0.26	0.39	0.58	0.82
922			0.07	0.19	0.54	0.86	1.00*	1.00*	1.00*	
923			0.08	0.43	0.76	1.00*	1.00*	1.00*	1.00*	
931			0.06	0.12	0.35	0.76	0.95	1.00*	1.00*	
932			0.07	0.03	0.03	0.20	0.52	0.59	0.83	1.00*
933			0.07	0.04	0.18	0.44	0.71	0.83	0.96	1.00*
Vert_Influent	1.00*	0.98	0.90	1.00*						
Vert_Effluent			0.02							

Vertical Tracer Test
Bromide Concentrations at Effluent Sampling Port (C/C_0)

Time (hrs)	Vertical Effluent Port
24.00	0.02
36.58	0.14
36.83	0.21
37.08	0.26
37.33	0.30
37.58	0.32
37.83	0.36
38.08	0.39
38.33	0.40
38.58	0.47
38.83	0.47
39.08	0.51
39.33	0.57
39.58	0.55
39.83	0.60
40.08	0.67
40.33	0.70
40.58	0.70
40.83	0.72
41.08	0.78
41.33	0.85
41.58	0.82
41.83	0.92

APPENDIX C

Carbon Tetrachloride Sorption Study
CT Concentrations at Internal Sampling Ports (C/C_0)

Location	24 hr	48 hr	72 hr	120 hr	146.5 hr	160.75 hr	184.25 hr	241 hr
111	0.65	0.77	0.70	0.80	0.68		0.82	
112	0.92	0.76	0.85	0.85	0.79		0.78	
113	0.84	0.75	0.90	0.77	1.00*		0.75	
121	0.69	0.77	0.81	0.79	1.00*		0.78	
122	0.79	0.87	0.83	0.93	0.72		0.88	
123	0.89	0.91	0.81	0.79	0.69		0.77	
131	0.71	0.69	0.75	0.67	0.56		0.82	
132	0.69	0.74	0.61	0.66	0.85		0.84	
133	0.72	0.72	0.87	0.90	0.85		0.85	
212								
222								
232								
311	0.54	0.61	0.91	0.82	1.00*			
312	0.76	0.75	0.88	0.88	1.00*			
313	0.37	0.72	0.76	0.97	0.97			
321	0.62	0.86	0.73	1.00*	0.89			
322	0.76	0.88	0.63	0.91	1.00*			
323	0.77	0.73	0.73	0.90	1.00*			
331	0.67	0.73	0.85	0.92	1.00*			
332	0.60	0.65	0.78	0.90	1.00*			
333	0.66	0.73	0.66	0.85	1.00*			
412								
422								
432								
511	0.25	0.75	0.74	0.98	0.95			
512	0.20	0.76	0.73	0.95	1.00*			
513	0.07	0.81	0.81	0.91	0.93			
521	0.12	0.70	0.64	0.87	0.89			
522	0.54	0.67	0.73	0.90	1.00*			
523	0.55	0.74	0.56	0.93	0.83			
531	0.37	0.76	0.68	0.92	1.00*			
532	0.29	0.74	0.81	1.00*	0.98			
533	0.35	0.66	0.82	0.91	1.00*			
612								
622								
632								

Location	24 hr	48 hr	72 hr	120 hr	146.5 hr	160.75 hr	184.25 hr	241 hr
711	0.04	0.60	0.74	0.79	0.91			
712	0.03	0.47	0.59	0.80	0.88			
713	0.01	0.31	0.46	0.63	0.81			
721	0.09	0.65	0.63	0.86	0.88			
722	0.05	0.43	0.54	0.79	0.86			
723	0.04	0.65	0.38	0.95	0.89			
731	0.12	0.60	0.73	0.90	0.76			
732	0.05	0.52	0.68	0.73	0.72			
733	0.04	0.56	0.66	0.79	0.77			
812								
822								
832								
911	0.04	0.26	0.47	0.66	0.70	0.78	0.80	
912	0.04	0.24	0.49	0.62	0.88	0.79	0.80	
913	0.02	0.09	0.46	0.50	0.80	0.76	0.67	
921	0.04	0.24	0.44	0.49	0.87	0.58	0.58	
922	0.04	0.13	0.62	0.68	0.89	0.81	0.75	
923	0.05	0.35	0.64	0.62	0.93	0.86	0.78	
931	0.06	0.35	0.58	0.52	0.85	0.83	0.75	
932	0.05	0.23	0.62	0.62	0.75	0.71	0.85	
933	0.05	0.25	0.54	0.54	0.83	0.75	0.68	
Vert_Influent	0.88	1.00*	1.00*	0.97	0.74	0.85	0.97	1.00*
Vert_Effluent		0.10	0.36	0.50	0.50	0.57	0.66	0.63

APPENDIX D

Inoculation
Bromide Concentrations at Internal Sampling Ports (C/C_0)

Location	0 min	15 min	30 min	45 min	60 min	75 min	90 min
312		0.94		1.00*		1.00*	1.00*
322		0.15	0.18	0.73	1.00*	1.00*	0.10
332		0.16		0.19	0.20	0.22	0.67
Hor_Effluent			0.19		0.19		0.06

Location	105 min	120 min	135 min	150 min	165 min	180 min
312	1.00*	0.98	1.00*	1.00*	0.98	0.86
322	1.00*	1.00*	1.00*	1.00*	0.98	0.86
332	1.00*	1.00*	0.98	0.98	0.94	0.83
Hor_Effluent		0.27		0.43		0.70

Inoculation
Mobile KC Concentrations at Internal Sampling Ports (C/C_0)

Location	0 min	15 min	30 min	45 min	60 min	75 min	90 min
Hor_Influent	0.93		1.00*		0.41		0.77
312		0.46	1.00*	0.74	0.89	1.00*	1.00*
322		0.00	0.00	0.01	0.08	1.00*	1.00*
332				0.00	0.00	0.00	0.00
Hor_Effluent							

Location	105 min	120 min	135 min	150 min	165 min	180 min
Hor_Influent		0.92		1.00*		1.00*
312		1.00*	1.00*	1.00*	1.00*	0.76
322	1.00*	1.00*	1.00*	1.00*	0.95	0.63
332	0.04	0.12	0.23	0.49	1.00*	1.00*
Hor_Effluent		0.00		0.01		0.04

APPENDIX E

Biocurtain
Carbon Tetrachloride Concentrations at Internal Sampling Ports (ppb)

Location	0 hr	1.5 hr	53.75 hr	77.75 hr	120.25 hr	144.25 hr	144.75 hr
111		0.00			23.02		
112		0.00			30.00		
113		0.16			8.84		
121		5.56			30.44		
122		1.49			18.86		
123		1.67			21.17		
131		42.91			18.85		
132		31.67			26.26		
133		42.56			26.25		
311		0.00			35.24		
312		0.00			29.89		
313		0.00			30.46		
321		0.17			28.00		
322		0.00			29.39		
323		2.00			13.78		
331		21.29			40.60		
332		4.86			40.86		
333		10.97			39.20		
511		0.00			7.64		
512		0.00			4.27		
513		0.00			1.27		
521		1.75			15.26		
522		0.38			8.96		
523		3.10			1.09		
531		33.16			39.68		
532		11.09			41.57		
533		40.63			43.97		

Location	0 hr	1.5 hr	53.75 hr	77.75 hr	120.25 hr	144.25 hr	144.75 hr
711		12.38			1.06		
712		2.97			1.47		
713		2.50			0.81		
721		40.65			2.27		
722		25.57			1.28		
723		31.49			1.80		
731		44.88			36.19		
732		43.43			37.59		
733		30.55			26.80		
911		37.84			5.23		
912		44.44			4.04		
913		39.47			13.70		
921		30.55			4.13		
922		32.46			14.11		
923		40.55			11.84		
931		44.83			35.76		
932		49.98			31.34		
933		38.56			34.76		
Vert_Influent		39.02	61.72	43.19	16.75		
Vert_Effluent		25.68	27.52	22.20	10.82		
Hor_Effluent						28.35	30.10

Biocurtain

Carbon Tetrachloride Concentrations at Internal Sampling Ports (ppb)

Location	145.25 hr	145.75 hr	146.25 hr	146.85 hr	288.25 hr
111					25.34
112					32.22
113					16.26
121					30.79
122					30.40
123					35.28
131					34.55
132					33.80
133					30.93
311					24.77
312					31.95
313					0.00
321					25.25
322					29.88
323					26.92
331					35.59
332					31.70
333					32.49
511					23.77
512					17.26
513					0.00
521					7.36
522					28.93
523					17.15
531					30.85
532					31.85
533					32.97

Location	145.25 hr	145.75 hr	146.25 hr	146.85 hr	288.25 hr
711					0.84
712					0.00
713					0.00
721					3.08
722					0.00
723					0.00
731					33.48
732					31.35
733					9.13
911					0.00
912					0.00
913					0.00
921					0.00
922					0.00
923					0.00
931					23.18
932					25.98
933					25.98
Vert_Influent					28.75
Vert_Effluent					3.23
Hor_Effluent	29.47	30.37	34.62	37.11	

REFERENCES

Anderson, M.P. and W.W. Woessner. 1992. Applied Groundwater Modeling: Simulation of Flow and Advective Transport. Academic Press, San Diego, 381 p.

Brennan, M.A. 2004. Effects of small-scale heterogeneity on tracer transport. M.S. Thesis, Department of Geological Sciences, Michigan State University.

Chapelle, F.H. 2001. Ground-Water Microbiology and Geochemistry. John Wiley & Sons Inc., New York, 477 p.

Clement, T.P. 1997. RT3D-A modular computer code for simulating reactive multi-species transport in 3-dimensional groundwater aquifers, Battelle Pacific Northwest National Laboratory Research Report, PNNL-SA-28967, September, 1997.

Criddle, C.S., J.T. Dewitt, D. Grbic-Garlic, and P.L. McCarty. 1990. Transformation of Carbon Tetrachloride by *Pseudomonas sp strain KC* under Denitrification Conditions. *Appl. Environ. Microbiol.* 56 (11): 3240 - 3246.

Davis, N. 1995. Added Microbe Converts Suspected Carcinogen. Centerpoint, 2 (4 – 5).

Dybas, M.J., G.M. Tatara, and C.S. Criddle. 1995. Localization and characterization of the carbon tetrachloride transformation activity of *Pseudomonas sp strain KC. Appl. Environ. Microbiol.* 61: 758 – 762.

Dybas M.J, M. Barcelona, S. Bezborodnikov, S. Davies, L. Forney, O. Kawka, T. Mayotte, L. Sepulveda-Torres, K. Smalla, M. Sneathen, J. Tiedje, T. Voice, D. Wiggert, M.E.Witt, C.S. Criddle. 1998. Pilot Scale Evaluation of Bioaugmentation for in-situ Remediation of a Carbon Tetrachloride Contaminated Aquifer. *Environ. Sci. Technol.*, 32 (22): 3598 – 3611.

Dybas, M.J., D.W. Hyndman, R. Heine, J. Tiedje, K. Linning, D. Wiggert, T. Voice, X. Zhao, L. Dybas, and C.S. Criddle. 2002. Development, Operation, and Long-Term Performance of a Full-Scale Biocurtain Utilizing Bioaugmentation. *Environ. Sci. Technol.* 36 (16): 3635 – 3644.

Ewer, K.A. 1997. Three-dimensional groundwater flow and contaminant transport in medium scale highly heterogeneous environments. M.S. Thesis, Department of Geological Sciences, Michigan State University.

Fetter, C.W. 1988. Applied Hydrogeology. Second Edition. Macmillan Publishing Company, New York, 592 p.

Fetter, C.W. 1999. Contaminant Hydrogeology. Second Edition. Prentice-Hall, Inc., New Jersey, 500 p.

Freeze, R.A. and J.A. Cherry. 1979. Groundwater. Prentice-Hall, Inc., Englewood Cliffs, New Jersey, 604 p.

Haggerty, R. and S.M. Gorelick. 1995. Multiple-rate mass transfer for modeling diffusion and surface reactions in heterogeneous media, *Water Resources Research.* 31(10): 2383-2400.

Halliburton NUS Environmental Co. 1991. Remedial Investigation and Feasibility Study of Remedial Alternatives, Plume A and Plume F, Village of Schoolcraft, Kalamazoo County, Michigan.

Harbaugh, A.W., E.R. Banta, M.C. Hill, and M.G. McDonald. 2000. MODFLOW-2000 The U.S. Geological Survey modular ground-water model – user guide to modularization concepts and the Ground-Water Flow Process: U.S. Geological Survey Open-File Report., 00-92, 121 p.

Huyakorn P.S. and G.F. Pinder. 1983. Computational Methods in Subsurface Flow. Academic Press, 473 p.

Hyndman, D.W., M.J. Dybas, L. Forney, R. Heine, T. Mayotte, M.S. Phanikumar, G. Tatara, J. Tiedje, T. Voice, R. Wallace, D. Wiggert, X. Zhao, and C.S. Criddle. 2000. Hydraulic Characterization and Design of a Full Scale Biocurtain. *Ground Water*, 38 (3): 462 – 474.

Johnson, W.P., P. Zhang, M.E. Fuller, T.D. Scheibe, B.J. Mailloux, T.C. Onstotte, M.F. Hubbard, S.S. Radtke, J. Kovacik, W.P. Holben. 2001. Ferrographic tracking of bacterial transport in the field at the Narrow Channel focus area, Oyster, VA. *Environ. Sci. Technol.* 35(1): 182-191.

Lee, C.H., T.A. Lewis, A. Paszczynski, R.L. Crawford. 1999. Identification of an extracellular catalyst of carbon tetrachloride dehalogenation from Pseudomonas Stutzeri strain KC as pyridine-2,6-bis(thiocarboxylate). Biochem. Biophys. Res. Commun., 261(3): 562-566.

Lewis, T.A. and R.L. Crawford. 1993. Physiological factors affecting carbon tetrachloride dehalogenation by the denitrifying bacterium *Pseudomonas sp strain KC. Appl. Environ. Microbiol.* 59: 1635-1641.

Lewis, T.A. and R.L. Crawford. 1999. Chemical Studies of Carbon Tetrachloride Transformation by *Pseudomonas sp strain KC. Novel Approaches for Bioremediation of Organic Pollutants*. R. Fass, Y. Flashner, and S. Reuveny Editors. Kluwer Academic, New York, pp. 1-10.

Mandle, R.J. 2002. Groundwater Modeling Guidance. Groundwater Modeling Program, Michigan Department of Environmental Quality.

Mayotte, T., M.J. Dybas, C.S. Criddle. 1996. Bench-scale evaluation of bioaugmentation to remediate carbon tetrachloride-contaminated aquifer materials. Ground Water, 34(2): 358-367.

Murphy, E.M., T.R. Ginn, A. Chilakapati, C.T. Resch, J.L. Phillips, T.W. Wietsma, and C.M. Spadoni. 1997. The influence of physical heterogeneity on microbial degrdataion and distribution in porous media. *Water Resources Research*, 33(5): 1087-1103.

Phanikumar, M.S., D.W. Hyndman, D.C. Wiggert, M.J. Dybas, M.E. Witt, and C.S. Criddle. 2002. Simulation of microbial transport and carbon tetrachloride biodegradation in intermittently-fed aquifer columns. *Water Resources Research, 38* (4), 10.1029/2001WR000289.

Phanikumar, M.S. and D.W. Hyndman. 2003. Interactions between sorption and biodegradation: Exploring bioavailability and pulsed nutrient injection efficiency. *Water Resources Research,* 39 (5), 1122,10.1029/2002WR001761.

Phanikumar, M.S. and D.W. Hyndman. 2003. Correction to "Interactions between sorption and biodegradation: Exploring bioavailability and pulsed nutrient injection efficiency." *Water Resources Research,* 39 (10), 1281,10.1029/2003WR002327.

Phanikumar, M.S., D.W. Hyndman, X. Zhao, and M.J. Dybas. 2005. A Three-Dimensional Model of Microbial Transport and Biodegradation at the Schoolcraft, Michigan Site. *Water Resources Research,* 41(5)10.1029/2004WR003376.

Radabaugh, P.D. 1998. Factors Affecting Transport of *Pseudomonas Stutzeri KC*, M.S. Thesis, Department of Civil and Environmental Engineering, Michigan State University.

Tatara, G.M., M.J. Dybas, and C.S. Criddle. 1993. Effects of Medium and Trace Metals on Kinetics of Carbon Tetrachliride Transformation by *Pseudomonas sp Strain KC. App. Env. Microbiology*, 59 (7): 2126 – 2131.

Tatara, G.M., M.J. Dybas, and C.S. Criddle. 1995. Biofactor-mediated transformation of carbon tetrachloride by diverse cell types. In Bioremediation of Chlorinated Solvents; Hinchee, R.E., Leeson, A, Semprinit, L., Eds.; Battelle Press: Colombus, OH, pp. 69-76.

Vidal-Gavilan, G. 2000. Multidimensional Transport of *Pseudomonas Stutzeri Strain KC* in a Model Aquifer System: Predicting CT Remediation. M.S. Thesis, Department of Civil and Environmental Engineering, Michigan State University.

Witt, M.E., M.J. Dybas, R.L. Heine, S. Nair, and C.S. Criddle, and D.C. Wiggert. 1995. Bioaugmentation and Transformation of Carbon Tetrachloride in a Model Aquifer. *Bioremediation 3: Bioaugmentation for Site Remediation*, Battelle Press, Columbus, 221 – 227.

Witt, M.E., M.J. Dybas, D.C. Wiggert, and C.S. Criddle. 1999. Use of Bioaugmentation for Continuous Removal of Carbon Tetrachloride in Model Aquifer Columns. *Env. Eng. Sci,* 16 (6): 475 – 485.

Zhao, X., M.J. Szafranski, M.A. Maraqa, and T.C. Voice. 1999. Desorption and Bioavailability of Carbon Tetrachloride in a Low Organic Content Sandy Soil. *Environmental Chemistry and Toxicology,* 18 (8): 1755 – 1762.

Zhao, X., R.B. Wallace, D.W. Hyndman, M.J. Dybas, and T.C. Voice. submitted. Heterogeneity of Chlorinated Hydrocarbon Sorption Properties in a Sandy Aquifer. *Journal of Contaminant Hydrology.*

MICHIGAN STATE UNIVERSITY
3 1293 02736